DISSERTATION

UNDERREPRESENTED DRIVERS OF AND VARIABILITY IN VOLATILE ORGANIC COMPOUND EMISSIONS FROM PLANTS

Submitted by

Mj Riches

Department of Chemistry

In partial fulfillment of the requirements

For the Degree of Doctor of Philosophy

Colorado State University

Fort Collins, Colorado

Summer 2022

Doctoral Committee:

Advisor: Delphine Farmer

Thomas Borch
Seth Davis
Grzegorz Szamel

ABSTRACT

UNDERREPRESENTED DRIVERS OF AND VARIABILITY IN
VOLATILE ORGANIC COMPOUND EMISSIONS FROM PLANTS

Volatile organic compounds released from plants interact with the atmosphere in complex ways, e.g., by contributing to the formation and removal of atmospheric oxidants and the production of secondary organic aerosol. These organic compounds include terpenes (polymers of C_5H_8), organic acids (e.g., formic and acetic), aldehydes (e.g., glycoaldehyde and 2-hexenal), and many other classes of compounds. These compounds are diverse in structure, preventing many assumptions as the physiochemical properties of each species is diverse. Even among the same class of compounds (e.g., $C_{10}H_{16}$ monoterpene isomers), the atmospheric implications of their emission and reactivity potential can range greatly, as some species contribute more towards the removal of ozone while others are more relevant to secondary organic aerosol formation. Given the diversity of these effects, the quantification and identification of these plant-emitted compounds is a key step to improve predictive models of their emissions and subsequent atmospheric impacts.

Measuring the emission of these volatile organic compounds is compounded by their low concentrations, high reactivity, and chemical diversity, and, as of today, there is no single instrument capable of fully investigating the suite of plant-derived emissions. To address this knowledge gap, we used a commercial portable photosynthesis system in combination with numerous analytical instruments, namely chemical ionization mass spectrometry, proton transfer

reaction mass spectrometry, and thermal desorption gas chromatography mass spectrometry. We present the modularity of this coupled technique and identify its limitations and the considerations which must be made when performing measurements in the field. We can investigate a greater suite of compounds by coupling the portable photosynthesis system with multiple trace gas instruments simultaneously. The system controls environmental conditions over a broad range applicable to plant physiology and we highlight how background interferences can be mitigated with pre- and post-leaf characterization. This technique provides photosynthetic parameters and direct measurements of leaf-level emissions to improve our understanding of the forces driving these emissions.

In addition to developing new analytical techniques, this dissertation identifies numerous environmental factors impacting volatile organic compound emissions that have been so far overlooked or incorrectly represented and expands upon their atmospheric implications. Specifically, we find that the first seasonal snow events cause an initial burst of emissions from a deciduous tree and further changes the identity of speciated compounds compared pre-snow conditions. In this case, excluding speciation of these compounds leads to an underestimation of the atmospheric burden on reactivity and secondary organic aerosol formation. We further identify humidity, which does not exist as a direct emission forcer in most models, as a necessary consideration. Humidity can either have a discrete or synergistic effect with temperature, again complicating integration into models, but inclusion is necessary to address changes in absolute emission rates and the temperature dependence of these emissions. As an overarching theme, this dissertation further presents compelling evidence for considering multiple scales of variability in leaf-level measurements; these measurements are often time consuming, but failure to account for such variability can grossly bias results.

ACKNOWLEDGEMENTS

I will start with my family- my father, who taught me to question what I know; my mother and brother, who have celebrated every step; my grandfather, who taught me that from the ashes comes new growth; my aunts, uncle, and cousins, without whom I'd feel much smaller; and Dozer, whose cuddles got me through many nights. I found a new family in graduate school, and while many have already left, their support and commiseration helped pull me through.

Endless thanks to my fifth-grade teacher Mr. Boemker, with whom I first experienced the joy of science, and my theatre teacher, Dr. Cresswell, who helped me find my voice. My undergraduate advisor, Dr. Longin, led me to study plants and to head to graduate school. The staff of the chemistry department keep things running and made my life easier. Stardew Valley, you were there for me in my darkest times. I would be remiss not to add Dr. Farmer, who challenged me, supported my science communication, and paid me to sit outside and tickle plants.

I thank my colleagues who gave me a sense of belonging and listened to my ramblings about plants. Many thanks to Matson and Erin for welcoming me into their office, for our many coffee breaks, and for teaching me everything I know about aerosols. I have been so lucky to have such a work environment and so much support along the way. I also acknowledge my failures and mistakes, which make me realize how far I have come and how much further I have to go.

I cannot thank anyone more than Alex. You have saved my research numerous times, from chipping away at ice to driving a pump through the mountains. I have loved you since middle school and my love for you has only grown all these years. You have helped me through the worst times and given me the best, and I cannot wait to continue our journey.

You are, in every sense of the word, my hero.

DEDICATION

To those who aren't here to see this

And to those who helped me see this through

TABLE OF CONTENTS

CHAPTER 1

MEASURING BIOSPHERE-ATMOSPHERE EXCHANGE OF SHORT LIVED CLIMATE FORCERS AND THEIR PRECURSORS[1]

Prologue

As our climate changes, so must our approach to constraining the impact of environmental perturbations on biogenic volatile organic compound (BVOC) emissions. Research in this field is constantly evolving, and improvements are made constantly both to measurements and modeling components. This dissertation highlights the importance of i) thorough instrument characterization, ii) considering often overlooked weather events, and iii) leaf-to-leaf, plant-to-plant, and day-to-day variability in leaf-level emission measurements. Furthermore, this dissertation identifies relative humidity as a key environmental parameter that is misrepresented or missing from models. We highlight the complexity and atmospheric importance of BVOC emissions in Chapter 1, with attention to some of the techniques used in the field to measure these compounds. Chapter 2 is an overview and thorough characterization of the measurement technique that we optimized and that is integral to the studies herein. Our field deployment during the first seasonal snow event, described in Chapter 3, offered rare insight to senescence-induced changes in BVOC emissions. Chapter 4 features results culminating from several months of field research, namely identifying the humidity dependence of various BVOC emissions and the discrete versus

[1] Farmer D.K., Riches M. Measuring biosphere–atmosphere exchange of short-lived climate forcers and their precursors. Accounts of Chemical Research. 2020 Jul 20;53(8):1427-35

synergistic role that humidity shares with temperature dependence. Future directions and ongoing works are discussed in the conclusion.

Conspectus

Exchange of reactive trace gases over the biosphere is a key source of reactive organic carbon to the atmosphere, and thus influences the formation of both ozone (O_3) and secondary organic aerosol (SOA). Both O_3 and aerosol particles are short-lived climate forcers and impact the radiative balance of the planet – and their sources and sinks are chemically complex. However, the biosphere also acts as a deposition sink for organic and inorganic compounds, including O_3, aerosols, and their precursors. Wet and dry deposition provides a key lever on the lifetime of trace gases and particles in the atmosphere - and thus on their potential to influence the radiative balance of the planet. The fluxes of reactive trace gases and particles are part of an atmospheric biogeochemical cycle that includes feedbacks through drought and other climate components.

Recent advances in measurement techniques have enabled new field observations of trace gas and particle fluxes. Our method development has focused on the leaf, branch and forest level, although satellite measurements coupled to modeling also provide promising new approaches to constraining trace gas fluxes. Leaf chamber measurements of volatile organic compound (VOC) emissions highlight leaf-to-leaf and plant-to-plant variability in both photosynthesis and emissions of individual VOCs, in addition to differences in emissions across different isomers of monoterpenes. Isomers obviously have different chemical properties (e.g. reaction rates with OH radicals, SOA yield), and thus hold different potentials as precursors for short-lived climate forcers.

The biosphere acts as both sources and sinks of the oxidation products of monoterpenes and other biogenic VOCs. Developments in chemical ionization mass spectrometry have recently enabled measurements of volatile organic acids, which demonstrate a strong temperature-

dependent ecosystem source, as well as a source from in-canopy chemistry. In-canopy chemistry also influences particle fluxes, although deposition should dominate their net exchange. Our field observations of chemically resolved particle fluxes demonstrate the simultaneous, competing processes driving forest exchange. To separate out these competing processes, black carbon is an inert tracer for particle deposition. Our recent measurements demonstrate the importance of wet deposition in controlling particle lifetime in the atmosphere. Overall, new measurement techniques have enabled both field and laboratory observations to improve our understanding of biosphere-atmosphere interactions and their influence on climate processes.

1. Introduction

The biosphere is both a source and a sink of short-lived climate forcers and their precursors. Direct, primary emissions of volatile organic compounds (VOCs) and nitrogen oxides provide precursors for important short-lived climate forcers, such as ozone (O_3) and secondary organic aerosol (SOA) particles (Fuentes et al., 2000; Scott et al., 2014). Importantly, forests act as sinks for both of these short-lived forcers, as well as the myriad intermediaries between VOCs and SOA (namely, oxygenated organic compounds) and particles in general. In fact, including dry deposition of oxygenated organic compounds can reduce modeled SOA on the order of 50% (Knote et al., 2015). The processes of wet and dry deposition control (or at least influence) the lifetimes of numerous climate-relevant components in the atmosphere – but remain poorly understood.

Coniferous and broadleaf forests, grasslands, and other ecosystems are dominated by plants that emit VOCs, ranging from terpenoids like isoprene (C_5H_8) and monoterpenes ($C_{10}H_{16}$) to oxygenated hydrocarbons like methanol. These VOCs are not in and of themselves climate forcers, but instead act as precursors for SOA and as key ingredients in O_3 production. VOCs can be oxidized in the atmosphere by O_3, hydroxyl radicals (OH) and nitrate (NO_3) radicals to form an array of products. This oxidation process kick-starts O_3 production by making hydroperoxyl (HO_2)

and peroxy (RO_2) radicals that react with nitric oxide (NO) to form nitrogen dioxide (NO_2), which in turn is photolyzed to form $O(^3P)$ that reacts with molecular oxygen (O_2) to produce O_3. The parent VOC that is oxidized in the initiation reaction with OH produces oxidized organic products that can undergo subsequent reactions with OH or other oxidants – in turn producing further oxidized volatile organic compounds (oVOCs). During this multi-generational VOC oxidation process, fragmentation reactions result in more volatile products that remain in the gas phase and continue to be oxidized, ultimately producing carbon dioxide (CO_2), a key greenhouse gas. Functionalization reactions produce less volatile products that can condense and form SOA.

Oxidation products include an array of organic moieties (Goldstein & Galbally, 2007; Heald & Kroll, 2020; Heald et al., 2008). Carboxylic acids are one common moiety found in the atmosphere but remain poorly understood. For example, the simplest carboxylic acid is formic acid, which is consistently observed in the atmosphere at far higher concentrations than can be explained by traditional models (Millet et al., 2015; F. Paulot et al., 2011; Stavrakou et al., 2012). This persistent model-measurement discrepancy highlights our poor understanding of atmospheric oxidation chemistry and biosphere sources of oVOCs. Particles play multiple roles in the atmosphere – as sinks for semi- and low-volatility gas-phase compounds; as transport mechanisms for pesticides and other toxic compounds; as direct light scatterers; and as cloud condensation nuclei (CCN) – particles that act as nuclei for the heterogeneous nucleation of water and thus form cloud droplets (Farmer et al., 2015; Scott et al., 2014). The links between plant emissions, particles and climate represent an atmospheric biogeochemical cycle (Figure 1.1). For example, in the Amazon, this SOA dominates CCN, while biological particles dominate ice nuclei (Pöschl et al., 2010). The resulting clouds influence the hydrological cycle, controlling precipitation over the forest and thus wet deposition of both trace gases and particles.

Biosphere-atmosphere exchange not only influences short-lived climate forcers, but also mediates multiple feedbacks in the climate system. For example, increased temperature enhances biogenic VOC emissions, thus enhancing both O_3 (warming effect) and SOA (cooling effect) - exemplifying both a positive and negative feedback (Scott et al., 2018). The effects of atmospheric CO_2, drought, nutrient additions, and O_3 damage to plants on biogenic VOC emissions are less well understood but may influence these feedbacks. For example, drought-stress can suppress biogenic isoprene emissions, impacting the temperature-dependence of regional ozone (Abeleira & Farmer, 2017). Not all VOCs respond to environmental perturbations identically - nor do they impact ozone and SOA production in the same way. For example, our laboratory experiments showed that different monoterpene isomers have unique photooxidation SOA yields (Friedman & Farmer, 2018). Combined with the fact that isomer emissions can have unique temperature dependencies (Tarvainen et al., 2005b; Tingey et al., 1980) and different drought responses (Bonn et al., 2019; Llusià & Peñuelas, 1998; Llusià et al., 2008), biosphere-atmosphere feedbacks on the climate system can be challenging to predict.

The impact of short-lived forcers on the radiative balance of the planet depends on both their potency (i.e., impact on radiative forcing per concentration unit in the atmosphere) and concentration. Ultimately, the concentration of any trace gas or particle in the atmosphere depends on the balance of sources and sinks. Thus, a rigorous understanding of the magnitude and mechanisms behind biosphere-atmosphere exchange is essential for capturing changes in short-lived climate forcers, and the role of human perturbations including land use change on our climate. This paper is not intended to be a comprehensive review of biosphere-atmosphere interactions of reactive trace gases – for that we recommend other publications (Carslaw et al., 2010; Fowler et al., 2009; Fuentes et al., 2000). Instead, we focus on some of our recent

contributions to our measurement and understanding of biosphere-atmosphere exchange of reactive trace gases and particles, and provide context for their insight into climate-relevant processes.

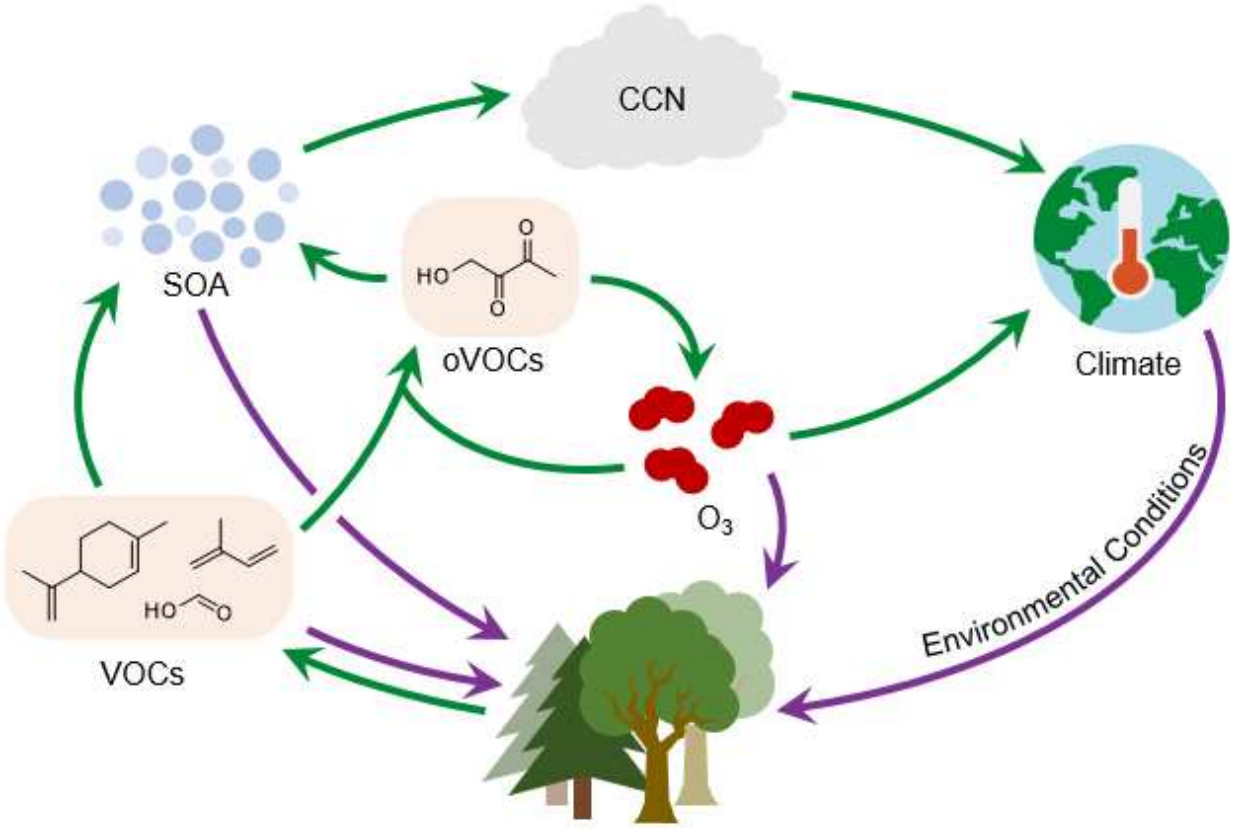

Figure 1.1. The terrestrial biosphere acts as both a source and sink of VOCs and their oxidation products. These organic gases contribute to the production of O_3 and SOA, both short-lived climate forcers that also deposit to ecosystems. However, the biosphere VOC source is impacted by climate conditions, resulting in a complex atmospheric biogeochemical cycle.

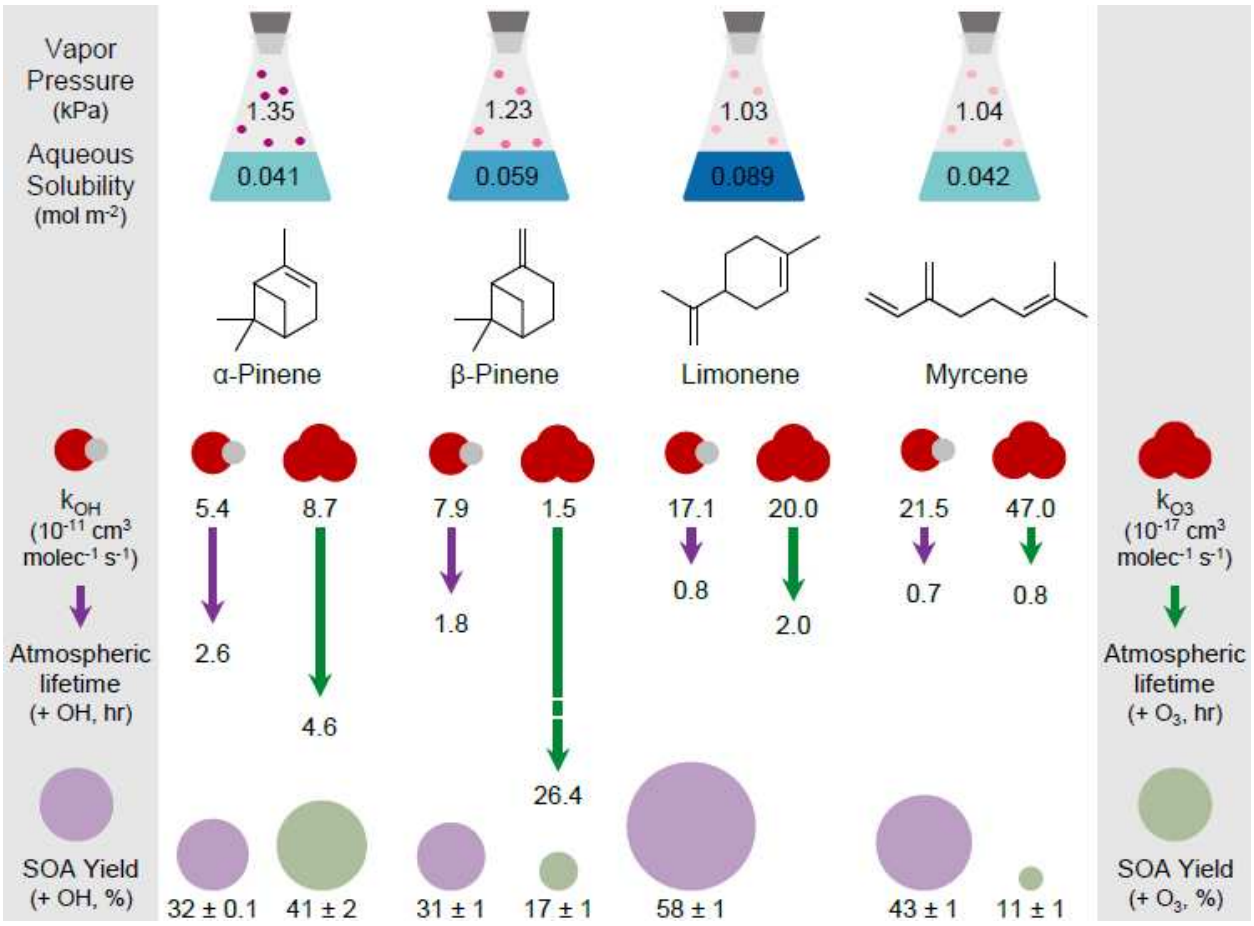

Figure 1.2. Chemical properties of select monoterpenes demonstrate that while VOCs are often lumped by elemental composition, different isomers can have different properties that influence their potential to form O_3 and SOA. Rate constants for the reaction with OH radical (kOH) and ozone (kO3) from Atkinson (1997). Estimated atmospheric lifetimes for OH (2.0×10^6 molec cm^{-3}, 12-hr avg) and O_3 (7×10^{11} molec cm^{-3}, 24-hr avg) from Atkinson and Arey (2003). Vapor pressure from Wilt et al. (1993). Aqueous solubility from Copolovici and Niinemets (2005). SOA mass yields from multiple sources (Lee, Goldstein, Keywood, et al., 2006; Lee, Goldstein, Kroll, et al., 2006).

2. Measurement techniques

Sensitive, specific and selective chemical detection techniques of both reactive trace gases and particles are essential for quantifying biosphere-atmosphere exchange. The measurement of trace gases is complicated by the chemical properties of any given species of interest. Some VOCs react with or partition to the surfaces of analytical instruments. VOCs have a broad range of atmospheric lifetimes on the order of minutes (Atkinson & Arey, 2003), requiring fast time-resolved measurements, to days, with respect to different atmospheric constituents.

2.1 Flux measurement approaches

Our understanding of biosphere-atmosphere exchange of reactive trace gases and particles is limited by our ability to observe the underlying processes. While numerous approaches exist to measure concentrations of reactive species (Farmer & Jimenez, 2010), measurement of fluxes over the biosphere is more challenging (Baldocchi et al., 1988). Flux measurements take place on the leaf, branch, or whole ecosystem level (Figure 1.3). In addition, concentration measurements - via either in situ field observations or ex situ remote sensing - can be coupled to chemical transport models to infer emission or deposition rates. Each of these techniques holds pros and cons: while more localized measurements over leaves or branches provide plant-level information about stomatal conductance and links to leaf area or specific leaf types (e.g., sun versus shade leaves), the fluxes can require sensitive measurement techniques, the measurements are limited to selected plants, and the enclosures themselves can influence the plant emissions (Ortega & Helmig, 2008). As a result of these challenges, leaf- and branch-level enclosures are poorly suited for long-term monitoring and are typically only used for short-term studies. Ecosystem-scale flux towers provide an integrated measurement across an ecosystem, incorporating all the plants and other components (e.g., soils, tree trunks). Flux towers can also be operated over relatively long timescales, though are typically only operated for weeks to months due to the challenges of maintaining reactive trace

gas and particle instruments over multiple years. However, these measurements can be challenging to interpret if too many different processes are occurring within the footprint of the measurement. Further, despite the intense work involved in flux studies, the measurements and controlling flux processes are not necessarily transferable from one site to another, let alone from one ecosystem to another. Multiple sites are essential for robust, broadly applicable conclusions. Coupling concentration measurements to models to derive flux estimates requires challenging assumptions in models, although recent work (Fu et al., 2019; Millet et al., 2008) on isoprene derived from satellite observations shows great promise. These larger scale calculations provide greater diversity of measurement sites, and potentially provide fluxes over longer time periods and more ecosystem types than in situ measurements could possibly provide. However, 'ground-truthing' these calculated fluxes through in situ measurements remains essential.

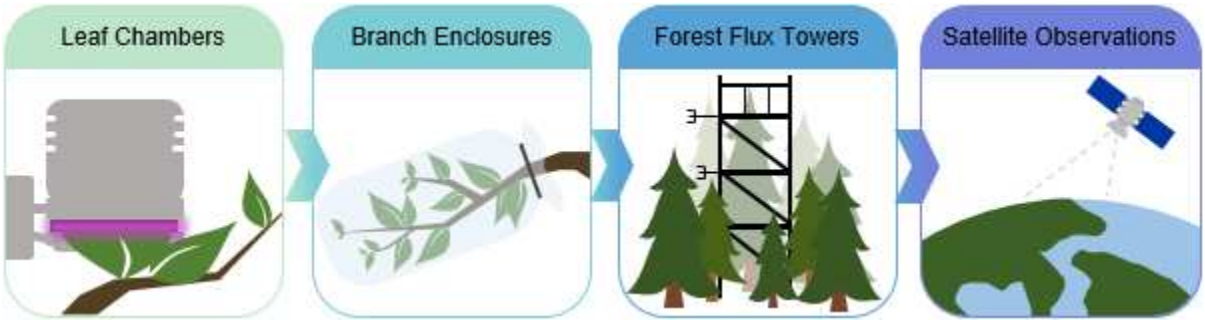

Figure 1.3. Multi-scale approaches to biosphere trace gas and particle emission measurements include direct measurements on leaves, branches, over ecosystem-scale footprints, and even by remote sensing coupled to measurements.

Leaf-level measurements typically use a small chamber over the leaf and use the difference in trace gas concentration observed in air entering versus exiting the chamber to calculate the plant emission rate. This approach has been used successfully in the community to investigate plant emissions of VOCs and volatile inorganic compounds. To measure leaf-level VOC emissions, we couple a portable photosynthesis system to trace-gas measurement systems (Riches et al., 2020).

This technique enables us to control environmental conditions (e.g., temperature, humidity, CO_2) over a known leaf area and to measure a variety of VOCs using different measurements systems, such as organic acids (via on-line mass spectrometry techniques) and monoterpenes (via thermal desorption of sorbent tubes coupled to off-line analysis). Branch enclosures are larger versions of leaf chambers, and hold the benefit of increased leaf surface area, and thus larger fluxes. However, the measurement of exact leaf surface area is more challenging. These enclosure measurement approaches are often limited in that the in-flow air is typically static in concentration, and thus ignores the potential for compensation points, in which the air concentration influences equilibria and thus the direction and magnitude of flux. However, on-going work in our group and others is investigating approaches to control ambient concentrations and thus investigate their influence on exchange processes.

Soil, leaf and branch enclosures enable us to investigate specific plant physiological processes and short-term responses to environmental conditions. One can scale from the leaf level to the entire forest canopy, but to understand long-term influences or the role of non-leaf ecosystem components or in-canopy chemistry, ecosystem level measurements are useful. Several micrometeorological approaches for ecosystem-scale measurements are available - each with their own chemical sensor requirements and assumptions. Flux-gradient and relaxed eddy accumulation techniques have been useful for measuring exchange over forests with sensors with lower time resolution or sensitivity, but eddy covariance remains the most direct ecosystem-level flux measurement approach (Baldocchi et al., 1988). However, eddy covariance flux measurement requires fast (typically 5-10 Hz) and sensitive detectors capable of making extended (at least 30 minutes) measurements without interruption or irregular change in background, calibration or other instrument parameters.

2.2 Instrument development

Much of our work has focused on developing measurement techniques that meet the eddy covariance criteria to be able to understand fluxes of reactive nitrogen oxides and oxidized organic compounds (Farmer et al., 2006; Fulgham et al., 2019). Chemical ionization mass spectrometry provides a particularly promising approach for eddy covariance fluxes due its speed, sensitivity, selectivity and capacity to measure multiple compounds at one time. For example, iodide reagent ions measure oxidized organic and inorganic species well, and have been used to measure eddy covariance fluxes of various species – including dinitrogen pentoxide (N_2O_5) and nitrylchloride ($ClNO_2$) over coastal water (Kim et al., 2014). However, like many reagent ions, iodide is susceptible to water interference; as water fluxes over ecosystems can be substantial due to transpiration, this interference can pose challenges to eddy flux data analysis. In contrast, acetate reagent ions are not sensitive to water vapor (Brophy & Farmer, 2016), and are useful for investigating different organic acid fluxes on a canopy level (Fulgham et al., 2019). While acetate reagent ions are particularly selective for organic and inorganic acids, this measurement approach is unable to measure the broad array of peroxide-, chlorine-, and nitrogen-containing molecules of iodide ionization.

Particles pose additional challenges for fast eddy covariance measurements. Particle size is the dominant control over deposition rates, although composition can also influence net ecosystem flux. No widely used commercially available instruments measure both size and composition fast enough for eddy covariance measurements, and most work to date has focused on total particle number and size-resolved number flux measurements in the accumulation mode. However, typical ambient accumulation mode particle size distributions hold substantial number in smaller sizes near 100 nm in diameter, but fewer particles in the larger (300+ nm) sizes. This size distribution challenges our ability to acquire adequate counts for size-resolved particle number

fluxes in larger modes on the rapid sub-second timescales of turbulence required for eddy covariance measurements. Optical measurement techniques count particle number, and are useful for size-resolved particle flux measurements (Vong et al., 2010) while aerosol mass spectrometry can detect particle chemical fluxes (Farmer et al., 2011) – and thus measure particle mass fluxes, but not number.

3. Flux observations

3.1 Volatile organic compounds

Numerous groups have measured VOC emissions from the biosphere using an array of techniques. Biogenic emission factors of VOCs vary greatly, both in terms of magnitude of emissions, and the way in which emissions respond to environmental conditions. VOCs can be temperature and/or light dependent, dependent on plant genetics and phenology, or may only be emitted during specific types of abiotic or biotic perturbations (Peñuelas & Llusià, 2001a). Our work has focused on leaf-level emissions through both on-line and off-line measurement techniques. Leaf-level measurements provide the opportunity to investigate how temperature or light impact plant emissions. However, individual leaves do not necessarily represent an entire plant, let alone a forest. Sampling many leaves on a single plant or multiple plants provide insight on this challenge of appropriately scaling from leaf-level measurements to entire plants or ecosystems.

Here, we provide an example of variability in limonene emissions of ponderosa lemon (*Citrus limon x Citrus medica*) plants using a leaf chamber (LI-6800 Portable Photosynthesis System, LI-COR) coupled to sorbent tubes for offline analysis using thermal desorption gas chromatography mass spectrometry (Riches et al., 2020) (Figure 1.4). We compared the intraplant variability with fifteen leaves on a single plant (1P x 15L) to the interplant variability with three leaves on each of five plants (5P x 3L). The averages of both sampling strategies are statistically

indistinguishable by a simple t-test (0.2 ± 0.6 mg m^{-2} h^{-1} for 1Px15L and 0.4 ± 0.9 mg m^{-2} h^{-1} for 5P x 3L, where uncertainty is the standard deviation). However, the large uncertainty on these averages emphasizes (1) the necessity for multiple leaf measurements, and (2) the high degree of variance in emissions across leaves and plants. Emissions vary over several orders of magnitude even within a single plant – and a single leaf can shift averaged VOC emission results. The high degree of variability in leaf-level monoterpene emissions is not necessarily reflected in plant photosynthetic metrics (e.g., stomatal conductance and CO_2 assimilation), which tend to show less intraplant variance than VOC emissions. We further note that emission variability differs between unstressed and stressed plants. Both the average limonene emission and variance associated with that average emission is significantly less in plants that have been drought-stressed (5P x 3L Drought, identical plants/leaves as 5P x 3L case, water withheld for 10 days beyond normal watering cycle) than well-watered (Figure 1.4).

3.2 Monoterpene isomers

VOCs can have structural isomers – molecules with the same elemental composition, but different structural arrangements of atoms. Structural isomers vary widely in their chemical properties and thus their atmospheric impacts. Monoterpenes ($C_{10}H_{16}$) provide particularly relevant examples of isomers in the atmosphere. Terpinolene and α-terpinene differ in structure only in the position of one of their double bonds (endo- and exo-cyclic, respectively), but terpinolene produces more SOA than α-terpinene upon oxidation with OH (up to 60x more SOA under certain conditions) (Friedman & Farmer, 2018). These chemical differences extend beyond SOA yield; monoterpene oxidation with OH also yields differences in oVOC products (Friedman & Farmer, 2018; Lee, Goldstein, Keywood, et al., 2006). These chemical differences in monoterpenes are often ignored in models to minimize computational expense by lumping all monoterpenes into a single representative system – typically α-pinene. However, different plants

emit isomers in different proportions, and those emissions and proportions may change in response to biotic (Faiola et al., 2019) and abiotic (Llusià & Peñuelas, 1998) stressors. Thus, a better understanding of the isomer-resolved differences in plant emissions of monoterpenes is essential for accurate prediction of atmospheric O_3 and SOA.

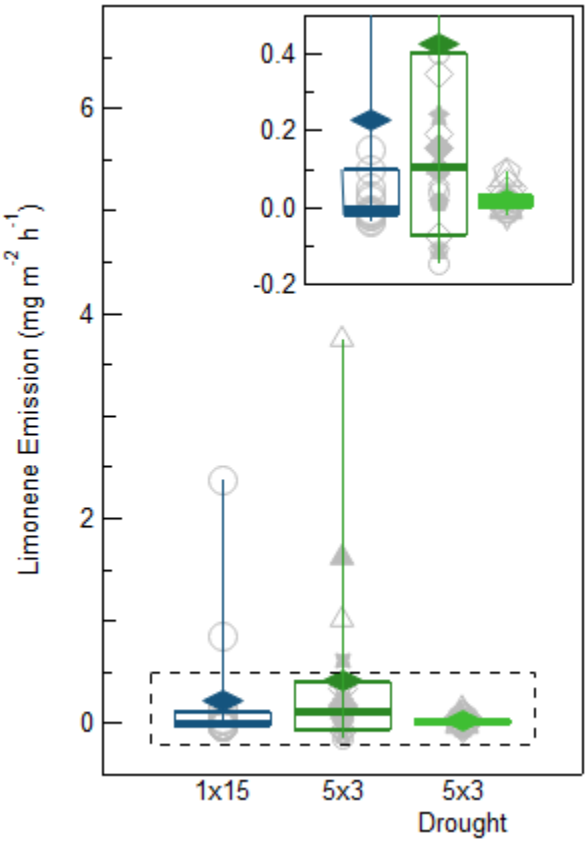

Figure 1.4. Box (25th, 50th, 75th percentiles) and whisker plots (0th and 100th percentiles) of the limonene emission variability in n=15 leaves of a single well-watered plant (1P x 15L); three leaves on each of five plants (5P x 3L); and the same leaves under drought conditions (5P x 3L Drought). The solid diamond represents averages. The insert highlights variability in 0th to 75th percentile region. Light grey open markers represent emission measurements from individual leaves, while grey marker shape indicates the plant identifier. Light grey closed markers represent the single-plant averages (n=3 leaves).

Figure 1.2 provides a compelling example of isomeric differences in relevant properties of myrcene, limonene, α-pinene and β-pinene. All are common biogenic monoterpenes with very different reactivities and properties. Myrcene and limonene have more double bonds than the pinene isomers and are thus more reactive. We do note that there are different approaches to measuring and reporting SOA yield from VOCs, which depend on oxidant, aerosol mass concentration, oxidant levels / reaction time, and presence of NO_x, but studies that investigate SOA yields of different monoterpene isomers, including ours, do consistently identify isomeric differences in yields.

3.3 Organic acids

While plants can emit oxygenated volatile organic compounds (oVOC) such as methanol, the bulk of the oVOC budget is formed in the atmosphere through multi-generational oxidation of biogenic hydrocarbons. We can consider four fates of oVOC: (1) further oxidation, which may contribute to O_3 production (or loss if oxidized by O_3), (2) partitioning and condensational growth of SOA, (3) dry deposition to surfaces, and (4) wet deposition. Thus, the removal of oVOC through deposition can influence the potential production of short-lived climate forcers.

Our work has aimed to understand sources and sinks of organic acids on several fronts. Formic acid is a particularly useful example molecule, as its sources have been widely investigated by multiple models. However, these models fail to capture diurnal trends in formic acid, consistent with underestimation of loss processes and potential overestimation of lifetimes.

Vertical gradient measurements of organic acids from the Boulder Atmospheric Observatory tower in the peri-urban environment of the Front Range of Colorado demonstrated persistent ground-level sources of several volatile organic acids (J. M. Mattila et al., 2018). Formic, propionic and butyric acids all showed higher mixing ratios near the ground than at 100 m above ground level - indicating emissions from a ground-level source through the day and night. In

contrast, pyruvic acid showed the opposite vertical profile, indicating a surface sink via dry deposition. The ground-level source of the smaller volatile organic acids is perplexing as the diurnal profiles show a rapid drop-off in gas-phase concentration in the afternoon and early evening. This diurnal profile is consistent with a relatively short lifetime driven by a loss process such as dry deposition. Soils are one potential source of these volatile organic acids: microbial activity (e.g. methanogenic bacteria) can produce formic acid, potentially causing substantial emissions. However, our lab measurements of soil emissions found that while both forest and managed soils in Colorado could release formic and acetic acids, the emission rates were too low to explain the observed vertical gradients - and would fail to impact model-measurement discrepancies on regional or global scales (Mielnik et al., 2018).

Consistent with the observed organic acid vertical gradients, our more direct eddy covariance measurements of volatile organic acid fluxes over a ponderosa pine forest in Colorado's Rocky Mountains showed persistent upward fluxes of volatile organic acids across multiple seasons (Fulgham et al., 2019). The fluxes showed a clear exponential dependence on temperature. Branch enclosures and soil chamber measurements failed to find adequate primary sources of these organic acids. In-canopy oxidation chemistry occurring below the height of our sensors provides a potential emission source. However, laboratory measurements of organic acid yields suggest that in-canopy formic acid production through OH oxidation and ozonolysis of monoterpenes is unable to fully explain the observed upward flux. Thus the underlying source of formic acid over forests remains 'missing', although overestimated dry deposition rates may be at least partially responsible for the flux budget discrepancies.

While oxidation chemistry in vertical gradients does not explain the observed fluxes on local scales due to the limited timescale for oxidation between monoterpene emission from leaves

and air moving through the plane of the sensor, this chemistry is still relevant on regional and global scales. Our laboratory chamber measurements indicate that isoprene oxidation alone could account for up to 70% of global formic acid (Link et al., 2020).

3.4 Reactive nitrogen oxides

Nitrogen deposition to the biosphere can provide an essential addition of nutrients - or a deleterious input of excess nutrient, acid or toxin to an ecosystem. For example, the addition of nitrogen in a remote forest can increase plant growth and thus CO_2 uptake, or it may cause plant damage and suppressed photosynthesis if the ecosystem is already saturated in nitrogen (Bobbink et al., 2010). Nitrogen can either be oxidized (e.g. nitric acid, particulate nitrate) or reduced (e.g. ammonia, particulate ammonium) when it deposits, and in either gas or particle phase. Long-term monitoring networks (e.g., the National Acid Deposition Program) provide insight on the trends and potential ecosystem impacts of deposition, but real-time observations are essential for understanding the mechanisms of particle deposition and interactions between different chemical components that influence ecosystem fluxes.

In-canopy chemistry is a particularly intriguing process that influences biosphere-atmosphere fluxes of nitrogen. Physical and chemical processes can change the form of molecules in the vertical space between biosphere surfaces and a sensor, thus creating a gradient in concentration and thus a spurious signal. For example, NO reacts with O_3 to form NO_2. If this reaction occurs in a forest canopy where soils are emitting NO but not NO_2, a forest flux measurement may detect a biosphere source of NO_2 - and spurious downward fluxes of O_3 and NO. Measurements by Goldstein and co-workers at Blodgett Forest in California showed clear evidence for VOC ozonolysis reactions influencing observed ozone deposition rates (Goldstein et al., 2004; Kurpius & Goldstein, 2003), while our measurements of reactive nitrogen oxides suggested that the subsequent oxidation chemistry could be rapid enough to influence the nitrogen

budget and form peroxy acyl nitrates ($R(O)ONO_2$) and nitric acid (HNO_3) within the forest canopy (Farmer & Cohen, 2008). While this extreme level of in-canopy chemistry has yet to be observed in other locations, the concept of rapid oxidation of reactive biogenic VOCs in forest canopies can been invoked to at least partially explain large fluxes of formic acid and other oxidized organic compounds from forests (Schobesberger et al., 2016; Wolfe et al., 2011).

3.5 Particles

Particle deposition to surfaces via wet and dry deposition is the key sink for atmospheric aerosols, controlling their lifetimes and thus potential impacts on climate. The single largest component of uncertainty in the role of particles in influencing climate is the loss rate of accumulation mode particles to the Earth's surface via dry deposition (Lee et al., 2013). While the impact on climate is largest over the ocean, the dry deposition of particles over the biosphere is poorly constrained by observations. The lack of measurements is driven by the challenge in making size-resolved particle measurements fast enough for eddy covariance flux analysis. Particle dry deposition is size-dependent, and driven by competing processes of Brownian diffusion, interception, impaction and gravitational settling (Slinn, 1982). Observational constraints on particle flux seem like an obvious way to validate these models, but chemistry can influence observed fluxes in complex ways.

In-canopy chemistry between VOCs and oxidants (O_3, OH or NO_3) can oxidize highly reactive VOCs, such as monoterpenes or sesquiterpenes, forming an array of products that are less volatile than their parent hydrocarbons. If the condensation of these products into SOA occurs in the forest canopy, this can create a vertical gradient in organic aerosol concentration that competes with vertical gradients induced by deposition processes. Further, gradients in temperature can cause partitioning of semi-volatile organic and inorganic components that also induce competing upward or downward fluxes. For example, well-enclosed forest canopies may be cooler lower in

the forest canopy than at the sensor height, which is usually several meters above the top of the canopy. Semi-volatile gases may condense onto particles in the forest canopy, thus inducing a vertical concentration gradient and apparent upward flux. Of course, open forest canopies may have thermal gradients that are warmer near the ground than at the sensor height and induce apparent downward particle fluxes.

Using aerosol mass spectrometry measurements of chemically-resolved particle fluxes over a ponderosa pine forest in California, we found that in-canopy oxidation of reactive terpenes produced enough SOA to compete with dry deposition and the thermal gradient-driven partitioning to cause an observed upward flux of organic aerosol from the forest (Farmer et al., 2013). While these observations mean that this particular forest can be considered a source of SOA to the atmosphere, we observed net deposition of total non-refractory submicron aerosol, indicating strong dry deposition of inorganic aerosol components. In contrast, our observations over a wet tropical forest in the Brazilian Amazon showed slight net deposition of total submicron aerosol, likely due to competing deposition and emission processes (Farmer et al., 2013). Several important themes have emerged from our investigations on particle fluxes: (1) competing processes impact observed particle fluxes including deposition, biological aerosol emission, in-canopy thermal gradients and subsequent SVOC partitioning, and in-canopy SOA formation; (2) chemically-resolved particle fluxes show clear differences - for example, less oxygenated organic aerosol tends to be emitted, while more oxygenated organic aerosol tends to deposit; and (3) wet deposition can be an important loss process for submicron aerosol, but is challenging to constrain as precipitation measurements contain both gas and aerosol components.

Black carbon is an inert tracer for particle deposition as it is unaffected by thermal gradients, in-canopy chemistry, or confounding wet deposition components of a gas-phase analog.

Recently, we used eddy covariance fluxes of black carbon to observe wet and dry deposition over a grassland site in Oklahoma. We observed refractory black carbon dry deposition velocities of 0.3 ± 0.2 mm/s by both mass and number, although substantial upward fluxes were observed; excluding upward fluxes resulted in much higher deposition velocities of 3.5 ± 0.3 mm/s by mass and 1.6 ± 0.3 mm/s by number (Emerson et al., 2018). This discrepancy raises a question that is persistent in the particle flux literature: are upward particle fluxes real? Upward particle fluxes have been observed from forests, but are often attributed to challenges with the eddy covariance micrometeorological technique, or the product of small near-zero fluxes (Lavi et al., 2013). In the case of black carbon, resuspension is the only likely source of upward fluxes, while for other aerosol types, gas-particle partitioning, aerosol formation, and biological aerosol sources may also contribute to observed particle emissions. Greater numbers of aerosol flux observations are essential for elucidating the driving processes behind these observed particle emissions.

However, the black carbon flux measurements provide additional insight on deposition of black carbon and the relative importance of wet and dry deposition. Comparing the observed wet and dry deposition fluxes, we find that dry deposition constituted only 6 ± 4% of total black carbon deposition at the site during the measurement period - though, the amount of precipitation and boundary layer height influence the relative proportion of wet and dry deposition (Emerson et al., 2018). These observations suggest lifetimes for black carbon of 30–90 days for dry deposition and 1–3 days for wet deposition - and a combined atmospheric lifetime of 7-11 days. These observationally constrained lifetimes are consistent with the model literature, which typically finds black carbon lifetimes of 5-11 days (Koch et al., 2009).

These particle flux observations collectively emphasize the role of dry deposition in influencing particle lifetimes. Obviously, the longer particles remain in the atmosphere, the greater

their potential radiative impact. Further observations to elucidate the competing processes that control particle fluxes from the terrestrial biosphere are essential for providing stronger constraints on these lifetimes - and for predicting how deposition rates will change over different land use types and under different climate conditions.

4. Conclusion

The biosphere is an important source and sink of reactive trace gases and particles, mediating the atmosphere through several feedbacks. Our approach to using detailed in situ chemical measurements to quantify fluxes and understand the underlying chemical processes has improved our understanding of in-canopy chemistry. However, using comprehensive measurements at single sites poses challenges in the generalizability of measurements. Despite the logistical challenges, expansion of biosphere-atmosphere interaction studies to multiple sites coupled to longer-term measurements is essential for understanding how the planet's surfaces interact with and influence atmospheric composition.

While observational constraints on deposition sinks or emission sources are essential for developing and validating models, flux measurements can be difficult to interpret. Observed fluxes over a canopy height represent the integral of all sources and sinks. For reactive trace gases, fluxes are the sum of direct emissions from or uptake to ecosystem surfaces, rapid in-canopy chemistry, and gas-particle partitioning along thermal gradients. Vertical gradients in size-resolved particle concentrations can be additionally influenced by vertical gradients in water vapor, which shift the particle size – and thus uptake by diffusion, impaction, interception, and gravitational settling processes. These complicating factors are often influenced by temperature, light, and relative humidity - parameters that simultaneously influence stomatal conductance and direct plant sources and sinks. Thus, measuring fluxes of reactive trace gases and particles is only the first part of the

biosphere-atmosphere interaction gauntlet; interpretation of the observations often requires models and supporting field and lab experimentation.

Emerging frontiers for research include a comprehensive understanding of the organic carbon (Millet et al., 2018) and nitrogen flux budget over ecosystems, ecosystem controls on ozone dry deposition (Clifton et al., 2020), and the potential role of feedbacks between the biosphere and atmosphere through reactive chemistry. For example, elevated ozone concentrations may increase emission of oVOCs (Beauchamp et al., 2005) and monoterpenes (Loreto et al., 2004), which in turn further contribute to the ozone and SOA production. Ultimately, measurements of biosphere-atmosphere exchange must be coupled to models to provide context and quantify the impact of the underlying exchange processes on radiative forcing - and how this will change under future land-use and climate conditions.

Support statement

We acknowledge the National Science Foundation for funding this analysis (NSF grant 1614315).

References

Abeleira, A. J., & Farmer, D. K. (2017). Summer ozone in the northern Front Range metropolitan area: weekend-weekday effects, temperature dependences, and the impact of drought. *Atmospheric Chemistry and Physics, 17*(11), 6517-6529.

Atkinson, R. (1997). Gas-phase tropospheric chemistry of volatile organic compounds: 1. Alkanes and alkenes. *Journal of Physical and Chemical Reference Data, 26*(2), 215-290.

Atkinson, R., & Arey, J. (2003). Gas-phase tropospheric chemistry of biogenic volatile organic compounds: a review. *Atmospheric Environment, 37*, S197-S219.

Baldocchi, D. D., Hicks, B. B., & Meyers, T. P. (1988). Measuring biosphere-atmosphere exchanges of biologically related gases with micrometeorological methods. *Ecology, 69*(5), 1331-1340.

Beauchamp, J., Wisthaler, A., Hansel, A., Kleist, E., Miebach, M., NIINEMETS, Ü., et al. (2005). Ozone induced emissions of biogenic VOC from tobacco: relationships between ozone uptake and emission of LOX products. *Plant, Cell Environ, 28*(10), 1334-1343.

Bobbink, R., Hicks, K., Galloway, J., Spranger, T., Alkemade, R., Ashmore, M., et al. (2010). Global assessment of nitrogen deposition effects on terrestrial plant diversity: a synthesis. *Ecological Applications, 20*(1), 30-59.

Bonn, B., Magh, R.-K., Rombach, J., & Kreuzwieser, J. (2019). Biogenic isoprenoid emissions under drought stress: different responses for isoprene and terpenes. *Biogeosciences, 16*(23), 4627-4645.

Brophy, P., & Farmer, D. K. (2016). Clustering, methodology, and mechanistic insights into acetate chemical ionization using high-resolution time-of-flight mass spectrometry. *Atmospheric Measurement Techniques, 9*(8), 3969-3986.

Carslaw, K. S., Boucher, O., Spracklen, D. V., Mann, G. W., Rae, J. G. L., Woodward, S., & Kulmala, M. (2010). A review of natural aerosol interactions and feedbacks within the Earth system. *Atmospheric Chemistry and Physics, 10*(4), 1701-1737.

Clifton, O. E., Fiore, A. M., Massman, W. J., Baublitz, C. B., Coyle, M., Emberson, L., et al. (2020). Dry deposition of ozone over land: processes, measurement, and modeling. *Rev Geophys*.

Copolovici, L. O., & Niinemets, Ü. (2005). Temperature dependencies of Henry's law constants and octanol/water partition coefficients for key plant volatile monoterpenoids. *Chemosphere, 61*(10), 1390-1400.

Emerson, E. W., Katich, J. M., Schwarz, J. P., McMeeking, G. R., & Farmer, D. K. (2018). Direct Measurements of Dry and Wet Deposition of Black Carbon Over a Grassland. *Journal of Geophysical Research-Atmospheres, 123*(21), 12277-12290.

Faiola, C. L., Pullinen, I., Buchholz, A., Khalaj, F., Ylisirniö, A., Kari, E., et al. (2019). Secondary organic aerosol formation from healthy and aphid-stressed Scots pine emissions. *Acs Earth and Space Chemistry, 3*(9), 1756-1772.

Farmer, D. K., Cappa, C. D., & Kreidenweis, S. M. (2015). Atmospheric Processes and Their Controlling Influence on Cloud Condensation Nuclei Activity. *Chemical Reviews, 115*(10), 4199-4217.

Farmer, D. K., Chen, Q., Kimmel, J. R., Docherty, K. S., Nemitz, E., Artaxo, P., et al. (2013). Chemically resolved particle fluxes over tropical and temperate forests. *Aerosol Science and Technology, 47*, 818-830.

Farmer, D. K., & Cohen, R. C. (2008). Observations of HNO_3, ΣAN, ΣPN and NO_2 fluxes: evidence for rapid HO_x chemistry within a pine forest canopy. *Atmospheric Chemistry and Physics, 8*(14), 3899-3917.

Farmer, D. K., & Jimenez, J. L. (2010). Real-time Atmospheric Chemistry Field Instrumentation. *Analytical Chemistry, 82*(19), 7879-7884.

Farmer, D. K., Kimmel, J. R., Phillips, G., Docherty, K. S., Worsnop, D. R., Sueper, D., et al. (2011). Eddy Covariance Measurements with High-Resolution Time-of-Flight Aerosol Mass Spectrometry: A New Approach to Chemically Resolved Aerosol Fluxes. *Atmospheric Measurement Techniques, 4*, 1275-1289

Farmer, D. K., Wooldridge, P. J., & Cohen, R. C. (2006). Application of thermal-dissociation laser induced fluorescence (TD-LIF) to measurement of HNO_3, Σalkyl nitrates, Σperoxy nitrates, and NO_2 fluxes using eddy covariance. *Atmospheric Chemistry and Physics, 6*, 3471-3486.

Fowler, D., Pilegaard, K., Sutton, M. A., Ambus, P., Raivonen, M., Duyzer, J., et al. (2009). Atmospheric composition change: Ecosystems-Atmosphere interactions. *Atmospheric Environment, 43*(33), 5193-5267.

Friedman, B., & Farmer, D. K. (2018). SOA and gas phase organic acid yields from the sequential photooxidation of seven monoterpenes. *Atmospheric Environment, 187*, 335-345.

Fu, D., Millet, D. B., Wells, K. C., Payne, V. H., Yu, S., Guenther, A., & Eldering, A. (2019). Direct retrieval of isoprene from satellite-based infrared measurements. *Nature Communications, 10*(1), 1-12.

Fuentes, J. D., Lerdau, M., Atkinson, R., Baldocchi, D., Bottenheim, J. W., Ciccioli, P., et al. (2000). Biogenic hydrocarbons in the atmospheric boundary layer: A review. *Bulletin of the American Meteorological Society, 81*(7), 1537-1575.

Fulgham, S. R., Brophy, P., Link, M., Ortega, J., Pollack, I., & Farmer, D. K. (2019). Seasonal flux measurements over a Colorado pine forest demonstrate a persistent source of organic acids. *Acs Earth and Space Chemistry, 3*(9), 2017-2032.

Goldstein, A. H., & Galbally, I. E. (2007). Known and unexplored organic constituents in the earth's atmosphere. *Environmental Science & Technology, 41*(5), 1514-1521.

Goldstein, A. H., McKay, M., Kurpius, M. R., Schade, G. W., Lee, A., Holzinger, R., & Rasmussen, R. A. (2004). Forest thinning experiment confirms ozone deposition to forest canopy is dominated by reaction with biogenic VOCs. *Geophysical Research Letters, 31*(22), L22106.

Heald, C., & Kroll, J. (2020). The fuel of atmospheric chemistry: Toward a complete description of reactive organic carbon. *Science Advances, 6*(6), eaay8967.

Heald, C. L., Goldstein, A. H., Allan, J. D., Aiken, A. C., Apel, E., Atlas, E. L., et al. (2008). Total observed organic carbon (TOOC) in the atmosphere: a synthesis of North American observations. *Atmospheric Chemistry and Physics, 8*(7), 2007-2025.

Kim, M., Farmer, D. K., & Bertram, T. H. (2014). Measurements of N2O5 and ClNO2 fluxes from the Scripps pier. *Proceedings of the National Academy of Sciences of the United States of America*, doi: 10.1073/pnas.1318694111.

Knote, C., Hodzic, A., & Jimenez, J. L. (2015). The effect of dry and wet deposition of condensable vapors on secondary organic aerosols concentrations over the continental US. *Atmospheric Chemistry and Physics, 15*, 1-18.

Koch, D., Schulz, M., Kinne, S., Bond, T., Balkanski, Y., Bauer, S., et al. (2009). Evaluation of black carbon estimations in global aerosol models. *Atmospheric Chemistry and Physics, 9*, 9001-9026.

Kurpius, M. R., & Goldstein, A. H. (2003). Gas-phase chemistry dominates O_3 loss to a forest, implying a source of aerosols and hydroxyl radicals to the atmosphere. *Geophysical Research Letters, 30*(7).

Lavi, A., Farmer, D. K., Segre, E., Moise, T., Rotenberg, E., Jimenez, J. L., & Rudich, Y. (2013). Fluxes of Fine Particles Over a Semi-Arid Pine Forest: Possible Effects of a Complex Terrain. *Aerosol Science and Technology, 47*(8), 906-915.

Lee, A., Goldstein, A. H., Keywood, M. D., Gao, S., Varutbangkul, V., Bahreini, R., et al. (2006). Gas-phase products and secondary aerosol yields from the ozonolysis of ten different terpenes. *Journal of Geophysical Research-Atmospheres, 111*, D07302.

Lee, A., Goldstein, A. H., Kroll, J. H., Ng, N. L., Varutbangkul, V., Flagan, R. C., & Seinfeld, J. H. (2006). Gas-phase products and secondary aerosol yields from the photooxidation of 16 different terpenes. *Journal of Geophysical Research-Atmospheres, 111*, D17305.

Lee, L. A., Pringle, K. J., Reddington, C. L., Mann, G. W., Stier, P., Spracklen, D. V., et al. (2013). The magnitude and causes of uncertainty in global model simulations of cloud condensation nuclei. *Atmospheric Chemistry and Physics, 13*, 8879–8914.

Link, M. F., Nguyen, T. B., Bates, K. H., Müller, J.-F., & Farmer, D. K. (2020). Can isoprene oxidation explain high concentrations of atmospheric formic and acetic acid over forests? *Acs Earth and Space Chemistry*.

Llusià, J., & Peñuelas, J. (1998). Changes in terpene content and emission in potted Mediterranean woody plants under severe drought. *Can J Bot, 76*(8), 1366-1373.

Llusià, J., Peñuelas, J., Alessio, G. A., & Estiarte, M. (2008). Contrasting species-specific, compound-specific, seasonal, and interannual responses of foliar isoprenoid emissions to experimental drought in a Mediterranean shrubland. *Int J Plant Sci, 169*(5), 637-645.

Loreto, F., Pinelli, P., Manes, F., & Kollist, H. (2004). Impact of ozone on monoterpene emissions and evidence for an isoprene-like antioxidant action of monoterpenes emitted by Quercus ilex leaves. *Tree physiology, 24*(4), 361-367.

Mattila, J. M., Brophy, P., Kirkland, J., Hall, S., Ullmann, K., Fischer, E. V., et al. (2018). Tropospheric sources and sinks of gas-phase acids in the Colorado Front Range. *Atmospheric Chemistry and Physics, 18*(16), 12315-12327.

Mielnik, A., Link, M., Mattila, J., Fulgham, S. R., & Farmer, D. K. (2018). Emission of formic and acetic acids from two Colorado soils. *Environmental Science: Processes & Impacts, 20*(11), 1537-1545. 10.1039/C8EM00356D.

Millet, D. B., Alwe, H. D., Chen, X., Deventer, M. J., Griffis, T. J., Holzinger, R., et al. (2018). Bidirectional ecosystem–atmosphere fluxes of volatile organic compounds across the mass spectrum: How many matter? *Acs Earth and Space Chemistry, 2*(8), 764-777.

Millet, D. B., Baasandorj, M., Farmer, D. K., Thornton, J. A., Baumann, K., Brophy, P., et al. (2015). A large and ubiquitous source of atmospheric formic acid. *Atmospheric Chemistry and Physics, 15*(11), 6283-6304.

Millet, D. B., Jacob, D. J., Boersma, K. F., Fu, T. M., Kurosu, T. P., Chance, K., et al. (2008). Spatial distribution of isoprene emissions from North America derived from formaldehyde column measurements by the OMI satellite sensor. *Journal of Geophysical Research-Atmospheres, 113*(D2).

Ortega, J., & Helmig, D. (2008). Approaches for quantifying reactive and low-volatility biogenic organic compound emissions by vegetation enclosure techniques - Part A. *Chemosphere, 72*(3), 343-364.

Paulot, F., Wunch, D., Crounse, J. D., Toon, G. C., Millet, D. B., DeCarlo, P. F., et al. (2011). Importance of secondary sources in the atmospheric budgets of formic and acetic acids. *Atmospheric Chemistry and Physics, 11*(5), 1989-2013.

Peñuelas, J., & Llusià, J. (2001). The complexity of factors driving volatile organic compound emissions by plants. *Biol Plant, 44*(4), 481-487.

Pöschl, U., Martin, S. T., Sinha, B., Chen, Q., Gunthe, S. S., Huffman, J. A., et al. (2010). Rainforest aerosols as biogenic nuclei of clouds and precipitation in the Amazon. *Science, 329*, 1513-1516.

Riches, M., Lee, D., & Farmer, D. K. (2020). Simultaneous leaf-level measurement of trace gas emissions and photosynthesis with a portable photosynthesis system. *Atmospheric Measurement Techniques*.

Schobesberger, S., Lopez-Hilfiker, F. D., Taipale, D., Millet, D. B., D'Ambro, E. L., Rantala, P., et al. (2016). High upward fluxes of formic acid from a boreal forest canopy. *Geophysical Research Letters, 43*(17), 9342-9351.

Scott, C. E., Monks, S. A., Spracklen, D. V., Arnold, S. R., Forster, P. M., Rap, A., et al. (2018). Impact on short-lived climate forcers increases projected warming due to deforestation. *Nature Communications, 9*.

Scott, C. E., Rap, A., Spracklen, D. V., Forster, P. M., Carslaw, K. S., Mann, G. W., et al. (2014). The direct and indirect radiative effects of biogenic secondary organic aerosol. *Atmospheric Chemistry and Physics, 14*(1), 447-470.

Slinn, W. G. N. (1982). Predictions for Particle Deposition to Vegetative Canopies. *Atmospheric Environment, 16*(7), 1785-1794.

Stavrakou, T., Muller, J. F., Peeters, J., Razavi, A., Clarisse, L., Clerbaux, C., et al. (2012). Satellite evidence for a large source of formic acid from boreal and tropical forests. *Nature Geoscience, 5*(1), 26-30.

Tarvainen, V., Hakola, H., Hellén, H., Bäck, J., Hari, P., & Kulmala, M. (2005). Temperature and light dependence of the VOC emissions of Scots pine. *Atmospheric Chemistry and Physics, 5*, 989–998.

Tingey, D. T., Manning, M., Grothaus, L. C., & Burns, W. F. (1980). Influence of light and temperature on monoterpene emission rates from slash pine. *Plant Physiology, 65*(5), 797-801.

Vong, R. J., Vong, I. J., Vickers, D., & Covert, D. S. (2010). Size-dependent aerosol deposition velocities during BEARPEX' 07. *Atmospheric Chemistry and Physics, 10*(12), 5749-5758.

Wilt, F. M., Miller, G. C., & Everett, R. L. (1993). Measurement of monoterpene hydrocarbon levels in vapor phase surrounding single-leaf pinyon (Pinus monophylla Torr. & Frem.: Pinaceae) understory litter. *Journal of Chemical Ecology, 19*(7), 1417-1428.

Wolfe, G. M., Thornton, J. A., Mckay, M., & Goldstein, A. H. (2011). Forest-atmosphere exchange of ozone: sensitivity to very reactive biogenic VOC emissions and implications for in-canopy photochemistry. *Atmospheric Chemistry and Physics, 11*, 7875-7891.

CHAPTER 2

SIMULTANEOUS LEAF-LEVEL MEASUREMENT OF TRACE GAS EMISSIONS AND PHOTOSYNTHESIS WITH A PORTABLE PHOTOSYNTHESIS SYSTEM[2]

Conspectus

Plants emit considerable quantities of volatile organic compounds (VOCs), the identity and amount of which vary with temperature, light and other environmental factors. Portable photosynthesis systems are a useful method for simultaneously quantifying in situ leaf-level emissions of VOCs and plant physiology. We present a comprehensive characterization of the LI-6800 portable photosynthesis system's ability to be coupled to trace gas detectors and measure leaf-level trace gas emissions, including limits in flow rates, environmental parameters, and VOC backgrounds. Instrument contaminants from the LI-6800 can be substantial but are dominantly complex molecules such as siloxanes that are structurally dissimilar to biogenic VOCs and thus unlikely to interfere with most leaf-level emissions measurements. We validate the method by comparing CO_2 assimilation calculated internally by the portable photosynthesis system to measurements taken with an external CO_2 gas analyzer; these assimilation measurements agree within 1 %. We also demonstrate both online and offline measurements of plant trace gas exchange using the LI-6800. Offline measurements by pre-concentration on adsorbent cartridges enable the detection of a broad suite of VOCs, including monoterpenes (e.g., limonene) and aldehydes (e.g., decanal). Online measurements can be more challenging if flow rates require dilution with

[2] Riches M, Lee D, Farmer DK. Simultaneous leaf-level measurement of trace gas emissions and photosynthesis with a portable photosynthesis system. Atmospheric Measurement Techniques. 2020 Aug 4;13(8):4123-39.

ultrapure zero air. We use high resolution time-of-flight chemical ionization mass spectrometry coupled to the LI-6800 to measure the direct plant emission of formic acid.

1. Introduction

Non-methane volatile organic compounds (VOCs) are readily oxidized in the atmosphere and thus impact atmospheric composition, climate and human health. As such, a quantitative understanding of VOC sources is essential for predicting future air quality and climate conditions. VOC oxidation impacts greenhouse gas mixing ratios by both producing tropospheric ozone and lowering OH radical mixing ratios, thereby increasing the lifetime of atmospheric methane (Kesselmeier & Staudt, 1999). Oxidized products of VOC precursors contribute to secondary organic aerosol (Faiola et al., 2018), which impacts climate and human health (Davidson et al., 2005; Pope III & Dockery, 2006). Biogenic emissions from plants dominate the global VOC source (Guenther et al., 1995; Lamarque et al., 2010; Lathière et al., 2006); terrestrial ecosystems and the ocean emit 1150 TgC yr^{-1} of VOCs globally (Guenther et al., 1995), relative to anthropogenic VOC sources, which account for only 142 TgC yr^{-1} globally (Singh, 1995). The most abundant group of biogenic VOCs (hereafter "BVOCs") are isoprenoids (Kesselmeier & Staudt, 1999), molecules comprised of $(C_5H_8)_n$ units. Isoprene (C_5H_8) contributes to roughly half of global BVOC emissions, while monoterpenes ($C_{10}H_{16}$) and sesquiterpenes ($C_{15}H_{24}$) account for an additional 18% combined (Guenther et al., 2012).

BVOC emissions are affected by a complex combination of factors, including temperature (Duhl et al., 2008; Sharkey & Yeh, 2001; Tarvainen et al., 2005a; Tingey et al., 1980), soil moisture (Ebel et al., 1995; Ormeño et al., 2007; Sharkey & Loreto, 1993), light (Owen et al., 2002; Sharkey & Loreto, 1993; Staudt & Seufert, 1995; Tarvainen et al., 2005a), CO_2 concentration (Francesco Loreto & Schnitzler, 2010; Wilkinson et al., 2009), plant developmental stage (Guenther, 1997; Holopainen, 2004; Kim et al., 2005; Zhang & Chen, 2009), mechanical

stress (Kaser et al., 2013; Markovic et al., 2016), and biotic stress (Mauck et al., 2010; Niinemets et al., 2013; Scala et al., 2013). While the effects of some environmental factors, such as temperature, are well-understood, the effects of other factors, such as CO_2 concentration, are less clear. Different VOCs also have different temperature responses, and different plant species have different temperature responses for the same VOC. While most VOC emissions increase exponentially with a linear increase in temperature (Niinemets et al., 2004; Peñuelas & Llusià, 2001b; Tingey et al., 1990) before reaching a maximum and rapidly decreasing (Grote et al., 2013), others are not sensitive with temperature (e.g., cis-β-ocimene) (Loreto et al., 1998). Temperature effects on VOC emissions are included in emission models, typically based on the results of short-term exposure experiments (Guenther et al., 2012; Guenther et al., 1993). Unlike temperature, the effect of changing CO_2 concentrations on BVOC emissions is under debate, even among plants of the same species (Loreto & Schnitzler, 2010). Under elevated CO_2 conditions, some studies observe no change in emissions (Constable et al., 1999; Kainulainen et al., 1998; Räisänen et al., 2008; Rapparini et al., 2003), while others observe a decrease (Sallas et al., 2003; Scholefield et al., 2004; Snow et al., 2003) or increase (Staudt et al., 2001) in VOC emissions relative to ambient CO_2. Despite its importance to atmospheric composition, biogenic VOC emission response to environmental change remains poorly understood.

Global emission inventories of BVOCs vary across models (Arneth et al., 2008; Grote et al., 2013). Monoterpenes are treated less consistently than isoprene: the standard deviation of monoterpene emissions across multiple emission models is 40% of the mean, compared to 10% for isoprene (Arneth et al., 2008). Emission models that group several VOCs together, such as the monoterpene isomers, may simplify the model, but this approach assumes that emissions are similar across the isomeric class and neglects differences in atmospheric reactivities of

compounds. For example, the lifetime for reaction with ozone between α-pinene and β-pinene differ between a few hours to a day (Atkinson & Arey, 2003), which consequently affects the SOA yield (Friedman & Farmer, 2018). Some models use plant photosynthesis to predict VOC emissions (Grote et al., 2013; Grote et al., 2014), though the correlation between plant physiology and VOC emission – let alone the response of these parameters to external environmental stressors – is not well understood. Model limitations are due, in part, to the limited availability of measurements, particularly simultaneous measurements of plant physiology and speciated VOC emissions.

VOC emissions are commonly quantified through canopy measurements (e.g., Ciccioli et al., 1999; Goldstein et al., 2004; Kaser et al., 2013; Rinne et al., 2007) and leaf or branch chamber headspace measurements (e.g., Guenther et al., 2000; Kessler & Baldwin, 2001; Komenda et al., 2001; Llusià et al., 2002). One approach to leaf-level studies couples a portable photosynthesis system (PPS) with a trace-gas analyzer, thus enabling simultaneous physiology and VOC emissions measurements (Brilli et al., 2007; Brilli et al., 2011; Geron, Owen, et al., 2006; Harley et al., 2014; Lerdau & Keller, 1997; Francesco Loreto & Velikova, 2001; Singsaas et al., 1999). The user can clamp the cuvette of the PPS onto a leaf and thereby control leaf-level parameters such as light wavelength and intensity, leaf temperature, humidity, airflow, and CO_2. Within the PPS, two infrared gas analyzers (IRGAs) determine the difference in gas concentration of CO_2 and water before and after the leaf cuvette. The system calculates physiological parameters including CO_2 assimilation rate (A), transpiration and stomatal conductance (for detailed calculations, refer to LI-COR, 2017). The CO_2 assimilation rate refers to the rate of photosynthetic CO_2 uptake into the leaf, transpiration is the rate at which water vapor is released from a leaf, and stomatal conductance is the rate at which CO_2 and water pass through the stomata of a leaf. Diverting the

PPS airflow to an external gas analyzer enables users to sample leaf emissions. Emissions analysis can be both *in situ* and real-time if online detection techniques are available, such as proton transfer reaction mass spectrometry (Brilli et al., 2007; PTR-MS; e.g. Brilli et al., 2011; Harley et al., 2014) or portable gas chromatography (e.g., Geron, Owen, et al., 2006; Lerdau & Keller, 1997; Loreto & Velikova, 2001; Singsaas et al., 1999). However, gas samples can also be collected for offline analysis by thermal desorption gas chromatography mass spectrometry (e.g., Geron, Owen, et al., 2006; Harley et al., 2014) and gas chromatography mass spectrometry canister analysis (e.g., Geron, Guenther, et al., 2006). These PPS-coupled techniques allow users to simultaneously obtain plant photosynthesis metrics and leaf-level VOC emissions.

While the PPS-VOC sampling technique has been used for decades, recent developments in PPSs provide new opportunities for leaf-level BVOC emission studies. The expanded ability to control environmental parameters, including leaf vapor pressure deficit, provides ample opportunity to study the connection between plant physiology and emission. However, PPSs have not been rigorously evaluated in the literature for leaf-level emissions. Here, we characterize the recently developed LI-6800 portable photosynthesis system for leaf-level emissions by quantifying the capabilities and limitations of this method. We investigate the instrumental limits of this approach, including acceptable flow rates and best practices. We demonstrate the utility of this technique for offline measurements using thermal desorption gas chromatography mass spectrometry and online measurements using time-of-flight chemical ionization mass spectrometry.

2. Instrumentation

We use a commercial portable photosynthesis system (LI-6800) with a Multiphase Flash™ Fluorometer (LI-COR, Nebraska) for CO_2 and H_2O gas exchange measurements. The PPS consists of two major components: the console, which includes the digital interface and the chemical

columns for control of air composition; and the head, which contains the 6 cm^2 leaf chamber and controls leaf temperature. The LI-6800 PPS controls environmental conditions at the leaf level, including: temperature, humidity, light intensity and wavelength, and CO_2. The PPS also controls airflow and fan speed. As described in the Introduction, the PPS uses IRGAs to detect gas concentrations of CO_2 and water from before (reference, REF) and after (sample, SAM) the leaf chamber. The LI-6800 PPS has ports on both of these sample lines; air collected from the REF subsampling port can be used as a system background for emissions that do not occur within the PPS itself, while air collected from the SAM port is representative of leaf emissions and the system background. In instances in which the analytes of interest are only emitted by plant tissue and not by the PPS, measurements taken from the REF port can be used to subtract the background from the SAM port samples.

We define our standard operating conditions in Table 2.1, along with the technical capabilities of the instrument and the acceptable range determined herein. We acquired response curves by altering a single environmental parameter (e.g., temperature), waiting for leaf photosynthesis (i.e., CO_2 assimilation) to stabilize to new conditions, and then collecting gas exchange and VOC measurements. To determine the parameters for photosynthesis stabilization, we monitored a leaf using the PPS for 20 min, and determined the natural variability in stomatal conductance and CO_2 assimilation. A standard deviation limit can be set for the stability parameters, but we found the natural variability in our citrus plants changes daily. Therefore, we determined stability using a limit on the slope of stomatal conductance (0.01 mol m^{-2} s^{-1} min^{-1}) and CO_2 assimilation (0.5 μmol m^{-2} s^{-1} min^{-1}) measurements over a 15 s period. Photosynthesis stabilization took anywhere from 30 s to 15 min, depending on how close the set environmental conditions were to ambient or prior conditions. Unless otherwise noted, we controlled the LI-6800

input gas stream with a CO_2 scrubber (soda lime, LI-COR 9964-090), desiccant (blue-indicating Drierite, LI-COR 622-04299), humidifier (Stuttgarter Masse, LI-COR 9968-165), and CO_2 (8 g cartridges, LI-COR 9968-227 and Leland 30404). The values for flow rate and chemical conditions are in Table 2.1; further details on the instrument specifications, including component precision, can be found in the instrument manual (LI-COR, 2017).

Table 2.1. User-defined standard, tested and operating conditions of environmental controls using the LI-6800.

	Chamber flow ($\mu mol\ s^{-1}$)	Chamber overpressure (kPa)	Fan speed (rpm)	RH (%)	Photon Flux Density[c] ($\mu mol\ m^{-2}\ s^{-1}$)	Temperature (°C)	CO_2 ($\mu mol\ mol^{-1}$)
Standard conditions	500	0.1	10000	50	750	25	400
Tested conditions[a]	0-1475	0.0-0.2	3000-14000	0-75	0-3000	10-38	0-2000
Operating conditions[b]	0-1400[d]	0.0 – 0.2	10000	0-90	0-3000	± 10 from ambient	0-2000[e]

[a] Provided values indicate the range at which the instrument functioned properly in conditions tested at 1.5 km above sea level, ~0.84 atm (8.6 kPa).
[b] Recommended operating values from (LI-COR, 2017).
[c] Saturating light conditions recommended for most uses. Operating range dependent on temperature, values shown are for 25 °C.
[d] At standard ambient temperature (25 °C) and pressure (100 kPa, 0.99 atm).
[e] Exact values limited on bulk flow rate, review (LI-COR, 2017) for further details.

Note that the LI-6800 denotes flow in terms of micromoles per second ($\mu mol\ s^{-1}$). All flows are given in liters per minute ($L\ min^{-1}$) we performed experiments at 1525 m above sea level and use an air pressure of 0.844 atm for conversion calculations when necessary.

The flow path of the PPS subsampling system is shown in Fig. 2.1. Ambient air is pulled into the PPS through the air inlet between 1.18 and 2.96 L min^{-1} (680-1700 μmol s^{-1}), and is then treated for humidity and CO_2. The bulk flow is automatically calculated by the PPS software to control the user-defined parameter for chamber airflow (described in Table 2.1). A subsample of this ambient air flows through the REF IRGA and when in use, the REF subsampling port, while the remaining air enters the leaf chamber. Air exiting the leaf chamber is split between the SAM subsampling port and the second SAM IRGA. Air from the SAM and REF IRGAs is removed as exhaust through the main exhaust line. During emissions sampling, the subsampling ports of the PPS can be simultaneously connected to trace gas analyzers, or alternated between a single analyzer with the other subsampling port closed. The air flow drawn out of the subsampling ports vary depending on emission sampling technique, and is described in more detail in Sect. 2.2.

The LI-6800 can be used with both online and offline emission sampling techniques. We use a chemical ionization mass spectrometer (CIMS) and an external CO_2 detector for online sampling, but we note that the principles of flow rate control are easily generalized for other trace gas analysis including PTR-MS. We use thermal desorption gas chromatography mass spectrometry for offline analysis. These systems are described in detail below.

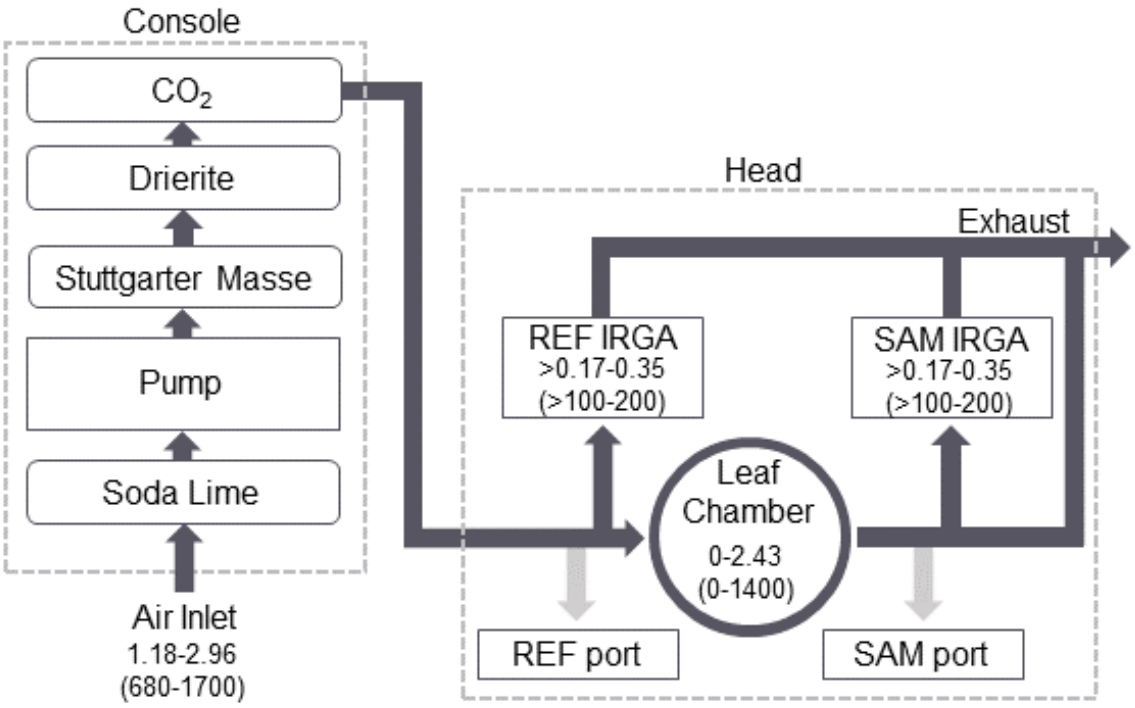

Figure 2.1. Flow chart diagram of air flow through the PPS during emissions sampling. Dashed lines delineate flow through the PPS console and the head. Dark grey lines show the flow through the PPS during photosynthesis measurements. Light grey lines indicate the additional flow path during emissions sampling. Values for flow rate are given in L min^{-1}, with μmol s^{-1} in parentheses. The order of the chemical treatment of air is shown for the console.

2.1 Portable Photosynthesis System

The PPS consists of the head (i.e., the device which clamps onto a leaf) (Fig. 2.2) and the console (i.e., the device which regulates environmental conditions and chemical use). The leaf chamber (Fig. 2.2A) was left unchanged while trace gas detector manifolds were connected to the SAM and REF subsampling ports (Fig. 2.2B and 2.C, respectively). A 3.175 mm brass hose barb fitting is attached to each of the subsampling ports, followed by a 38 mm piece of flexible tubing (Tygon™, 6.35 mm o.d., 3.175 mm i.d.) that connects to a 1/4" stainless steel tee (Ultra-Torr). On each of the remaining ports (one perpendicular (Fig. 2.2B_2, C_2) and one lateral (Fig. 2.2B_1, C_1), a 38 mm piece of polytetrafluoroethylene (PTFE) tubing (6.35 mm o.d., 3.175 mm i.d.) connects to

a 6.35 mm perfluoroalkoxy alkane (PFA) fitting. The PFA fittings are capped unless actively used. For sorbent tube sampling, a cap on the lateral port (Fig. 2B_1 for SAM, C_1 for REF) is replaced with a 6.35 mm fitting, and the sorbent tube (Fig. 2D) is fit directly in line. The external pump (Fig. 2E) is placed downstream of the tube and ensures constant flow through the sorbent tube.

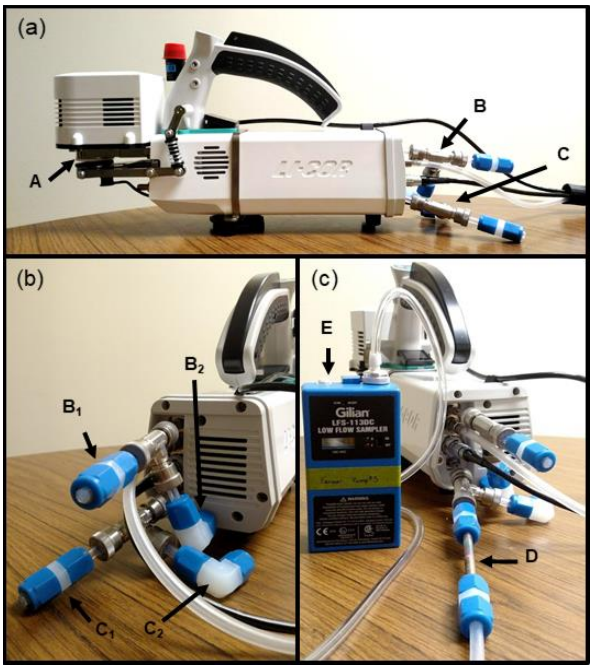

Figure 2.2. Photograph of the emissions subsampling manifold for the LI-6800. The profile view (a) highlights the leaf chamber (A), SAM subsampling port (B) and REF subsampling port (C). The back view (b), highlights the SAM and REF sampling ports (B_1 and C_1, respectively) and overflow ports (B_2 and C_2, respectively). Panel (c) shows an example setup of sorbent tube (D) emission collection with an external pump (E) sampling the REF subsampling port.

When subsampling the PPS air for BVOC emissions, an external pump subsamples air through the REF and/or SAM subsampling ports. The external pump ensures constant flow through the BVOC measurement system. The bulk flow through the system (F_I) is controlled by an internal pump in the console and any additional pumps used by trace gas analyzers on the REF or SAM subsampling ports. Thus the total air inlet flow is the sum of flows through REF port (F_R), SAM port (F_S) and the exhaust (F_E):

$$F_I = F_R + F_S + F_E \quad (1)$$

where F_E includes flow from the internal REF and SAM IRGAs. The IRGAs each require at least 0.17 L min^{-1} (100 μmol s^{-1}) - though a flow above 0.35 L min^{-1} (200 μmol s^{-1}) is preferential - and the inlet flow can be a maximum of 2.96 L min^{-1} (1700 μmol s^{-1}). Due to the instrumental limitations of these flows, sampling flows (F_R and F_S) must not reach so high as to interfere with PPS function. For thermal desorption sampling, whereby flow rates typically reach 0.2 L min^{-1}, samples can simultaneously be collected through both subsampling ports. The instrument will automatically calculate the split of flows between the IRGAs to account for system requirements. While higher flows (e.g., 1 L min^{-1}) can be sampled via the subsampling ports, the user will need to manually adjust the flow splits using the digital user interface on the console (LI-COR, 2017). Using higher flow rates to accommodate sampling from the SAM port will impact the flow through the leaf chamber, and thus the conditions experienced by the leaf tissue. The impact of increased flow rates should be investigated for individual species.

2.2 Online measurements: TOF-CIMS

The PPS trace gas sampling scheme described above is well-suited for online trace gas detection. Here, we use two systems: (1) a CO2 analyzer and (2) a high resolution time-of-flight chemical ionization mass spectrometer (TOF-CIMS; Aerodyne Research Inc. and Tofwerk AG) (Brophy & Farmer, 2015) coupled to iodide reagent ions (Lee et al., 2014) to detect gas-phase formic acid. Details of the TOF-CIMS are in S1.

For external comparison of leaf CO_2 exchange with the internal IRGAs, we use an external CO_2 analyzer (LI-840A, Li-Cor, Nebraska), which was alternately connected to the REF and the SAM subsampling ports. The LI-840A analyzer requires 1L min^{-1} of flow.

The TOF-CIMS pulls 1.9 L min^{-1}, exceeding the maximum threshold for the PPS subsampling ports. To decrease the flow, we dilute the subsampled air with 2.00 ± 0.05 L min^{-2} of

ultrahigh purity zero air (UZA; Airgas) at the inlet to the CIMS. The diluting flow is controlled by a mass flow controller (MKS Instruments, Mass Flo® Controller, 1179B).

We calculate formic acid emission rates as follows:

$$C_P = C_C * \frac{Q_C}{Q_P} \quad (2)$$

where C_P is the mixing ratio of the VOC coming from the PPS (mol mol^{-1}), C_C is the mixing ratio of the VOC identified by the CIMS (mol mol^{-1}), Q_C is the total flow pulled by the CIMS (L min^{-1}), and Q_P is the flow taken from the PPS subsampling port (L min^{-1}). To get C_C, a calibration is used to convert integrated peak area into concentration; the resulting value is then divided by the time over which the integration occurred.

We then convert the leaf chamber flow (Q_L) from liters per minute (L min^{-1}) to moles per minute (mol min^{-1}) using:

$$Q_L(mol\ min^{-1}) = \frac{Q_L(L\ min^{-1}) * P}{R * T} \quad (3)$$

where P is atmospheric pressure, R is the gas constant, and T is air temperature. Using Eqs. (2) and (3), we obtain:

$$E_{VOC} = \frac{C_P * Q_L}{S} \quad (4)$$

where E_{VOC} is the VOC emission rate (mol m^{-2} min^{-1}), and S is the leaf area (m^2).

2.3 Offline measurements: sorbent tubes

Thermal desorption (TD) gas chromatography mass spectrometry (GC/MS) is an offline sampling technique commonly used to sample atmospheric volatile and semi-volatile organic compounds (Harper, 2000). This technique pre-concentrates trace gases on sorbent tubes, which are stainless steel or glass tubes of specific dimensions that are filled with adsorbent materials. Different adsorbents target different analytes. Tenax TA is a general adsorbent, which has a

sampling range of 7 to 26 carbons (C_7-C_{26}), and is relatively hydrophobic (Dettmer & Engewald, 2002). Other adsorbents, such as carbon molecular sieves (e.g., Carboxen 563) collect smaller molecules (C_2-C_5), but are sensitive to atmospheric humidity (Dettmer & Engewald, 2002). As air flows through the sorbent tubes, atmospheric constituents adsorb onto the surface. The tubes are then rapidly heated, and the compounds thermally desorbed into an airstream for analysis by GC/MS. Here we use an autosampler (Ultra-xr, Markes Intl.) and thermal desorption unit (Unity-xr, Markes Intl.) coupled to a gas chromatograph (TRACE 1310, Thermo Scientific) mass spectrometer (TSQ 8000 Evo Triple Quadrupole GC-MS/MS, Thermo Scientific).

Details of the TD-GC/MS method are in Sect. S2. Briefly, we use the TD-GC/MS with Tenax adsorbent cartridges to quantify seven monoterpenes, summarized in Table 2.2.

Table 2.2. Summary of monoterpenes quantified using TD GC/MS.

Compound ($C_{10}H_{16}$)	RT [a] (min)	RSD [b] (%)	LOD [c] (ng)	Emission Rate LOD [d] (ng m^{-2} min^{-1})
α-pinene	3.716 ± 0.008	8.2	0.137	11.4
β-pinene	4.44 ± 0.01	7.4	0.082	6.8
α-terpinene	5.173±0.008	4.5	0.071	5.9
p-cymene	5.354±0.009	5.6	0.111	9.2
d-limonene	5.47±0.01	3.5	0.054	4.5
γ-terpinene	6.306±0.009	2.4	0.085	7.1
terpinolene	7.35±0.01	2.6	0.050	4.2

[a] Retention time
[b] Relative standard deviation (n=10)
[c] Limit of detection, calculated using the propagation of errors approach (Bernal, 2014)
[d] Based on a 20 min sampling time

We calculate leaf-level VOC emissions from the cartridge samples as follows:

$$E_{VOC} = \frac{m_{VOC} * Q_L}{V * S} \quad (5)$$

where E_{VOC} is the VOC emission rate (ng m^{-2} min^{-1}); m_{VOC} is the mass of the VOC (ng), as determined by the thermal desorption calibration; Q_L is the flow through the leaf chamber (L min^{-1}); V is the total volume of air sampled with the sorbent tube (L), sampling flow multiplied by sampling time; and S is the leaf surface area (m^2). For all measurements in this paper, we selected leaves that filled the chamber, for a total measured leaf area of 6 cm^2. However, this technique is still applicable for leaves that do not fill the chamber due to size or shape; for such leaves, leaf area must be determined separately (e.g., via image processing (Chaudhary et al., 2012), or via calculations based on geometric measurements (Sellin, 2000)).

2.4 Sampling protocol

The sampling protocol involves clamping the PPS leaf chamber onto a leaf, waiting for the leaf to adapt to the leaf chamber conditions, collecting trace gas measurements from the SAM and REF subsampling ports, and then either removing the leaf chamber and moving to a new leaf (single emission point), or changing the environmental conditions to investigate leaf-level emission responses to temperature, light, relative humidity, or CO_2 (Table 2.1). Photosynthesis may be measured simultaneously at any point in the sampling protocol and is independent of emission measurements.

Once the PPS has undergone its standard warm-up (≤45 min), we set the PPS to the standard environmental conditions and allow the instrument to equilibrate without a leaf present, with the leaf chamber closed (<15 min; the further the ambient conditions deviate from standard conditions, the longer the instrument takes to equilibrate). We match the IRGAs to one another (LI-COR, 2017) prior to collecting an emissions measurement, when the CO_2 or humidity values

change or within an hour since the last match. To collect a system background ("blank"), we connect a sorbent tube to the SAM subsampling port and use an external handheld pump to sample emissions (0.2 L min^{-1}; 20 min). The tube is then removed, and the subsampling port capped. To sample leaf emissions, we enclose a leaf in the PPS chamber and allow the leaf to acclimate at standard conditions (30 s to 35 min). A sorbent tube and external pump connected to the SAM subsampling port sample the leaf emissions (0.2 L min^{-1}; 20 min). For CIMS measurements, we collect a system blank from the PPS (no leaf) by sampling the SAM subsample port for at least 5 min (at 1 Hz). After enclosing the leaf in the PPS chamber, we monitor the stability of both photosynthesis and volatile emissions. We typically find that the leaf and detector system require at least 5 min to stabilize.

If there are no internal sources or sinks to the VOCs of interest (or these interactions are quantifiable), gas measurements may be simultaneously taken from both the REF and SAM subsample ports (with flow considerations, as described in Sect. 2.1). With this method, REF measurements provide the background for subtraction from the SAM emissions measurements.

At this point, users may make continuous measurements, survey measurements, or response measurements. A continuous measurement allows for the subsequent measurement of the same leaf tissue at the same environmental conditions (i.e., one leaf throughout the day). A survey measurement allows for the measurement of multiple leaves under one set of environmental conditions (i.e., sampling emissions from multiple leaves on the same plant). Importantly, each time a leaf is physically placed in the PPS chamber, it requires time (30 s – 35 min, depending on environmental conditions) to acclimate. A response measurement allows for the measurement of a single leaf at different environmental conditions (e.g., sampling emissions as a function of temperature).

Leaves must acclimate to new environmental conditions. However, the time required for a leaf to adapt to placement in the chamber or changing environmental conditions is inconsistently reported in leaf-level photosynthesis studies. Some studies allow leaves to acclimate until photosynthesis reaches stability or steady-state (e.g., Bunce, 2008; Domurath et al., 2012), though those terms are often undefined. Some studies use an upper (e.g., Yang et al., 2010) or a lower (e.g., Lang et al., 2013) time limit to allow photosynthesis to reach stability. When exact equilibration times are mentioned, they vary greatly between perturbations and between studies. For emissions measurements, equilibration times of both photosynthesis and BVOC emission must be considered. Using the CIMS, we determined that it takes 10-15 min for both photosynthesis and formic acid to reach stability after being clamped or after an environmental change.

We investigated the potential for VOCs in the leaf chamber to persist from one experiment to another, after the leaf has been removed, through adsorption on gaskets or chamber surfaces ("carryover"). Carryover can cause spuriously high emission measurements. To investigate carryover, we collected a system blank (no leaf present; SAM port) before introducing a ponderosa lemon (*Citrus limon x Citrus medica*) leaf into the chamber for the next 8 hours at varying temperatures. We observe no consistent evidence that longer periods in the leaf chamber impact photosynthesis or VOC emission. Citrus is believed to influence regional atmospheric chemistry due to their VOC emissions (Hodges & Spreen, 2006; Park et al., 2013). As a cocktail-sized, slow-growing plant with large leaves, this species was suitable for laboratory and greenhouse experiments. Immediately after removing the leaf at the end of the day, we collected a second system blank (no leaf present; SAM port).

We observed no carryover of monoterpenes (α-pinene, β-pinene, limonene, cis-β-ocimene, or γ-terpinene) or caryophyllene. The only identifiable plant emissions with observable signal (%

of initial, i.e., leaf in chamber) that persisted after the leaf was removed were citral (27%) and 2-ethyl-1-hexanol (92%).

We also observed carryover of long-chain acids including palmitoleic acid (49%), pentadecanoic acid (47%), hexadecanoic acid (85%) and oleic acid (88%). Squalene (89%) also had substantial carryover. These compounds could have been introduced via the cuticular wax of leaves (Fernandes et al., 1964) or through human contact. However, these signals appear at retention times between 15 and 17 min and are thus unlikely to interfere with the signals of more volatile species.

Volatility likely plays a role in the carryover of compounds. Squalene, citral, and the long-chain acids have lower volatility than the monoterpenes. However, 2-ethyl-1-hexanol is of similar volatility to the monoterpenes yet persists after the leaf has been removed. Carryover should thus be investigated for specific compounds prior to extensive studies.

2.5 Leaf chamber conditions

The PPS control of environmental conditions enables the acquisition of short-term response curves for trace gas emissions, which are typically used to parameterize biogenic VOC emissions in atmospheric chemical transport models. Table 2.1 summarizes the ranges in parameters we find to be feasible for each environmental parameter.

The PPS regulates CO_2 and light well. However, both temperature and humidity regulation in the PPS depend on the balance between the ambient and desired conditions. Relative humidity (RH) is constrained so as to not reach condensing conditions, so the extent of RH control depends on the temperature of the leaf chamber. For example, when aiming for high PPS temperatures (>30 °C), the PPS can have difficulty simultaneously maintaining high (>50 %) RH. When ambient temperatures are low (<4 °C), the PPS is challenged to maintain RH >35 %. This instrumental challenge occurs because temperature control in the PPS is limited by the heat exchanger; as the

heat exchanger approaches the dew point, the PPS takes proactive measures and slows the heating or cooling of the system. We find two approaches to deal with PPS temperature and RH problems: (i) temperature may be set independently of humidity, or (ii) temperature may be ramped slowly while humidity is maintained.

Of all the controllable environmental conditions, temperature takes the longest for the PPS to regulate (10 ± 2 min to warm an empty chamber from 18 to 33 °C). Cooling takes twice as long as heating and introducing a leaf into the chamber increases time necessary to cool by 35 % and time necessary to heat by 26 %. External fans improved the chamber temperature control at higher ambient temperatures, as did placing ice packs beside the air-inlet, around the chemical tubes, beside the leaf chamber, and on the side of the head.

The LI-6800 also enables direct control of the leaf vapor pressure deficit but achieving a large dynamic range in vapor pressure deficit is subject to the same constraints as simultaneously changing temperature and RH in the PPS.

3. Internal PPS versus external CO_2 measurements

The LI-6800 PPS internally measures leaf-level CO_2 exchange with the SAM and REF IRGAs as a core measurement, providing CO_2 assimilation (μmol m^{-2} s^{-1}). Assimilation provides a useful metric of validation against external leaf-level emissions, and we compare leaf-level CO_2 assimilation measured internally by the LI-6800 PPS and externally through the subsampling manifold and an external CO_2 analyzer. Here, we used the CO_2 assimilation of a basil leaf (*Ocimum basilicum*) to verify that the use of an external subsampling port supports the same values as the PPS's internal IRGA systems.

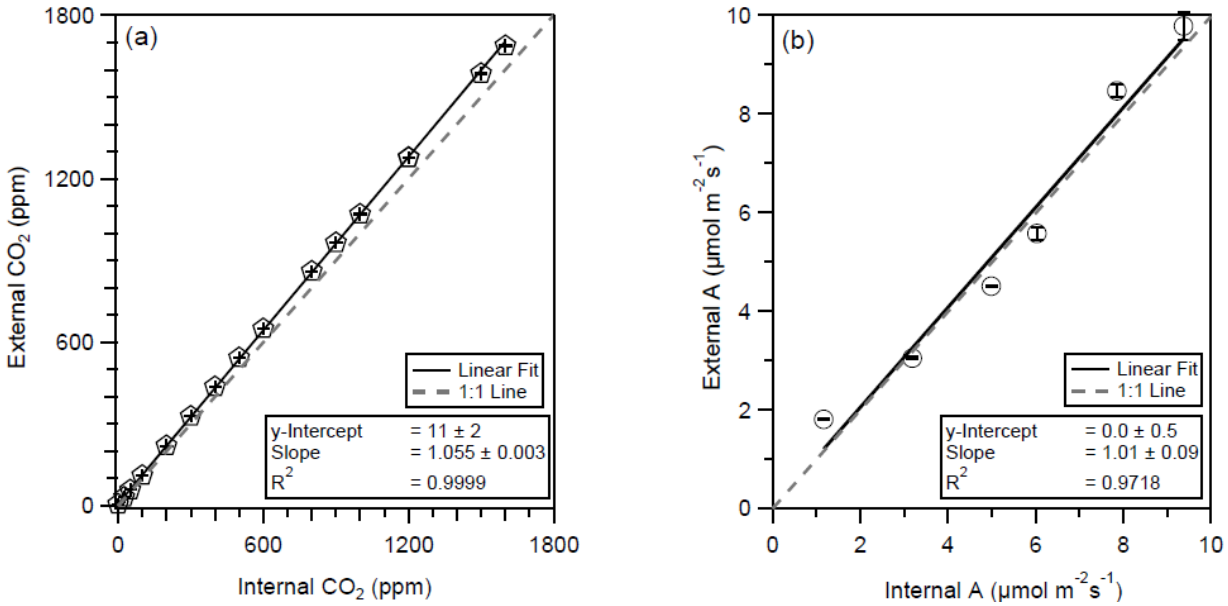

Figure 2.3. Correlation plots of CO_2 mixing ratio (pentagons, left panel) and CO_2 assimilation (A, circles, right panel) as calculated internally by the PPS (x-axis) and externally by the CO_2 analyzer (y-axis). A 1:1 line is present as a grey, dashed line. Linear regression fit is shown with a solid line, and fit parameters accompany in text, ± standard error of the fit. Error bars represent the standard deviation of values.

We connected an external CO_2 analyzer (LI-840A, LI-COR, Nebraska) to the PPS (no leaf) and varied the CO_2 mixing ratio to determine the sensitivity of external CO_2 measurements (using the LI-840A) with the internal LI-6800 CO_2 measurements. The LI-6800 can control the CO_2 mixing ratio in one of two locations: before (REF) or in (SAM) the leaf chamber. First, we compare CO_2 measurements between the internal (LI-6800) and external (LI-840A) CO_2 analyzers. We internally controlled the REF CO_2 mixing ratio and measured the subsequent CO_2 mixing ratio externally though each subsampling port. We then controlled the SAM CO_2 mixing ratio and repeated the external measurements. All comparison experiments showed a strong correlation between internal and external CO_2 measurements ($r^2 > 0.9999$). The controlled CO_2 mixing ratio for both experiments ranged from 0 to 1600 ppm. We found that the external CO_2 measurement was 5.5 % higher than the internal measurement, which we attribute to systematic differences in

instrument calibration (Fig. 2.3). We find no evidence of leaks at below-ambient CO_2 mixing ratios.

We then compared CO_2 assimilation (sampling with leaf) between the internal PPS determination and the external measurements accounting for observed flows. This external CO_2 assimilation measurement and calculation approach parallels our coupled PPS+online sampling trace gas measurement, and provides validation of the sampling approach. For CO_2 assimilation comparisons, we controlled the SAM CO_2 mixing ratios and monitored the REF CO_2 mixing ratios externally. We accounted for the calibration offset between internal and external CO_2 detectors. With the external CO_2 analyzer connected to the REF subsampling port and a leaf in the chamber, we set the PPS CO_2 mixing ratio to 200, 400, 600, 800, and 1000 μmol CO_2 mol^{-1}. The PPS measured photosynthesis 10 times within 10 min while we externally monitored CO_2 mixing ratios from the REF port (1 Hz).

We calculate CO_2 assimilation (A) as:

$$A = \frac{Q_{L,c} * \left([CO_2]_R - [CO_2]_S * \frac{1 - [H_2O]_{R,c}}{1 - [H_2O]_{S,c}} \right)}{S} \quad (6)$$

(adapted from LI-COR, 2017) where $Q_{L,c}$ is the flow through the leaf chamber (μmol s^{-1}), multiplied by the leak correction factor (unitless, provided by the PPS); $[CO_2]_R$ and $[CO_2]_S$ are the mixing ratios of CO_2 (μmol mol^{-1}), as determined by the REF and SAM infrared gas analyzers, respectively; $[H_2O]_{R,c}$ and $[H_2O]_{S,c}$ are the mixing ratios of H_2O (mol mol^{-1}), as determined by the REF and SAM infrared gas analyzers, respectively; and S is the leaf area (m^2). We take $[H_2O]_{R,c}$ and $[H_2O]_{S,c}$ from the LI-6800.

The internally and externally calculated CO_2 assimilations correlate well ($r^2 = 0.97$) with 1 % difference between the two approaches (Fig. 2.3).

4. Trace gas background in the PPS

Background contamination reduces analyte signal accuracy. Co-eluting peaks in a gas chromatogram add additional difficulty in determining the exact peak area of a VOC analyte. When a chromatogram features heavy background contamination from a system, the chromatograms can become busy, challenging untargeted peak identification. Here we investigate the background VOCs in the PPS.

The REF port can be measured simultaneously with the SAM port to provide a background measurement of air entering the leaf chamber, but not any internal PPS sources of interference in the leaf chamber.

The PPS is made of materials that can emit volatile compounds. While the PPS background may not contribute substantial background signals when using certain targeted analytical techniques (e.g., selected ion monitoring GC/MS), untargeted techniques, such as full scan GC/MS, are susceptible to background interference. TD-GC/MS chromatograms of the PPS (no leaf, 30 °C) revealed substantial background contamination, especially compared to the background of the Tenax tubes themselves (Figs. 2.4 and 2.6). The total integrated ion counts of identifiable peaks were 49 % higher background from the SAM port versus the REF, highlighting the problem of only using the REF port as a background for VOC analysis. These peak counts are substantially higher (by ~80 %) than the blank Tenax sorbent tube itself. The primary differences in the integrated peak area between SAM and REF are due to the five largest peaks, three of which are siloxanes. Siloxanes are commonly used in consumer products, including textiles, cosmetics, paint, and electronics (Fromme, 2018; Tilley & Fry, 2015), and were 41 % higher in the SAM than REF ports. The other two largest peaks are isobornyl acrylate (a film-forming agent) and n-

octyl acrylate (an adhesive and coating component). While unlikely to interfere with leaf VOC emissions, co-elution with these peaks may lead to unidentified emissions in untargeted approaches. As a result of this work, we recommend taking frequent backgrounds from the SAM port to ensure no chamber background interference for analytes of interest.

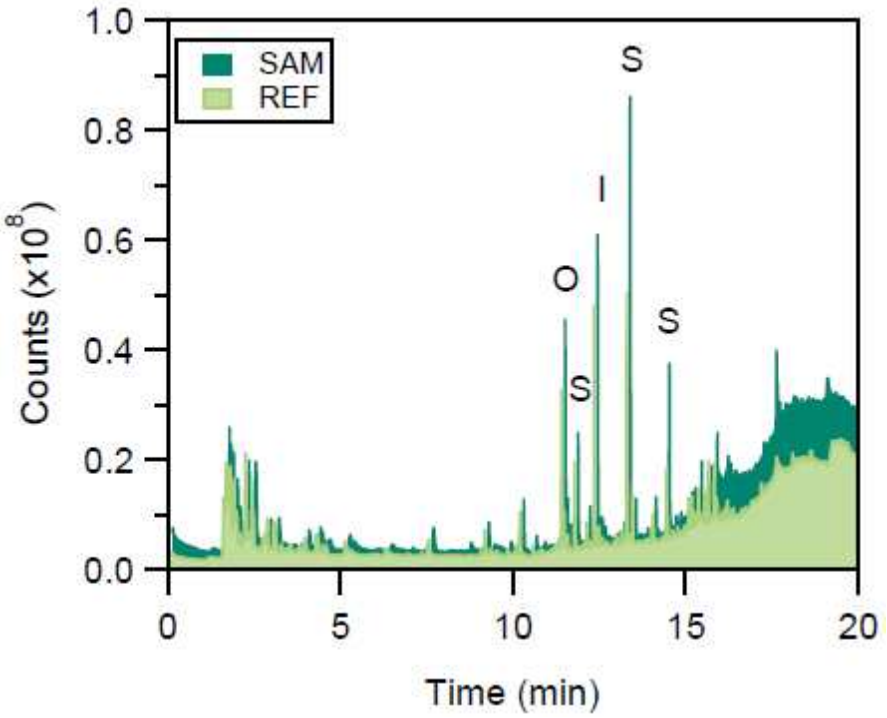

Figure 2.4. Stacked chromatograms of the background composition of the LI-6800, comparing measurements taken from the REF (light green) and SAM (dark green) ports as sampled by TD-GC-MS (20 minutes at 0.2 L min^{-1}, sampled on Tenax cartridges). The five largest peaks are labeled: S is the result of a siloxane, I is that of isobornyl acrylate and O is of n-octyl acrylate.

Figure 2.5 categorizes the signals from the SAM background by functional groups, highlighting the complexity and potential interference for biogenic trace gas emission analysis. The large background signals caution against using bulk signal measurements (e.g., total observed carbon, or total observed reactivity) from the PPS without careful background analysis. Instead, targeted approaches like extracted ion chromatography (EIC) are a promising way to exclude spurious background signals. Figure 2.6 highlights the differences between the full chromatogram

(total ion counts) and an EIC, for which we selected for monoterpenes. This approach clearly separates leaf-emissions that are not present in the blank, including β-pinene (4.210 min), limonene (5.175 min) and β-ocimene (5.561 min). By minimizing background contamination with EIC, we clearly observe differences between strongly- and weakly-emitting leaves (Fig. 2.6). Therefore, we recommend an EIC approach for the semi-targeted identification and analysis of monoterpenes and aldehydes.

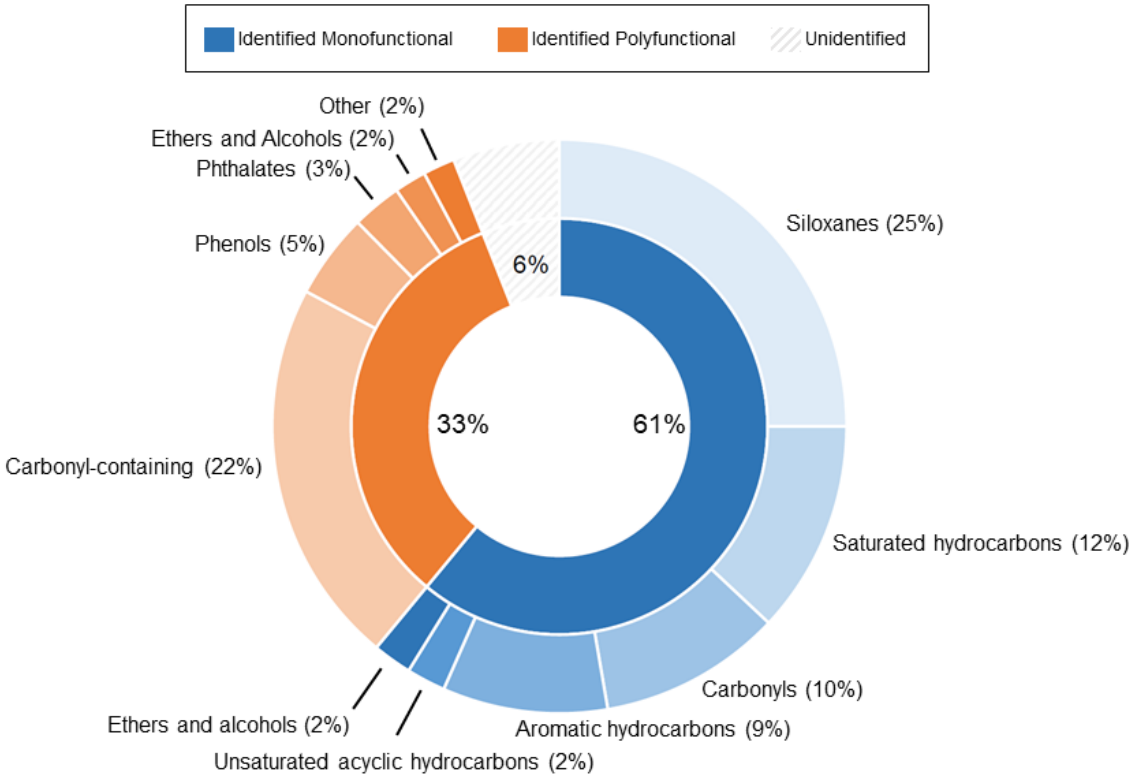

Figure 2.5. Pie chart summarizing the background composition of the LI-6800 with no leaf in the chamber, collected using the SAM port of the PPS. Percentages are provided to indicate the contribution of each class of compounds to the total integrated peak area. The inner pie chart shows the division of total ion counts for identified monofunctional (containing a single functional group), identified polyfunctional (containing multiple functional groups) and unidentified (yellow stripes) peaks. Identification required an integrated peak area over 50,000 counts and a NIST library match score of at least 500. The outer pie chart shows the subsequent breakdown of both identified classes.

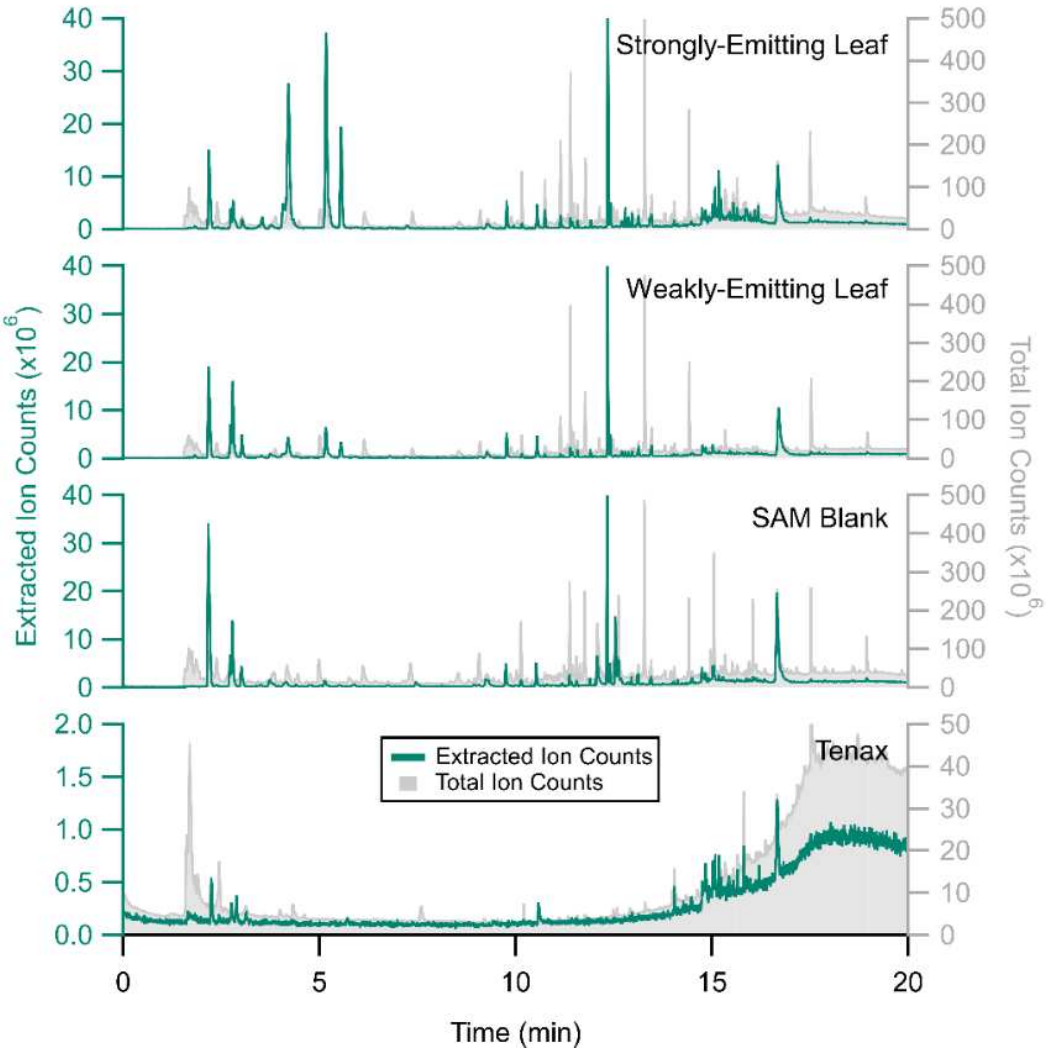

Figure 2.6. Stacked chromatograms comparing extracted ion chromatograms (EIC using *m/z* 136, 135, 93 and 91, left, in green) with the total ion chromatogram (TIC, right, in grey) for a Tenax blank, a SAM blank, a weakly- and a strongly- emitting citrus leaf (*Citrus limon* × *Citrus medica*). Note the difference in axis scales between EIC and TIC. While several background peaks remain in the EIC, there are substantially fewer in the 10+ minute range. Peak height of EIC isobornyl acrylate (RT = 12.3 min) in has been truncated. Note that retention times differ from Table 2.2; the column length had been shortened by the time of these measurements.

We investigated three approaches to minimizing the PPS backgrounds. We replaced the Drierite desiccant with silica gel orange (Sigma-Aldrich, 13767-2.5KG-R) and the Stuttgarter Masse humidifier with Perlite (Miracle Gro®, 74278430). We also installed fresh air filters at each chemical column, IRGA and the air-inlet. After each change, we flushed the system with heated

air (35 °C at a flow rate of 1300 μmol s^{-1} for 30 min) before collecting system blanks under standard conditions, but none of these changes substantially decreased the background signals (Fig. 2.S1 in the Supplement).

The air entering the PPS is ambient, and thus prone to change throughout the day as sources and sinks vary. While the PPS includes several filters within the system, they do not filter all biogenic hydrocarbons – including monoterpenes. This is a particular problem in greenhouses, where low exchange rates, warm temperatures and large concentrations of plants lead to high ambient biogenic VOC emissions. We investigated the potential to filter monoterpenes from inlet air at the Plant Growth Facilities at Colorado State University. We added a home-built charcoal filter (30.5 cm piece of 85 cm o.d. stainless steel tubing filled with activated charcoal Norit (®, Sigma-Aldrich, 29204-500G) and filtered with glass wool and stainless-steel mesh on either end) to the air inlet of the PPS. This filter completely removed all background α-pinene from 0.04 ppb to below detection limit but was less effective in subsequent outdoor experiments. As the ambient concentration of VOCs varies with time of day, we recommend using a charcoal filter and taking simultaneous REF and SAM measurements to account for interference from input air. Alternately, zero air can replace ambient input air at the PPS inlet, per manufacturer's instructions (LI-COR, 2017).

5. Case studies

Despite this background interference, the LI-6800 has the potential to investigate plant gas exchange for an array of molecules with an array of trace gas instrumentation. Here, we provide case studies with both online (Sect. 5.1; CIMS) and offline (Sect 5.2 and 5.3; TD-GC-MS) analysis. TD offers the benefit that the sorbent tubes are easily portable, though sample collection and analysis are time intensive. CIMS offers the benefit of online, real-time data acquisition, however the instrument itself is less portable and provides no definitive compound identities.

These case studies maintained standard conditions unless otherwise noted, and each study used different plants. Further information on plant growth conditions can be found in Sect. S4.

5.1 Formic acid emissions

Organic acids account for roughly 25 % of global non-methane VOCs (Khare et al., 1999) and contribute to secondary organic aerosol (Yatavelli et al., 2014). Despite their ubiquity, models typically underestimate ambient concentrations of formic acid, even the structurally simplest of organic acids, implying a missing source (Alwe et al., 2019; Paulot et al., 2011). This missing source of formic acid is not soils (Mielnik et al., 2018), but flux studies (Fulgham et al., 2019) and vertical gradient measurements (Mattila et al., 2018) suggest a direct ecosystem source. Here we demonstrate the capacity of the PPS coupled to a CIMS system to investigate leaf-level organic acid sources from *Mentha spicata* (spearmint), a culinary herb of economic importance due to the production of its essential oil.

We generated a temperature response curve on a spearmint leaf connected to the PPS with a CIMS detector. We generated three temperature response curve replicates, each with temperatures varying from 21 to 35 °C. The leaf was acclimated (as described in Sect. 2) at each new temperature for at least 5 min, during which time the CIMS sampled the REF port to determine the system background. We then simultaneously measured leaf-level emissions of formic acid and photosynthetic parameters for 5 min.

CO_2 assimilation and formic acid emission both varied with temperature for this leaf (Fig. 2.7). As temperature increases, CO_2 assimilation increases up to a maximum value of 14.2 μmol m^{-2} s^{-1} at 26 °C. This CO_2 assimilation follows the expected cubic fit (Yamori et al., 2010). In contrast, formic acid continues to increase above the photosynthesis maximum, with maximum emission (2.30 μg m^{-2} min^{-1}) occurring at 29 °C. However, we emphasize that this represents a single experiment using the CIMS to demonstrate the utility of coupling the CIMS to the PPS,

rather than an extensive or replicated experiment of formic acid emissions. Thus, these observations should be considered a case study, rather than emissions ratios to be used in models. While the terpenoids of the essential oils of spearmint have been investigated (Delfine et al., 2005), stored and emitted compounds may differ. There is a need for studies focusing on the leaf-level emission rate of VOCs, including monoterpenes and formic acid. This case study demonstrates the potential for the PPS to be coupled to real-time measurements in exploring less-studied BVOCs, such as organic acids, at a leaf level.

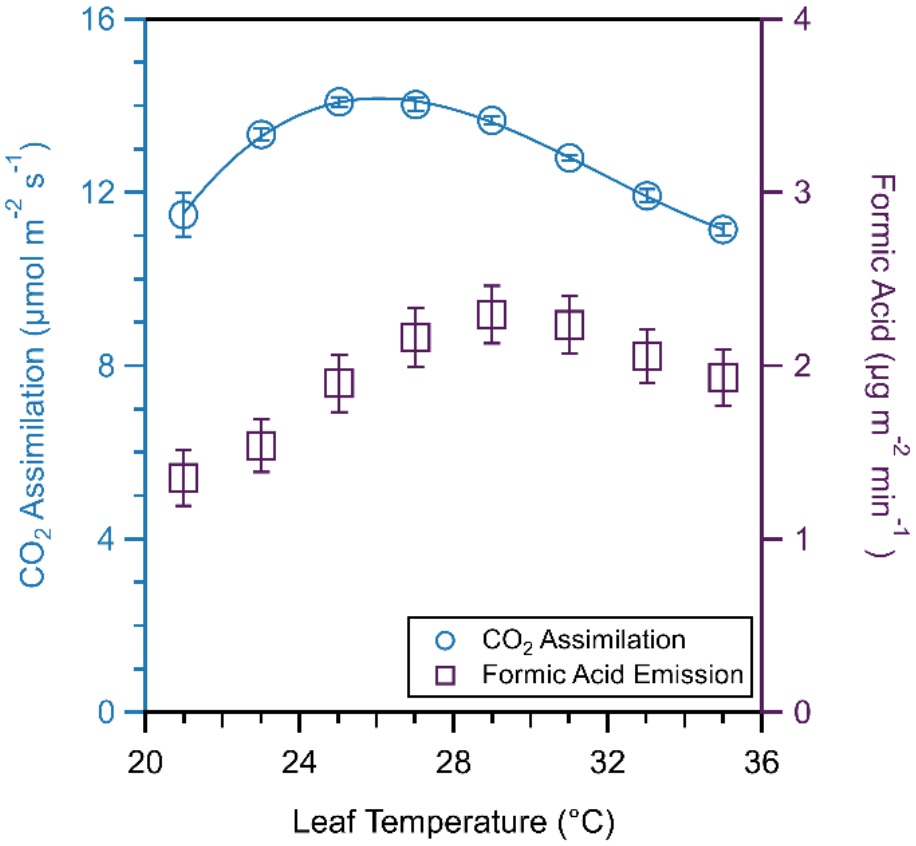

Figure 2.7. CO_2 assimilation (blue circles) and formic acid emission (purple squares) temperature response curve of one spearmint leaf. Temperatures varied by 2 °C from 21 to 35 °C. CO_2 assimilation follows the expected cubic fit. We collected assimilation and formic acid emission measurements for five minutes and averaged the values of each; error bars represent the standard deviation of those averages.

5.2 Decanal emissions

C_6 – C_{10} aldehydes are an understudied class of plant BVOC emissions (Ciccioli et al., 1993; S Owen et al., 1997; Wildt et al., 2003). Aldehydes can contribute to free radical formation in the atmosphere through photolysis or reaction with OH radicals (Atkinson, 1986). Decanal (C_{10}-aldehyde) is present in atmospheric mixing ratios of parts per trillion by volume (ppt_v) to parts per billion by volume (ppb_v) (Ciccioli et al., 1993), and is emitted by plants in response to stress (Wildt et al., 2003). Here, we demonstrate the potential for offline measurements (i.e., the TD-GC/MS) coupled to the PPS to investigate plant emissions of C_6-C_{10} aldehydes. Figure 2.8 shows the temperature response curve of a single leaf on a basil plant (*Ocimum basilicum*), a popular culinary herb. We collected single sorbent tubes for 20 min at each point as we varied temperature by ~3 °C from 18 to 35 °C. The LI-6800 simultaneously measured photosynthesis every 30 s. Background decanal concentrations in ambient air were 11 ± 1 ppb (average ± standard deviation).

CO_2 assimilation increases over the entire range of temperatures, beginning to stabilize around 33 °C. The CO_2 assimilation values for this study are within the range of values from previous studies (Golpayegani & Tilebeni, 2011). A cubic fit to assimilation suggests that 35 °C was the maxim in assimilation, which would decrease at higher temperatures. In contrast to photosynthesis, decanal exhibits bidirectional exchange. As temperature increases, decanal emissions are initially zero or negative (i.e., lower than the background concentration of input air), and then show enhanced uptake with increasing temperature before a turnover point at which emission rapidly increases. The temperature response is inconsistent with stored pools (Grote et al., 2013), suggesting a more complex biochemical pathway.

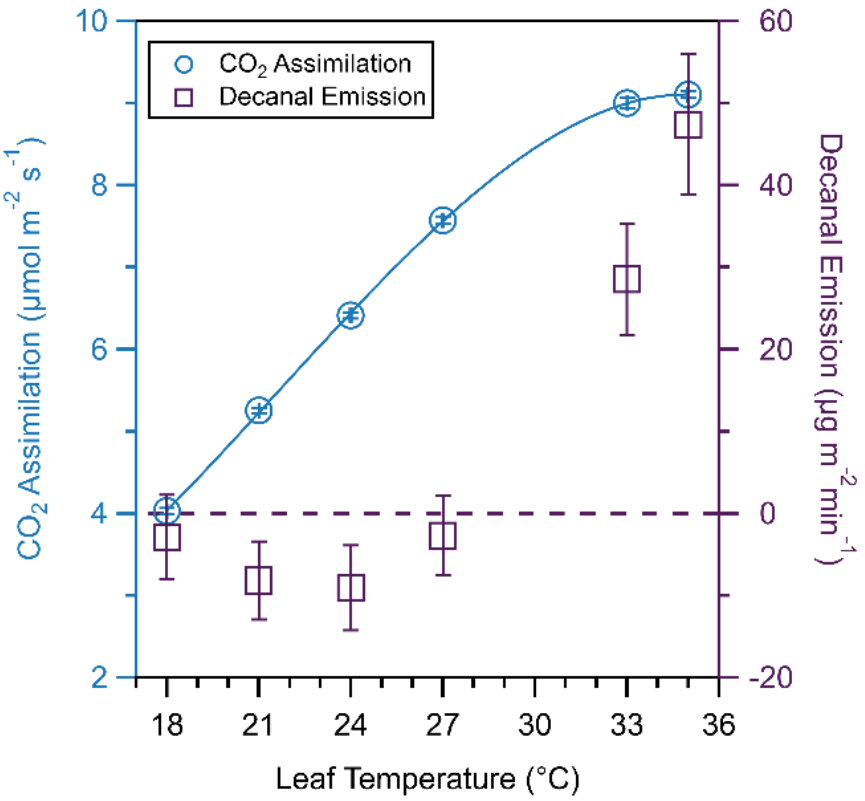

Figure 2.8. CO_2 assimilation (blue circles) and decanal emission (purple squares) temperature response curve of one basil leaf. CO_2 assimilation is fit to a cubic function. We collected CO_2 assimilation values ten times over 20 minutes and averaged the values; error bars represent the standard deviation of those measurements. Error bars for decanal emission represent instrumental error. The dashed line denotes 0 µg m^{-2} min^{-1} decanal emission.

The observed uptake of decanal below 27 °C supports the idea of a turnover point and bidirectional exchange of VOCs (Millet et al., 2018; Niinemets et al., 2014). Further investigation of turnover points as a function of varying input air VOC concentrations are warranted. Essential oil emissions of monoterpenes are quantified for basil (Tarchoune et al., 2013); however, the leaf-level emission of decanal is understudied, and has not yet been investigated for this species. The range of decanal emissions vary greatly in this study, but our findings suggest that, at high temperatures, decanal may be more strongly emitted than previously found. Our highest emissions at 35 °C are over 200 times greater than emission rates found from canola plants (Wildt et al.,

2003). There is a need for further study investigating the interspecies differences in aldehyde emissions, in addition to the light and temperature dependencies of decanal emissions.

The temperature response of photosynthetic metrics can be used to compare the thermotolerance between species or between plants of the same species. For example, this study suggests that basil has a photosynthetic maximum at temperatures greater than spearmint (35 °C, Fig. 2.8;26 °C Fig. 2.7, respectively), despite the fact that basil had a lower overall CO_2 assimilation rate. At temperatures above the maximum, photosynthesis and plant productivity may be inhibited (Berry & Bjorkman, 1980), suggesting that basil may have a higher thermotolerance than spearmint. We note that this comparison only considers short-term temperature increases, and further investigations would be necessary to determine the acclimation potential of these plant species to higher temperatures. The temperature response of trace gases can be used to further investigate the mechanisms by which different compounds are emitted. Comparing the emission of less-studied compounds like decanal to better-studied compounds like monoterpenes can improve the understanding of the regulating factors in leaf-level BVOC emissions.

5.3 Monoterpen emissions

The PPS-coupled emission sampling method is portable, which we take advantage of in our third case study. While BVOC emission studies often quantify emissions in terms of dry leaf weight, *in situ* measurements enable us to collect data based on leaf area, which is used in many emissions models.

To investigate the difference in limonene and γ-terpinene emissions between plants of different species, we sampled two shaded leaves of each of three tree species during the summer of 2019 in the Colorado State University Arboretum in Fort Collins, CO. We sampled: *Ginkgo biloba* (ginkgo), *Morus alba* (mulberry), and *Juglans regia* (walnut). These species cover a variety of uses: ginkgo is one of the longest living tree species and is used in dietary supplements

(Strømgaard & Nakanishi, 2004), mulberry is a primary food source for silkworms and is used for paper production (He et al., 2013), and walnut is of economic importance as timber (Ares & Brauer, 2004). These three species are considered low emitters of monoterpenes (Benjamin & Winer, 1998); our identification and quantification of their monoterpene emissions highlight the sensitivity of this technique.

Emissions were taken at 27±2 °C, near-ambient CO_2 (414 ppm), and under saturating light conditions (2000 μmol m^{-2} s^{-1}). We simultaneously sampled monoterpene emissions using the sorbent cartridges (30 min collection) and photosynthesis (30 s time resolution) at each temperature. Leaf temperature was difficult to regulate in the field. The PPS maintained a 25 °C leaf temperature with ambient temperatures up to 29 °C, but it could not keep leaf temperatures below 28 °C when ambient temperatures increased, even with shading and ice packs.

Previous studies have identified monoterpene emissions in ginkgo (Li et al., 2009), mulberry (Papiez et al., 2009), and walnut (Casado et al., 2008); however, these studies calculate emission rates in units of dry weight. Models that rely on leaf area to calculate monoterpene fluxes must thus account for differences between dry weight and leaf area. Alternatively, emissions collected via this method are already normalized to surface area, and do not require a major conversion.

Here, limonene emissions from all species were an order of magnitude greater than γ-terpinene, by factors of 10-20 (Fig. 2.9). This ratio can change based on genotype; for example, the ratio of limonene to γ-terpinene emissions in different black walnut genotypes ranges from 4.1:1 to 1:1.7 (Blood et al., 2018). Monoterpene emission rates from individual leaves varied, though this variance was more notable for γ-terpinene than limonene, in agreement with previous

studies (Blood et al., 2018). For example, we found that limonene emission rates differed by 24 % between the two mulberry leaves, whereas γ-terpinene differed by 46 %.

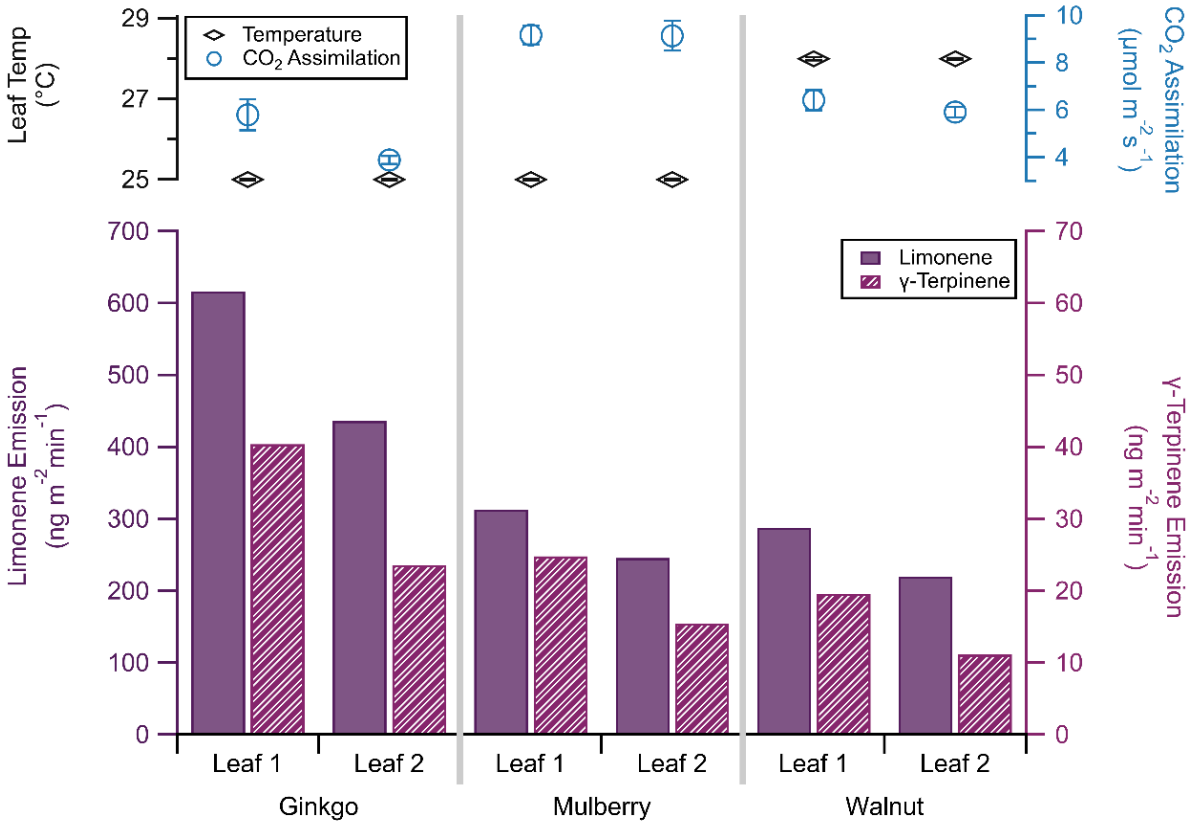

Figure 2.9. Limonene (solid bars, left bottom axis) and γ-terpinene (striped bars, right bottom axis) emission of two leaves from each of three plant species: ginkgo, mulberry, and walnut. Note that the scale of the limonene emission axis is ten times that of the γ-terpinene emission axis. Leaf temperature (black diamonds, left top axis) and CO_2 assimilation (blue circles, right top axis) are included, with standard deviation bars (n = 60).

Within leaves of a single plant, chamber temperature and subsequent CO_2 assimilation rates were similar (<0.5 % difference in assimilation between leaves of the same plant), and observed CO_2 assimilation rates agreed with previous measurements (Baraldi et al., 2019; Nicodemus et al., 2008; Pandey et al., 2003). This discrepancy in variance between CO_2 assimilation and monoterpene emissions on a single plant highlights the limitation of tying modeled photosynthesis

rates to VOC emissions and warrants further investigation. We focus on two monoterpenes here, however, this field survey approach to trace gas VOC emissions can provide a species-specific monoterpene emission cassette.

We provide an example monoterpene emission cassette. Figure 2.10 puts those emissions into an atmospheric context. We show that, although α-pinene contributes to 22% of the measured emissions, it only contributes to 7% of overall OH formation and 0.5% of ozone formation. Although α-terpinene contributes to 20% of the measured emissions, it is the dominating factor in both OH and ozone formation (44% and 98%, respectively). This technique allows for the speciation necessary to understand both the factors which influence emission rates and their subsequent atmospheric impact.

This case study supports previous findings that leaf emissions can vary between leaves of one tree (Staudt et al., 2001), between trees of one species (Staudt et al., 2001), and between trees of different species (Benjamin et al., 1996) – but that trace gas sampling with the PPS is a viable method for investigating these sources of variance. We further highlight the importance of speciated monoterpene analysis, and this technique's application for such analyses.

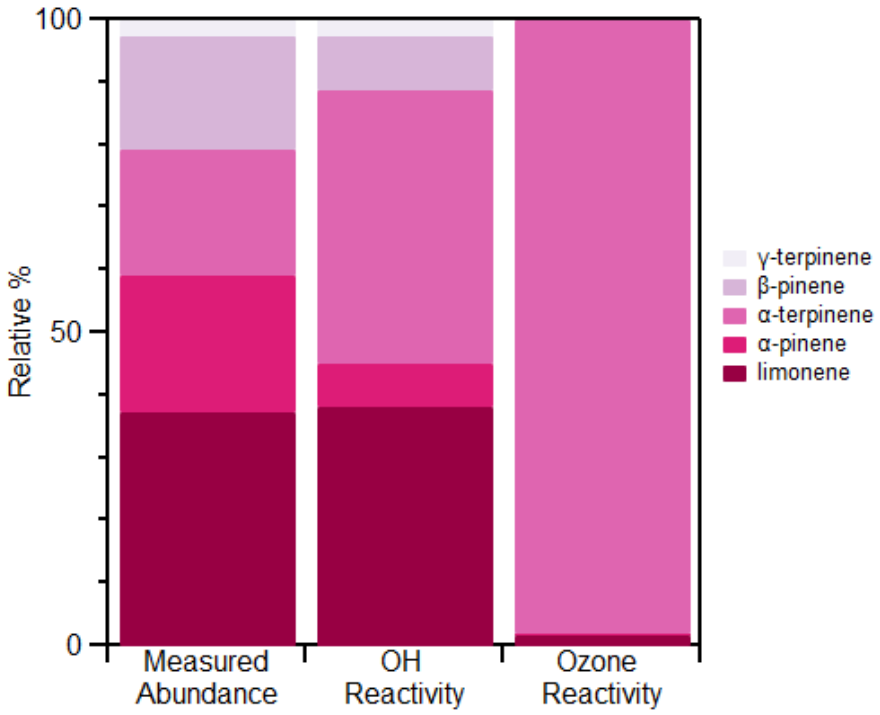

Figure 2.10. Relative measured abundance of all quantified monoterpenes from Ginkgo Leaf 1 (Fig. 2.9), and the subsequent relative contribution to both OH Reactivity and Ozone Reactivity. OH and ozone reactivity were calculated using k_{OH} and k_{ozone} rate constants from Atkinson (1997).

6. Conclusion

This study shows the utility of a new PPS coupled with both online and offline analysis for the analysis of leaf-level gas emissions, as well as the limitations and caveats associated with those measurements. In particular, trace gas measurements with high airflow needs (> 1 L min^{-1}) must be used carefully. Using an external CO_2 monitor to calculate CO_2 assimilation rates, we verify the integrity of the subsampling manifold and provide relevant equations for calculations of plant gas exchange.

The PPS-coupling described herein has substantial potential for improving our understanding of plant emissions. For example, different CIMS ionization sources can target different types of organic molecules (e.g. acetate ionization for organic acids vs iodide ionization for oxygenated organics), and different sorbent materials in thermal desorption tubes enable the detection of different compounds (i.e., Tenax for monoterpenes vs graphitic carbon for isoprene).

However, we emphasize the importance of carefully considering potential contaminants from the PPS itself, and the use of frequent system background measurements through both the SAM port in the absence of a leaf, and the REF port in the presence of the leaf. The further potential to control the composition of the airflow into the PPS will enable the investigation of compensation points.

Support statement

We thank Dr. Karolien Denef for assistance with the GC/MS in the Central Instrument Facility CORE at Colorado State University and Elizabeth Gordon (Li-Cor, Inc.). We thank James Mattila for his assistance with CIMS calculations, and Tyson Berg and Jarod Snook for their assistance with data collection. This research has been supported by the National Science Foundation (grant no. 1614315) and the Eppley Foundation for Research.

References

Abeleira, A. J., & Farmer, D. K. (2017). Summer ozone in the northern Front Range metropolitan area: weekend-weekday effects, temperature dependences, and the impact of drought. *Atmospheric Chemistry and Physics, 17*(11), 6517-6529.

Alwe, H. D., Millet, D. B., Chen, X., Raff, J. D., Payne, Z. C., & Fledderman, K. (2019). Oxidation of volatile organic compounds as the major source of formic acid in a mixed forest canopy. *Geophysical Research Letters, 46*(5), 2940-2948.

Ares, A., & Brauer, D. (2004). Growth and nut production of black walnut in relation to site, tree type and stand conditions in south-central United States. *Agroforestry systems, 63*(1), 83-90.

Arneth, A., Monson, R., Schurgers, G., Niinemets, Ü., & Palmer, P. (2008). Why are estimates of global terrestrial isoprene emissions so similar (and why is this not so for monoterpenes)? *Atmospheric Chemistry and Physics, 8*(16), 4605-4620.

Atkinson, R. (1986). Kinetics and mechanisms of the gas-phase reactions of the hydroxyl radical with organic compounds under atmospheric conditions. *Chemical Reviews, 86*(1), 69-201.

Atkinson, R. (1997). Gas-phase tropospheric chemistry of volatile organic compounds: 1. Alkanes and alkenes. *Journal of Physical and Chemical Reference Data, 26*(2), 215-290.

Atkinson, R., & Arey, J. (2003). Gas-phase tropospheric chemistry of biogenic volatile organic compounds: a review. *Atmospheric Environment, 37*, 197-219.

Atkinson, R., & Arey, J. (2003). Gas-phase tropospheric chemistry of biogenic volatile organic compounds: a review. *Atmospheric Environment, 37*, S197-S219.

Baldocchi, D. D., Hicks, B. B., & Meyers, T. P. (1988). Measuring biosphere-atmosphere exchanges of biologically related gases with micrometeorological methods. *Ecology, 69*(5), 1331-1340.

Baraldi, R., Chieco, C., Neri, L., Facini, O., Rapparini, F., Morrone, L., et al. (2019). An integrated study on air mitigation potential of urban vegetation: From a multi-trait approach to modeling. *Urban Forestry & Urban Greening, 41*, 127-138.

Beauchamp, J., Wisthaler, A., Hansel, A., Kleist, E., Miebach, M., Niinemets, Ü., et al. (2005). Ozone induced emissions of biogenic VOC from tobacco: relationships between ozone uptake and emission of LOX products. *Plant, Cell Environ, 28*(10), 1334-1343.

Benjamin, M. T., Sudol, M., Bloch, L., & Winer, A. M. (1996). Low-emitting urban forests: a taxonomic methodology for assigning isoprene and monoterpene emission rates. *Atmospheric Environment, 30*(9), 1437-1452.

Benjamin, M. T., & Winer, A. M. (1998). Estimating the ozone-forming potential of urban trees and shrubs. *Atmospheric Environment, 32*(1), 53-68.

Bernal, E. (2014). Limit of detection and limit of quantification determination in gas chromatography. In *Advances in gas chromatography*: IntechOpen.

Berry, J., & Bjorkman, O. (1980). Photosynthetic response and adaptation to temperature in higher plants. *Annual Review of plant physiology, 31*(1), 491-543.

Blood, B., Klingeman, W., Paschen, M., Hadžiabdić, Đ., Couture, J., & Ginzel, M. (2018). Behavioral responses of Pityophthorus juglandis (Coleoptera: Curculionidae: Scolytinae) to volatiles of black walnut and Geosmithia morbida (Ascomycota: Hypocreales: Bionectriaceae), the causal agent of Thousand Cankers Disease. *Environmental entomology, 47*(2), 412-421.

Bobbink, R., Hicks, K., Galloway, J., Spranger, T., Alkemade, R., Ashmore, M., et al. (2010). Global assessment of nitrogen deposition effects on terrestrial plant diversity: a synthesis. *Ecological Applications, 20*(1), 30-59.

Bonn, B., Magh, R.-K., Rombach, J., & Kreuzwieser, J. (2019). Biogenic isoprenoid emissions under drought stress: different responses for isoprene and terpenes. *Biogeosciences, 16*(23), 4627-4645.

Brilli, F., Barta, C., Fortunati, A., Lerdau, M., Loreto, F., & Centritto, M. (2007). Response of isoprene emission and carbon metabolism to drought in white poplar (Populus alba) saplings. *New Phytologist, 175*(2), 244-254.

Brilli, F., Ruuskanen, T. M., Schnitzhofer, R., Müller, M., Breitenlechner, M., Bittner, V., et al. (2011). Detection of plant volatiles after leaf wounding and darkening by proton transfer reaction "time-of-flight" mass spectrometry (PTR-TOF). *PLoS One, 6*(5), e20419.

Brophy, P., & Farmer, D. (2015). A switchable reagent ion high resolution time-of-flight chemical ionization mass spectrometer for real-time measurement of gas phase oxidized species: characterization from the 2013 southern oxidant and aerosol study. *Atmospheric Measurement Techniques, 8*(7), 2945-2959.

Brophy, P., & Farmer, D. K. (2016). Clustering, methodology, and mechanistic insights into acetate chemical ionization using high-resolution time-of-flight mass spectrometry. *Atmospheric Measurement Techniques, 9*(8), 3969-3986.

Bunce, J. (2008). Acclimation of photosynthesis to temperature in Arabidopsis thaliana and Brassica oleracea. *Photosynthetica, 46*(4), 517-524.

Carslaw, K. S., Boucher, O., Spracklen, D. V., Mann, G. W., Rae, J. G. L., Woodward, S., & Kulmala, M. (2010). A review of natural aerosol interactions and feedbacks within the Earth system. *Atmospheric Chemistry and Physics, 10*(4), 1701-1737.

Casado, D., Gemeno, C., Avilla, J., & Riba, M. (2008). Diurnal variation of walnut tree volatiles and electrophysiological responses in Cydia pomonella (Lepidoptera: Tortricidae). *Pest Management Science: formerly Pesticide Science, 64*(7), 736-747.

Chaudhary, P., Godara, S., Cheeran, A., & Chaudhari, A. K. (2012). Fast and accurate method for leaf area measurement. *International journal of computer applications, 49*(9), 22-25.

Ciccioli, P., Brancaleoni, E., Frattoni, M., Cecinato, A., & Brachetti, A. (1993). Ubiquitous occurrence of semi-volatile carbonyl compounds in tropospheric samples and their possible sources. *Atmospheric Environment. Part A. General Topics, 27*(12), 1891-1901.

Ciccioli, P., Brancaleoni, E., Frattoni, M., Di Palo, V., Valentini, R., Tirone, G., et al. (1999). Emission of reactive terpene compounds from orange orchards and their removal by within-canopy processes. *Journal of Geophysical Research: Atmospheres, 104*(D7), 8077-8094.

Clifton, O. E., Fiore, A. M., Massman, W. J., Baublitz, C. B., Coyle, M., Emberson, L., et al. (2020). Dry deposition of ozone over land: processes, measurement, and modeling. *Rev Geophys*.

Constable, J. V., Litvak, M. E., Greenberg, J. P., & Monson, R. K. (1999). Monoterpene emission from coniferous trees in response to elevated CO2 concentration and climate warming. *Global Change Biology, 5*(3), 252-267.

Copolovici, L. O., & Niinemets, Ü. (2005). Temperature dependencies of Henry's law constants and octanol/water partition coefficients for key plant volatile monoterpenoids. *Chemosphere, 61*(10), 1390-1400.

Davidson, C. I., Phalen, R. F., & Solomon, P. A. (2005). Airborne particulate matter and human health: A review. *Aerosol Science and Technology, 39*(8), 737-749.

Delfine, S., Loreto, F., Pinelli, P., Tognetti, R., & Alvino, A. (2005). Isoprenoids content and photosynthetic limitations in rosemary and spearmint plants under water stress. *Agriculture, ecosystems & environment, 106*(2-3), 243-252.

Dettmer, K., & Engewald, W. (2002). Adsorbent materials commonly used in air analysis for adsorptive enrichment and thermal desorption of volatile organic compounds. *Analytical and bioanalytical chemistry, 373*(6), 490-500.

Domurath, N., Schroeder, F.-G., & Glatzel, S. (2012). *Light response curves of selected plants under different light conditions.* Paper presented at the VII International Symposium on Light in Horticultural Systems 956.

Duhl, T., Helmig, D., & Guenther, A. (2008). Sesquiterpene emissions from vegetation: a review.

Ebel, R. C., Mattheis, J. P., & Buchanan, D. A. (1995). Drought stress of apple trees alters leaf emissions of volatile compounds. *Physiologia Plantarum, 93*(4), 709-712.

Emerson, E. W., Katich, J. M., Schwarz, J. P., McMeeking, G. R., & Farmer, D. K. (2018). Direct Measurements of Dry and Wet Deposition of Black Carbon Over a Grassland. *Journal of Geophysical Research-Atmospheres, 123*(21), 12277-12290.

Faiola, C. L., Buchholz, A., Kari, E., Yli-Pirilä, P., Holopainen, J. K., Kivimäenpää, M., et al. (2018). Terpene Composition Complexity Controls Secondary Organic Aerosol Yields from Scots Pine Volatile Emissions. *Scientific Reports, 8*(1), 3053

Faiola, C. L., Pullinen, I., Buchholz, A., Khalaj, F., Ylisirniö, A., Kari, E., et al. (2019). Secondary organic aerosol formation from healthy and aphid-stressed Scots pine emissions. *Acs Earth and Space Chemistry, 3*(9), 1756-1772.

Farmer, D. K., Cappa, C. D., & Kreidenweis, S. M. (2015). Atmospheric Processes and Their Controlling Influence on Cloud Condensation Nuclei Activity. *Chemical Reviews, 115*(10), 4199-4217.

Farmer, D. K., Chen, Q., Kimmel, J. R., Docherty, K. S., Nemitz, E., Artaxo, P., et al. (2013). Chemically resolved particle fluxes over tropical and temperate forests. *Aerosol Science and Technology, 47*, 818-830.

Farmer, D. K., & Cohen, R. C. (2008). Observations of HNO_3, ΣAN, ΣPN and NO_2 fluxes: evidence for rapid HO_x chemistry within a pine forest canopy. *Atmospheric Chemistry and Physics, 8*(14), 3899-3917.

Farmer, D. K., & Jimenez, J. L. (2010). Real-time Atmospheric Chemistry Field Instrumentation. *Analytical Chemistry, 82*(19), 7879-7884.

Farmer, D. K., Kimmel, J. R., Phillips, G., Docherty, K. S., Worsnop, D. R., Sueper, D., et al. (2011). Eddy Covariance Measurements with High-Resolution Time-of-Flight Aerosol Mass Spectrometry: A New Approach to Chemically Resolved Aerosol Fluxes. *Atmospheric Measurement Techniques, 4*, 1275-1289

Farmer, D. K., Wooldridge, P. J., & Cohen, R. C. (2006). Application of thermal-dissociation laser induced fluorescence (TD-LIF) to measurement of HNO_3, Σalkyl nitrates, Σperoxy nitrates, and NO_2 fluxes using eddy covariance. *Atmospheric Chemistry and Physics, 6*, 3471-3486.

Fernandes, A. S., Baker, E., & Martin, J. (1964). Studies on plant cuticle: VI. The isolation and fractionation of cuticular waxes. *Annals of Applied Biology, 53*(1), 43-58.

Fowler, D., Pilegaard, K., Sutton, M. A., Ambus, P., Raivonen, M., Duyzer, J., et al. (2009). Atmospheric composition change: Ecosystems-Atmosphere interactions. *Atmospheric Environment, 43*(33), 5193-5267.

Friedman, B., & Farmer, D. K. (2018). SOA and gas phase organic acid yields from the sequential photooxidation of seven monoterpenes. *Atmospheric Environment, 187*, 335-345.

Fromme, H. (2018). Cyclic Volatile Methylsiloxanes: Occurrence and Exposure.

Fu, D., Millet, D. B., Wells, K. C., Payne, V. H., Yu, S., Guenther, A., & Eldering, A. (2019). Direct retrieval of isoprene from satellite-based infrared measurements. *Nature Communications, 10*(1), 1-12.

Fuentes, J. D., Lerdau, M., Atkinson, R., Baldocchi, D., Bottenheim, J. W., Ciccioli, P., et al. (2000). Biogenic hydrocarbons in the atmospheric boundary layer: A review. *Bulletin of the American Meteorological Society, 81*(7), 1537-1575.

Fulgham, S. R., Brophy, P., Link, M., Ortega, J., Pollack, I., & Farmer, D. K. (2019). Seasonal flux measurements over a Colorado pine forest demonstrate a persistent source of organic acids. *Acs Earth and Space Chemistry, 3*(9), 2017-2032.

Geron, C., Guenther, A., Greenberg, J., Karl, T., & Rasmussen, R. (2006). Biogenic volatile organic compound emissions from desert vegetation of the southwestern US. *Atmospheric Environment, 40*(9), 1645-1660.

Geron, C., Owen, S., Guenther, A., Greenberg, J., Rasmussen, R., Bai, J. H., et al. (2006). Volatile organic compounds from vegetation in southern Yunnan Province, China: Emission rates and some potential regional implications. *Atmospheric Environment, 40*(10), 1759-1773.

Goldstein, A., McKay, M., Kurpius, M., Schade, G., Lee, A., Holzinger, R., & Rasmussen, R. (2004). Forest thinning experiment confirms ozone deposition to forest canopy is dominated by reaction with biogenic VOCs. *Geophysical Research Letters, 31*(22).

Goldstein, A. H., & Galbally, I. E. (2007). Known and unexplored organic constituents in the earth's atmosphere. *Environmental Science & Technology, 41*(5), 1514-1521.

Goldstein, A. H., McKay, M., Kurpius, M. R., Schade, G. W., Lee, A., Holzinger, R., & Rasmussen, R. A. (2004). Forest thinning experiment confirms ozone deposition to forest canopy is dominated by reaction with biogenic VOCs. *Geophysical Research Letters, 31*(22), L22106.

Golpayegani, A., & Tilebeni, H. G. (2011). Effect of biological fertilizers on biochemical and physiological parameters of basil (Ociumum basilicm L.) medicine plant. *Am Eurasian J Agric Environ Sci, 11*, 411-416.

Grote, R., Monson, R. K., & Niinemets, Ü. (2013). Leaf-level models of constitutive and stress-driven volatile organic compound emissions. In *Biology, controls and models of tree volatile organic compound emissions* (pp. 315-355): Springer.

Grote, R., Morfopoulos, C., Niinemets, Ü., Sun, Z., Keenan, T. F., Pacifico, F., & Butler, T. (2014). A fully integrated isoprenoid emissions model coupling emissions to photosynthetic characteristics. *Plant, Cell & Environment, 37*(8), 1965-1980.

Guenther, A. (1997). Seasonal and spatial variations in natural volatile organic compound emissions. *Ecological Applications, 7*(1), 34-45.

Guenther, A., Geron, C., Pierce, T., Lamb, B., Harley, P., & Fall, R. (2000). Natural emissions of non-methane volatile organic compounds, carbon monoxide, and oxides of nitrogen from North America. *Atmospheric Environment, 34*(12-14), 2205-2230.

Guenther, A., Hewitt, C. N., Erickson, D., Fall, R., Geron, C., Graedel, T., et al. (1995). A global model of natural volatile organic compound emissions. *Journal of Geophysical Research: Atmospheres, 100*(D5), 8873-8892.

Guenther, A., Jiang, X., Heald, C., Sakulyanontvittaya, T., Duhl, T., Emmons, L., & Wang, X. (2012). The Model of Emissions of Gases and Aerosols from Nature version 2.1 (MEGAN2. 1): an extended and updated framework for modeling biogenic emissions.

Guenther, A. B., Zimmerman, P. R., Harley, P. C., Monson, R. K., & Fall, R. (1993). Isoprene and monoterpene emission rate variability: model evaluations and sensitivity analyses. *Journal of Geophysical Research: Atmospheres, 98*(D7), 12609-12617.

Harley, P., Eller, A., Guenther, A., & Monson, R. K. (2014). Observations and models of emissions of volatile terpenoid compounds from needles of ponderosa pine trees growing in situ: control by light, temperature and stomatal conductance. *Oecologia, 176*(1), 35-55.

Harper, M. (2000). Sorbent trapping of volatile organic compounds from air. *Journal of Chromatography A, 885*(1-2), 129-151.

He, N., Zhang, C., Qi, X., Zhao, S., Tao, Y., Yang, G., et al. (2013). Draft genome sequence of the mulberry tree Morus notabilis. *Nature communications, 4*(1), 1-9.

Heald, C., & Kroll, J. (2020). The fuel of atmospheric chemistry: Toward a complete description of reactive organic carbon. *Science Advances, 6*(6), eaay8967.

Heald, C. L., Goldstein, A. H., Allan, J. D., Aiken, A. C., Apel, E., Atlas, E. L., et al. (2008). Total observed organic carbon (TOOC) in the atmosphere: a synthesis of North American observations. *Atmospheric Chemistry and Physics, 8*(7), 2007-2025.

Hodges, A. W., & Spreen, T. H. (2006). Economic impacts of citrus greening (HLB) in Florida. In.

Holopainen, J. K. (2004). Multiple functions of inducible plant volatiles. *Trends in plant science, 9*(11), 529-533.

Kainulainen, P., Holopainen, J., & Holopainen, T. (1998). The influence of elevated CO 2 and O 3 concentrations on Scots pine needles: changes in starch and secondary metabolites over three exposure years. *Oecologia, 114*(4), 455-460.

Kaser, L., Karl, T., Guenther, A., Graus, M., Schnitzhofer, R., Turnipseed, A., et al. (2013). Undisturbed and disturbed above canopy ponderosa pine emissions: PTR-TOF-MS measurements and MEGAN 2.1 model results.

Kaser, L., Karl, T., Schnitzhofer, R., Graus, M., Herdlinger-Blatt, I., DiGangi, J., et al. (2013). Comparison of different real time VOC measurement techniques in a ponderosa pine forest. *Atmospheric Chemistry and Physics, 13*(5), 2893-2906.

Kesselmeier, J., & Staudt, M. (1999). Biogenic volatile organic compounds (VOC): an overview on emission, physiology and ecology. *Journal of atmospheric chemistry, 33*(1), 23-88.

Kessler, A., & Baldwin, I. T. (2001). Defensive function of herbivore-induced plant volatile emissions in nature. *Science, 291*(5511), 2141-2144.

Khare, P., Kumar, N., Kumari, K., & Srivastava, S. (1999). Atmospheric formic and acetic acids: An overview. *Reviews of geophysics, 37*(2), 227-248.

Kim, J.-C., Kim, K.-J., Kim, D.-S., & Han, J.-S. (2005). Seasonal variations of monoterpene emissions from coniferous trees of different ages in Korea. *Chemosphere, 59*(11), 1685-1696.

Kim, M., Farmer, D. K., & Bertram, T. H. (2014). Measurements of N2O5 and ClNO2 fluxes from the Scripps pier. *Proceedings of the National Academy of Sciences of the United States of America*

Knote, C., Hodzic, A., & Jimenez, J. L. (2015). The effect of dry and wet deposition of condensable vapors on secondary organic aerosols concentrations over the continental US. *Atmospheric Chemistry and Physics, 15*, 1-18.

Koch, D., Schulz, M., Kinne, S., Bond, T., Balkanski, Y., Bauer, S., et al. (2009). Evaluation of black carbon estimations in global aerosol models. *Atmospheric Chemistry and Physics, 9*, 9001-9026.

Komenda, M., Parusel, E., Wedel, A., & Koppmann, R. (2001). Measurements of biogenic VOC emissions: sampling, analysis and calibration. *Atmospheric Environment, 35*(12), 2069-2080.

Kurpius, M. R., & Goldstein, A. H. (2003). Gas-phase chemistry dominates O_3 loss to a forest, implying a source of aerosols and hydroxyl radicals to the atmosphere. *Geophysical Research Letters, 30*(7).

Lamarque, J.-F., Bond, T. C., Eyring, V., Granier, C., Heil, A., Klimont, Z., et al. (2010). Historical (1850–2000) gridded anthropogenic and biomass burning emissions of reactive gases and aerosols: methodology and application. *Atmospheric Chemistry and Physics, 10*(15), 7017-7039.

Lang, Y., Wang, M., Zhang, G., & Zhao, Q. (2013). Experimental and simulated light responses of photosynthesis in leaves of three tree species under different soil water conditions. *Photosynthetica, 51*(3), 370-378.

Lathière, J., Hauglustaine, D. A., Friend, A. D., De Noblet-Ducoudré, N., Viovy, N., & Folberth, G. A. (2006). Impact of climate variability and land use changes on global biogenic volatile organic compound emissions. *Atmos. Chem. Phys., 6*(8), 2129-2146.

Lavi, A., Farmer, D. K., Segre, E., Moise, T., Rotenberg, E., Jimenez, J. L., & Rudich, Y. (2013). Fluxes of Fine Particles Over a Semi-Arid Pine Forest: Possible Effects of a Complex Terrain. *Aerosol Science and Technology, 47*(8), 906-915.

Lee, A., Goldstein, A. H., Keywood, M. D., Gao, S., Varutbangkul, V., Bahreini, R., et al. (2006). Gas-phase products and secondary aerosol yields from the ozonolysis of ten different terpenes. *Journal of Geophysical Research-Atmospheres, 111*, D07302.

Lee, A., Goldstein, A. H., Kroll, J. H., Ng, N. L., Varutbangkul, V., Flagan, R. C., & Seinfeld, J. H. (2006). Gas-phase products and secondary aerosol yields from the photooxidation of 16 different terpenes. *Journal of Geophysical Research-Atmospheres, 111*, D17305.

Lee, B. H., Lopez-Hilfiker, F. D., Mohr, C., Kurtén, T., Worsnop, D. R., & Thornton, J. A. (2014). An iodide-adduct high-resolution time-of-flight chemical-ionization mass spectrometer: Application to atmospheric inorganic and organic compounds. *Environmental science & technology, 48*(11), 6309-6317.

Lee, L. A., Pringle, K. J., Reddington, C. L., Mann, G. W., Stier, P., Spracklen, D. V., et al. (2013). The magnitude and causes of uncertainty in global model simulations of cloud condensation nuclei. *Atmospheric Chemistry and Physics, 13*, 8879–8914.

Lerdau, M., & Keller, M. (1997). Controls on isoprene emission from trees in a subtropical dry forest. *Plant, Cell & Environment, 20*(5), 569-578.

LI-COR. (2017). *Using the LI-6800 Portable Photosynthesis System* (Vol. 1.3).

Li, D., Chen, Y., Shi, Y., He, X., & Chen, X. (2009). Impact of elevated CO 2 and O 3 concentrations on biogenic volatile organic compounds emissions from Ginkgo biloba. *Bulletin of environmental contamination and toxicology, 82*(4), 473-477.

Link, M. F., Nguyen, T. B., Bates, K. H., Müller, J.-F., & Farmer, D. K. (2020). Can isoprene oxidation explain high concentrations of atmospheric formic and acetic acid over forests? *Acs Earth and Space Chemistry*.

Llusià, J., & Peñuelas, J. (1998). Changes in terpene content and emission in potted Mediterranean woody plants under severe drought. *Can J Bot, 76*(8), 1366-1373.

Llusià, J., Peñuelas, J., Alessio, G. A., & Estiarte, M. (2008). Contrasting species-specific, compound-specific, seasonal, and interannual responses of foliar isoprenoid emissions to experimental drought in a Mediterranean shrubland. *Int J Plant Sci, 169*(5), 637-645.

Llusià, J., Peñuelas, J., & Gimeno, B. (2002). Seasonal and species-specific response of VOC emissions by Mediterranean woody plant to elevated ozone concentrations. *Atmospheric Environment, 36*(24), 3931-3938.

Loreto, F., Förster, A., Dürr, M., Csiky, O., & Seufert, G. (1998). On the monoterpene emission under heat stress and on the increased thermotolerance of leaves of Quercus ilex L. fumigated with selected monoterpenes. *Plant, Cell & Environment, 21*(1), 101-107.

Loreto, F., Pinelli, P., Manes, F., & Kollist, H. (2004). Impact of ozone on monoterpene emissions and evidence for an isoprene-like antioxidant action of monoterpenes emitted by Quercus ilex leaves. *Tree physiology, 24*(4), 361-367.

Loreto, F., & Schnitzler, J.-P. (2010). Abiotic stresses and induced BVOCs. *Trends in Plant Science, 15*(3), 154-166.

Loreto, F., & Velikova, V. (2001). Isoprene produced by leaves protects the photosynthetic apparatus against ozone damage, quenches ozone products, and reduces lipid peroxidation of cellular membranes. *Plant Physiology, 127*(4), 1781-1787.

Markovic, D., Nikolic, N., Glinwood, R., Seisenbaeva, G., & Ninkovic, V. (2016). Plant responses to brief touching: a mechanism for early neighbour detection? *PLoS One, 11*(11), e0165742.

Mattila, J. M., Brophy, P., Kirkland, J., Hall, S., Ullmann, K., Fischer, E. V., et al. (2018). Tropospheric sources and sinks of gas-phase acids in the Colorado Front Range.

Mattila, J. M., Brophy, P., Kirkland, J., Hall, S., Ullmann, K., Fischer, E. V., et al. (2018). Tropospheric sources and sinks of gas-phase acids in the Colorado Front Range. *Atmospheric Chemistry and Physics, 18*(16), 12315-12327.

Mauck, K. E., De Moraes, C. M., & Mescher, M. C. (2010). Deceptive chemical signals induced by a plant virus attract insect vectors to inferior hosts. *Proceedings of the National Academy of Sciences, 107*(8), 3600-3605.

Mielnik, A., Link, M., Mattila, J., Fulgham, S. R., & Farmer, D. K. (2018). Emission of formic and acetic acids from two Colorado soils. *Environmental Science: Processes & Impacts, 20*(11), 1537-1545.

Millet, D. B., Alwe, H. D., Chen, X., Deventer, M. J., Griffis, T. J., Holzinger, R., et al. (2018). Bidirectional ecosystem–atmosphere fluxes of volatile organic compounds across the mass spectrum: How many matter? *Acs Earth and Space Chemistry, 2*(8), 764-777.

Millet, D. B., Baasandorj, M., Farmer, D. K., Thornton, J. A., Baumann, K., Brophy, P., et al. (2015). A large and ubiquitous source of atmospheric formic acid. *Atmospheric Chemistry and Physics, 15*(11), 6283-6304.

Millet, D. B., Jacob, D. J., Boersma, K. F., Fu, T. M., Kurosu, T. P., Chance, K., et al. (2008). Spatial distribution of isoprene emissions from North America derived from formaldehyde column measurements by the OMI satellite sensor. *Journal of Geophysical Research-Atmospheres, 113*(D2).

Nicodemus, M. A., Salifu, F. K., & Jacobs, D. F. (2008). Growth, nutrition, and photosynthetic response of black walnut to varying nitrogen sources and rates. *Journal of Plant Nutrition, 31*(11), 1917-1936.

Niinemets, Ü., Fares, S., Harley, P., & Jardine, K. J. (2014). Bidirectional exchange of biogenic volatiles with vegetation: emission sources, reactions, breakdown and deposition. *Plant, Cell & Environment, 37*(8), 1790-1809.

Niinemets, Ü., Kännaste, A., & Copolovici, L. (2013). Quantitative patterns between plant volatile emissions induced by biotic stresses and the degree of damage. *Frontiers in Plant Science, 4*, 262.

Niinemets, Ü., Loreto, F., & Reichstein, M. (2004). Physiological and physicochemical controls on foliar volatile organic compound emissions. *Trends in plant science, 9*(4), 180-186.

Ormeño, E., Mevy, J., Vila, B., Bousquet-Mélou, A., Greff, S., Bonin, G., & Fernandez, C. (2007). Water deficit stress induces different monoterpene and sesquiterpene emission changes in Mediterranean species. Relationship between terpene emissions and plant water potential. *Chemosphere, 67*(2), 276-284.

Ortega, J., & Helmig, D. (2008). Approaches for quantifying reactive and low-volatility biogenic organic compound emissions by vegetation enclosure techniques - Part A. *Chemosphere, 72*(3), 343-364.

Owen, S., Boissard, C., Street, R., Duckham, S., Csiky, O., & Hewitt, C. (1997). Screening of 18 Mediterranean plant species for volatile organic compound emissions. *Atmospheric Environment, 31*, 101-117.

Owen, S., Harley, P., Guenther, A., & Hewitt, C. (2002). Light dependency of VOC emissions from selected Mediterranean plant species. *Atmospheric Environment, 36*(19), 3147-3159.

Pandey, S., Kumar, S., & Nagar, P. (2003). Photosynthetic performance of Ginkgo biloba L. grown under high and low irradiance. *Photosynthetica, 41*(4), 505-511.

Papiez, M. R., Potosnak, M. J., Goliff, W. S., Guenther, A. B., Matsunaga, S. N., & Stockwell, W. R. (2009). The impacts of reactive terpene emissions from plants on air quality in Las Vegas, Nevada. *Atmospheric Environment, 43*(27), 4109-4123.

Park, J.-H., Goldstein, A., Timkovsky, J., Fares, S., Weber, R., Karlik, J., & Holzinger, R. (2013). Active atmosphere-ecosystem exchange of the vast majority of detected volatile organic compounds. *Science, 341*(6146), 643-647.

Paulot, F., Wunch, D., Crounse, J. D., Toon, G., Millet, D. B., DeCarlo, P. F., et al. (2011). Importance of secondary sources in the atmospheric budgets of formic and acetic acids. *Atmospheric Chemistry and Physics, 11*(5), 1989-2013.

Paulot, F., Wunch, D., Crounse, J. D., Toon, G. C., Millet, D. B., DeCarlo, P. F., et al. (2011). Importance of secondary sources in the atmospheric budgets of formic and acetic acids. *Atmospheric Chemistry and Physics, 11*(5), 1989-2013. <Go to ISI>://000288368900010

Peñuelas, J., & Llusià, J. (2001a). The complexity of factors driving volatile organic compound emissions by plants. *Biol Plant, 44*(4), 481-487.

Peñuelas, J., & Llusià, J. (2001b). The complexity of factors driving volatile organic compound emissions by plants. *Biologia Plantarum, 44*(4), 481-487.

Pope III, C. A., & Dockery, D. W. (2006). Health effects of fine particulate air pollution: lines that connect. *Journal of the Air & Waste Management Association, 56*(6), 709-742.

Pöschl, U., Martin, S. T., Sinha, B., Chen, Q., Gunthe, S. S., Huffman, J. A., et al. (2010). Rainforest aerosols as biogenic nuclei of clouds and precipitation in the Amazon. *Science, 329*, 1513-1516.

Räisänen, T., Ryyppö, A., & Kellomäki, S. (2008). Effects of elevated CO2 and temperature on monoterpene emission of Scots pine (Pinus sylvestris L.). *Atmospheric Environment, 42*(18), 4160-4171.

Rapparini, F., Baraldi, R., Miglietta, F., & Loreto, F. (2003). Isoprenoid emission in trees of Quercus ilex with lifetime exposure to naturally high CO2 environment. *Plant, Cell & Environment*.

Riches, M., Lee, D., & Farmer, D. K. (2020). Simultaneous leaf-level measurement of trace gas emissions and photosynthesis with a portable photosynthesis system. *Atmospheric Measurement Techniques*.

Rinne, J., Taipale, R., Markkanen, T., Ruuskanen, T., Hellén, H., Kajos, M., et al. (2007). Hydrocarbon fluxes above a Scots pine forest canopy: measurements and modeling. *Atmospheric Chemistry and Physics, 7*(12), 3361-3372.

Sallas, L., Luomala, E.-M., Utriainen, J., Kainulainen, P., & Holopainen, J. K. (2003). Contrasting effects of elevated carbon dioxide concentration and temperature on Rubisco activity, chlorophyll fluorescence, needle ultrastructure and secondary metabolites in conifer seedlings. *Tree Physiology, 23*(2), 97-108.

Scala, A., Allmann, S., Mirabella, R., Haring, M., & Schuurink, R. (2013). Green leaf volatiles: a plant's multifunctional weapon against herbivores and pathogens. *International journal of molecular sciences, 14*(9), 17781-17811.

Schobesberger, S., Lopez-Hilfiker, F. D., Taipale, D., Millet, D. B., D'Ambro, E. L., Rantala, P., et al. (2016). High upward fluxes of formic acid from a boreal forest canopy. *Geophysical Research Letters, 43*(17), 9342-9351.

Scholefield, P., Doick, K., Herbert, B., Hewitt, C. S., Schnitzler, J. P., Pinelli, P., & Loreto, F. (2004). Impact of rising CO2 on emissions of volatile organic compounds: isoprene emission from Phragmites australis growing at elevated CO2 in a natural carbon dioxide spring. *Plant, Cell & Environment, 27*(4), 393-401.

Scott, C. E., Monks, S. A., Spracklen, D. V., Arnold, S. R., Forster, P. M., Rap, A., et al. (2018). Impact on short-lived climate forcers increases projected warming due to deforestation. *Nature Communications, 9*.

Scott, C. E., Rap, A., Spracklen, D. V., Forster, P. M., Carslaw, K. S., Mann, G. W., et al. (2014). The direct and indirect radiative effects of biogenic secondary organic aerosol. *Atmospheric Chemistry and Physics, 14*(1), 447-470.

Sellin, A. (2000). Estimating the needle area from geometric measurements: application of different calculation methods to Norway spruce. *Trees, 14*(4), 215-222.

Sharkey, T. D., & Loreto, F. (1993). Water stress, temperature, and light effects on the capacity for isoprene emission and photosynthesis of kudzu leaves. *Oecologia, 95*(3), 328-333.

Sharkey, T. D., & Yeh, S. (2001). Isoprene emission from plants. *Annual review of plant biology, 52*(1), 407-436.

Singh, H. B. (1995). *Composition, chemistry, and climate of the atmosphere*: Van Nostrand Reinhold Company.

Singsaas, E. L., Laporte, M. M., Shi, J.-Z., Monson, R. K., Bowling, D. R., Johnson, K., et al. (1999). Kinetics of leaf temperature fluctuation affect isoprene emission from red oak (Quercus rubra) leaves. *Tree Physiology, 19*(14), 917-924.

Slinn, W. G. N. (1982). Predictions for Particle Deposition to Vegetative Canopies. *Atmospheric Environment, 16*(7), 1785-1794.

Snow, M. D., Bard, R. R., Olszyk, D. M., Minster, L. M., Hager, A. N., & Tingey, D. T. (2003). Monoterpene levels in needles of Douglas fir exposed to elevated CO2 and temperature. *Physiologia Plantarum, 117*(3), 352-358.

Staudt, M., Joffre, R., Rambal, S., & Kesselmeier, J. (2001). Effect of elevated CO2 on monoterpene emission of young Quercus ilex trees and its relation to structural and ecophysiological parameters. *Tree Physiology, 21*(7), 437-445.

Staudt, M., Mandl, N., Joffre, R., & Rambal, S. (2001). Intraspecific variability of monoterpene composition emitted by Quercus ilex leaves. *Canadian Journal of Forest Research, 31*(1), 174-180.

Staudt, M., & Seufert, G. (1995). Light-dependent emission of monoterpenes by holm oak (Quercus ilex L.). *Naturwissenschaften, 82*(2), 89-92.

Stavrakou, T., Muller, J. F., Peeters, J., Razavi, A., Clarisse, L., Clerbaux, C., et al. (2012). Satellite evidence for a large source of formic acid from boreal and tropical forests. *Nature Geoscience, 5*(1), 26-30.

Strømgaard, K., & Nakanishi, K. (2004). Chemistry and biology of terpene trilactones from Ginkgo biloba. *Angewandte Chemie International Edition, 43*(13), 1640-1658.

Tarchoune, I., Baâtour, O., Harrathi, J., Cioni, P. L., Lachaâl, M., Flamini, G., & Ouerghi, Z. (2013). Essential oil and volatile emissions of basil (Ocimum basilicum) leaves exposed to NaCl or Na2SO4 salinity. *Journal of Plant Nutrition and Soil Science, 176*(5), 748-755.

Tarvainen, V., Hakola, H., Hellén, H., Bäck, J., Hari, P., & Kulmala, M. (2005a). Temperature and light dependence of the VOC emissions of Scots pine. *Atmospheric Chemistry and Physics, 5*(4), 989-998.

Tarvainen, V., Hakola, H., Hellén, H., Bäck, J., Hari, P., & Kulmala, M. (2005b). Temperature and light dependence of the VOC emissions of Scots pine. *Atmospheric Chemistry and Physics, 5*, 989–998.

Tilley, S. K., & Fry, R. C. (2015). Priority environmental contaminants: understanding their sources of exposure, biological mechanisms, and impacts on health. In *Systems Biology in Toxicology and Environmental Health* (pp. 117-169): Elsevier.

Tingey, D., Turner, D., & Weber, J. (1990). Factors controlling the emissions of monoterpenes and other volatile organic compounds. *Trace gas emission by plants.*, 93-119.

Tingey, D. T., Manning, M., Grothaus, L. C., & Burns, W. F. (1980). Influence of light and temperature on monoterpene emission rates from slash pine. *Plant Physiology, 65*(5), 797-801.

Vong, R. J., Vong, I. J., Vickers, D., & Covert, D. S. (2010). Size-dependent aerosol deposition velocities during BEARPEX' 07. *Atmospheric Chemistry and Physics, 10*(12), 5749-5758.

Wildt, J., Kobel, K., Schuh-Thomas, G., & Heiden, A. (2003). Emissions of oxygenated volatile organic compounds from plants Part II: emissions of saturated aldehydes. *Journal of atmospheric chemistry, 45*(2), 173-196.

Wilkinson, M. J., Monson, R. K., Trahan, N., Lee, S., Brown, E., Jackson, R. B., et al. (2009). Leaf isoprene emission rate as a function of atmospheric CO2 concentration. *Global Change Biology, 15*(5), 1189-1200.

Wilt, F. M., Miller, G. C., & Everett, R. L. (1993). Measurement of monoterpene hydrocarbon levels in vapor phase surrounding single-leaf pinyon (Pinus monophylla Torr. & Frem.: Pinaceae) understory litter. *Journal of Chemical Ecology, 19*(7), 1417-1428.

Wolfe, G. M., Thornton, J. A., Mckay, M., & Goldstein, A. H. (2011). Forest-atmosphere exchange of ozone: sensitivity to very reactive biogenic VOC emissions and implications for in-canopy photochemistry. *Atmospheric Chemistry and Physics, 11*, 7875-7891.

Yamori, W., Evans, J. R., & Von Caemmerer, S. (2010). Effects of growth and measurement light intensities on temperature dependence of CO2 assimilation rate in tobacco leaves. *Plant, Cell & Environment, 33*(3), 332-343.

Yang, X., Wang, X., & Wei, M. (2010). Response of photosynthesis in the leaves of cucumber seedlings to light intensity and CO2 concentration under nitrate stress. *Turkish Journal of Botany, 34*(4), 303-310.

Yatavelli, R., Stark, H., Thompson, S., Kimmel, J., Cubison, M., Day, D., et al. (2014). Semicontinuous measurements of gas–particle partitioning of organic acids in a ponderosa pine forest using a MOVI-HRToF-CIMS. *Atmospheric Chemistry and Physics, 14*(3), 1527-1546.

Zhang, P., & Chen, K. (2009). Age-dependent variations of volatile emissions and inhibitory activity toward Botrytis cinerea and Fusarium oxysporum in tomato leaves treated with chitosan oligosaccharide. *Journal of Plant Biology, 52*(4), 332-339.

CHAPTER 3

THE FIRST SEASONAL SNOWFALL IMPACTS PLANT PHOTOSYNTHESIS AND MONOTERPENE EMISSIONS[3]

Conspectus

Biogenic monoterpene emissions impact regional and global atmospheric chemistry. While the impact of short-term temperature fluctuations on emissions is well-understood, the role of weather events is not. Here we simultaneously measure photosynthesis and speciated monoterpene emissions from leaves of one cultivar of *Liriodendron tulipifera* prior to, during, and following the first seasonal snow event. We find that leaves act as a sink to atmospheric monoterpenes during snow, and subsequently release a surge of monoterpenes the following day, an order of magnitude higher than pre-snow emission rates. We further find that as senescence continues, the characteristic profile of the emissions changes in favor of β-ocimene, a highly reactive species. While summed monoterpene emission decreases throughout senescence, the enhanced β-ocimene emission increases hydroxyl radical reactivity compared to pre-snow conditions. Our findings highlight the importance of speciated monoterpene measurements in considering biosphere-atmosphere exchange of biogenic hydrocarbons.

1. Introduction

Non-methane volatile organic compounds are ubiquitous and highly reactive in the atmosphere, contributing to the formation and removal of secondary organic aerosol and

[3] Riches M, Snook J, Farmer DK. The first seasonal snowfall impacts plant photosynthesis and monoterpene emissions. *Reviewed and Resubmitted to Geophysical Research Letters.*

greenhouse gases (Faiola et al., 2018; Kesselmeier & Staudt, 1999). Biogenic sources of volatile organic compounds dominate the global budget, globally contributing to 1150 TgC yr^{-1} relative to the 142 TgC yr^{-1} from anthropogenic sources (Guenther et al., 1995; Singh, 1995). Of those biogenic sources, monoterpene isomers ($C_{10}H_{16}$) constitute 15% of the emissions (Guenther et al., 2012). Despite structural similarities, different monoterpene isomers have different atmospheric reactivities (e.g., Atkinson, 1990), and our understanding of these isomers are further complicated by the differences in the factors that influence their emissions. Monoterpene emissions are influenced by several abiotic factors, the most well-known including temperature (e.g., Guenther et al., 1993; Jardine et al., 2017; Tingey et al., 1980), light (e.g., Kuhn et al., 2004; Nishimura et al., 2015; Staudt & Seufert, 1995) and soil moisture (e.g., Bonn et al., 2019; Staudt et al., 2002; Wu et al., 2015). These abiotic factors are incorporated into existing emissions parameterizations that are used in local, regional and global models to investigate how biogenic volatile organic compounds and their resulting atmospheric chemistry influences air quality and climate-relevant composition. While much is known about the influence of these individual abiotic factors on monoterpene emissions, other factors, including weather events (e.g., Haase et al., 2011; Janson, 1993) and insect herbivory (e.g., Copolovici et al., 2011; Litvak & Monson, 1998), are less understood and their effects are not included in model predictions.

Few studies investigate the changes in monoterpene emissions due to extreme weather events. Extreme precipitation events are increasing in response to climate change (Trenberth et al., 2000). Both hail (Kaser et al., 2013) and summer storms (Haase et al., 2011) have been noted to increase overall monoterpene emissions. There are few studies that highlight the effects of seasonal snow events on summed monoterpene emissions (Holzinger et al., 2006). However, studies of CO_2 influence on both emitted and stored monoterpenes clearly show that changing

environmental conditions can cause different impacts across monoterpene isomers. Some isomers increase in response to a given change while others decrease – and that changes in summed monoterpenes do not reflect the complexity of speciated compounds (Loreto et al., 2001; Loreto & Schnitzler, 2010; Snow et al., 2003).

Here we summarize the changes of monoterpene emissions over the course of the first seasonal snow event, and the subsequent death (senescence) of the leaves. We investigate the changes in temperature response of these emissions. Our observations highlight the importance of considering speciated monoterpenes, as the chemical identity impacts reactivity with hydroxyl radicals and potential for secondary chemistry. We further provide the first description of monoterpene emissions from the Emerald City cultivar of Tulip Trees (*Liriodendron tulipifera* 'JFS-Oz'), the parent of which are often considered to be non-emitters of monoterpenes (Wang et al., 2016).

2. Methods

This study took place at the Colorado State University Arboretum (40° 34' 9" N, 105° 5' 31" W, 1546 m elevation) between 3 October and 15 October 2019. We measured the most abundant monoterpene emissions and photosynthesis on 6-15 leaves from a single plant before, during, and after the first seasonal snow event. Samples that were acquired prior to the snow event (3-9 October) are labelled "pre-snow", while those collected during snowfall (10 October) are "during", and those after snow (11-15 October) are "post-snow". Snow remained on the ground throughout the duration of the study, suggesting a limited role of water availability in controlling the observed VOC emissions.

We measured emissions from one mature and visually healthy *Liriodendron tulipifera* (tulip tree) of the Emerald City cultivar ('JFS-Oz') at least an hour and a half after sunrise and before sunset. We randomly selected leaves that were accessible by ground measurements (maximum 1.7 m above ground) and received direct sunlight for at least 1 hour during the day. Leaves were identified and tagged non-invasively so that they could be resampled throughout the course of the study.

We sampled monoterpene emissions using Tenax sorbent tubes (Markes Intl., C1-CXXX-5003) coupled with a portable photosynthesis system (LI-COR, Inc., LI-6800). The portable photosynthesis system monitors carbon dioxide (CO_2) and water with infrared gas analyzers before and after the leaf chamber to determine the CO_2 assimilation and stomatal conductance of the leaf. We subsample air flow before each infrared gas analyzer using two handheld low-flow pumps (Markes Intl. ACTI-VOC and Sensidyne Gilian LFS-113DC) onto sorbent tubes and use the difference to quantify emissions. We describe the interface between the PPS and sorbent tubes elsewhere (Riches et al., 2020).

The portable photosynthesis system was equipped with a 6 cm^2 leaf chamber and external light source (LI-COR, Inc. Multiphase Flash™ Fluorometer). We controlled air through the leaf chamber at a flow rate of 500 μmol s^{-1} (0.87 L min^{-1}), with a CO_2 concentration near ambient (414 ppm) and saturating light conditions (photon flux density = 2000 μmol m^{-2} s^{-1}). Unless otherwise stated, we maintained leaf temperature at 25 °C and relative humidity (RH) at 50%. During leaf sampling, we allow a leaf to reach a steady rate (5-40 min) in the chamber before collecting samples with the sorbent tubes. We simultaneously logged photosynthesis measurements once every 30 seconds. We altered either relative humidity or temperature to investigate perturbation effects on emissions, holding all other parameters constant. Relative humidity was difficult to

maintain above 40% during and after the snow event; we apply a correction factor determined by the fit parameters to account for varying RH.

Emission rates for some monoterpenes vary with RH (Schade et al., 1999). Of the eight monoterpene isomers we investigated, three (α-pinene, d-limonene, γ-terpinene) had a negative correlation between emission rate and RH ($r^2 > 0.9$), one (terpinolene) had a weakly negative correlation ($r^2 \approx 0.5$), and one (p-cymene) had a positive correlation ($r^2 = 0.7$). The other three monoterpenes (α-terpinene, β-pinene, β-ocimene) had no correlation to RH ($r^2 < 0.05$) (see S1 for details). We find no consistent relationship between the emission-RH correlation and chemical properties of the isomers. In particular, we find no pattern with octanol-air partition coefficients, octanol-water partition coefficients, volatility, or Henry's law constants. Further, compounds in the same families can behave differently. For example, α-pinene had a negative emission-RH correlation while β-pinene had none; α-terpinene had no correlation while terpinolene and γ-terpinene had a negative emission-RH correlation. p-Cymene is the one monoterpene that increased in emission rate with RH; while p-cymene uniquely contains an aromatic ring, its chemical properties are numerically similar to other monoterpenes. This observation suggests that RH impacts on VOC emission are unlikely driven by chemical properties, but that instead RH affects plant physiology, which in turn affects the expression of p-cymene uniquely from other compounds. It is worth noting that p-cymene is produced through the same biochemical pathway and at the same biosynthetic sites as other monoterpenes (Maffei, 2010). While we have no metric to investigate the physiological driver of p-cymene in this study, we suggest that the humidity dependence may be due more to storage of monoterpenes than the active biosynthesis of them.

We analyzed the sorbent tubes using a thermal desorption unit with an autosampler (Markes Intl., Unity-xr and Ultra-xr), which injected desorbed sample into a gas chromatograph

(Thermo Scientific TRACE 1310 with ZB-5HT-MS column) with mass spectrometry detection (Thermo Scientific TSQ 8000 Eco Triple Quadrupole GC-MS/MS; electron impact source). Riches et al. (2020) provides further details on the thermal desorption and subsequent gas chromatography mass spectrometry of the samples.

We analyzed all data using Igor Pro 7.07 (Wavemetrics, Inc.). Our in-house chromatography analysis procedure creates and subtracts a baseline, then locates and integrates peaks from each chromatogram. The software also generated and applied calibration curves for α-pinene, β-pinene, α-terpinene, γ-terpinene, d-limonene, β-ocimene, p-cymene and terpinolene based on known standard samples. Once calibrated, each value was normalized for sampling time, background subtracted, and converted to an emission rate (ng m^{-2} min^{-1}).

3. Results and discussion

Photosynthesis and stomatal conductance were largely positive pre-snow, except for a single leaf which remained dormant through the entirety of the study. During the snow event, however, photosynthesis was quenched, and all leaves but one showed negligible photosynthesis. This decrease was immediate and persisted for the remainder of the study (Figure 3.1).

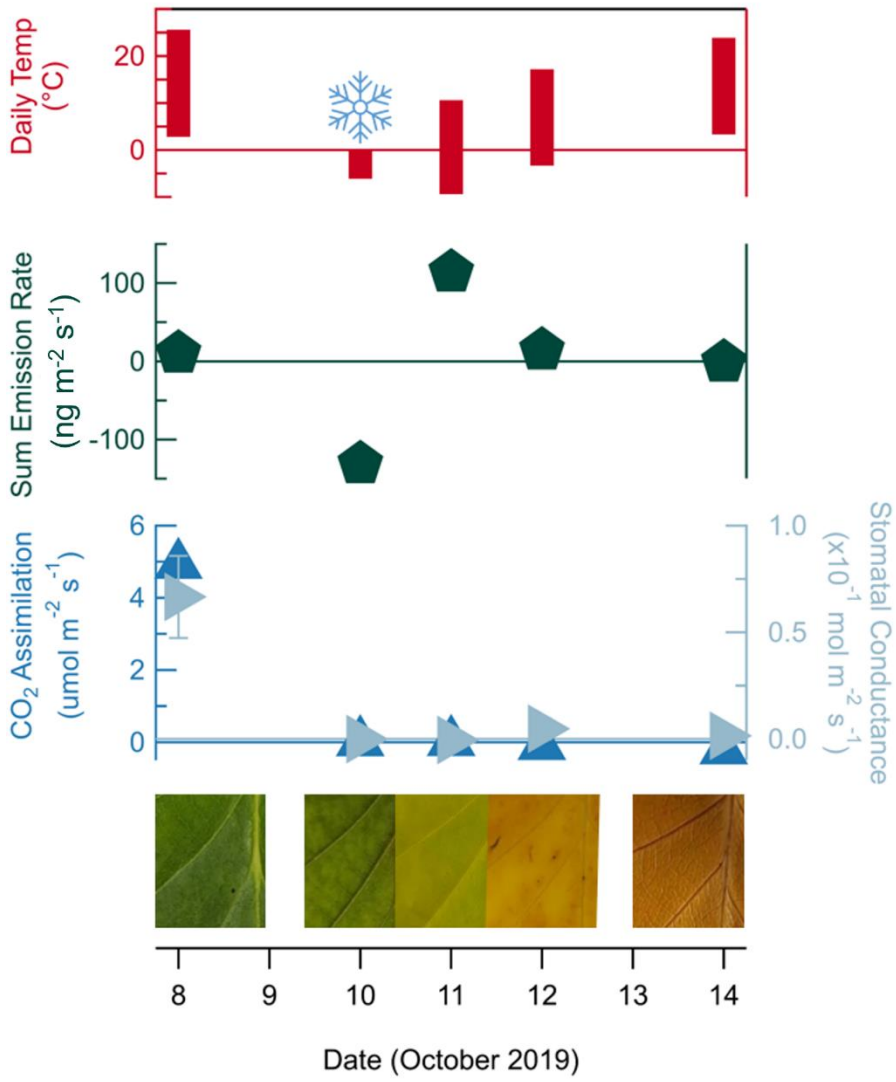

Figure 3.1. Daily temperature ranges (red bars), sum monoterpene emission rate (dark green pentagons), leaf senescence (photos), CO_2 assimilation (dark blue upright triangles), and stomatal conductance (light blue right triangles) over the duration of the study. Snowflake indicates the first seasonal snow. These results and their associated photographs are for a single leaf. Whiskers on CO_2 assimilation and stomatal conductance are standard deviation.

Monoterpene emissions, however, did not follow photosynthesis throughout the study (Figure 3.1). Emission independent of stomatal conductance agrees with previous studies (e.g., Owen et al., 2002). However, the temporal response of emissions differed for each isomer, and the overall effects of snow changed day-by-day (Figure 3.2), highlighting the complexity of the impact of snow on the plant. Pre-snow, there was a net emission of monoterpenes, with limonene

dominating the emission profile. During snow, leaves largely acted as a monoterpene sink, with the notable exception of limonene, which continued to emit. However, the very next day, net emission trended positive, with nearly all monoterpenes emitted including β-ocimene, which until this point had always been taken up by the leaves. Two days following snow, the emission profile resembled pre-snow conditions, but after four days, there was an inversion between limonene and β-ocimene, with the former driving the uptake and the latter becoming the dominant positive emission.

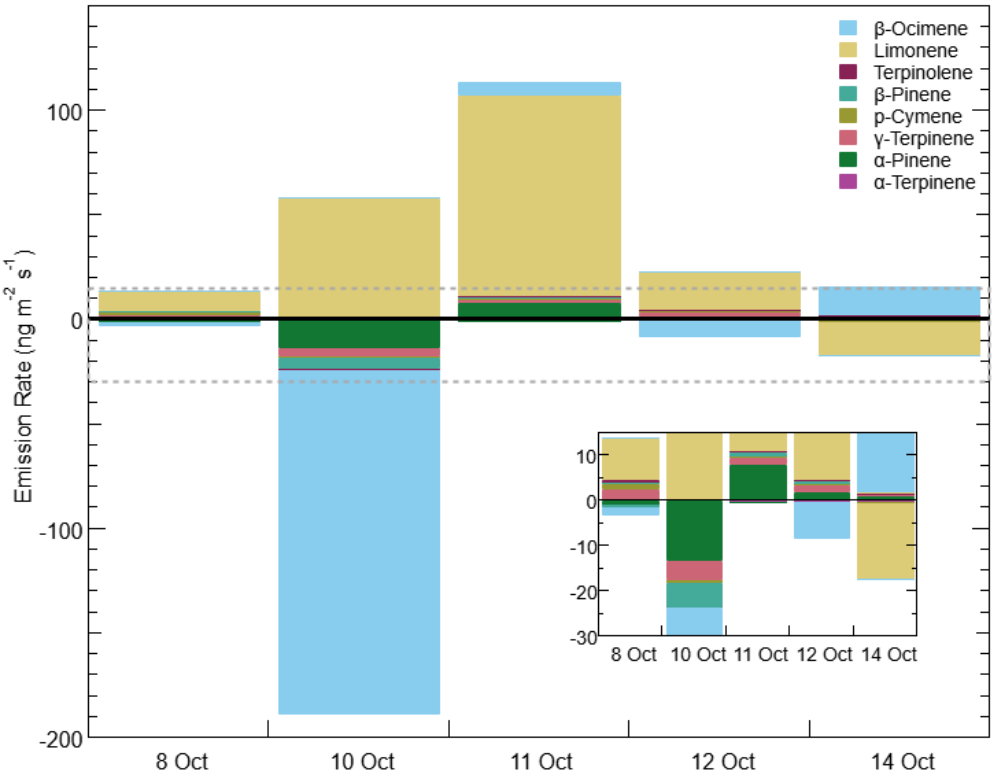

Figure 3.2. Stacked bar chart of daily emission rate of eight monoterpenes on a single leaf. Insert highlights the region between -30 and 15 ng m^{-2} s^{-1}. A negative emission rate indicates leaf-level uptake of the compound.

Although daily temperatures were similar on 8 October and 14 October, monoterpene emissions except for β-ocimene were largely quenched by the latter date. The suppression of α-pinene emissions upon senescence has been previously observed in rubber trees (*Hevea brasiliensis*, Chen & Cao, 2008); however, while their study also noted suppressed β-pinene emissions, we observe no change. Unlike previous observations by Holzinger et al. (2006), the increase in post-snow emissions were short lived. The difference in these observations is likely in part due to differences in plant species, ours not being an evergreen species and thus less resilient to the impacts of snow.

Even as leaves undergo senescence and are photosynthetically inactive, leaves remain a source and sink for different monoterpenes (Faiola et al., 2014; Isidorov et al., 2010). The release of monoterpenes could be a result of a) previously synthesized monoterpenes that are stored within the leaf being emitted, or b) ongoing physiological functions that actively synthesize monoterpenes (Owen & Peñuelas, 2005). As we show, at no point do we find a consistent response of monoterpene emissions to snow, as the overall trend post-snow is complex. Further work is necessary to determine the underlying physiological mechanism for these emission changes, but the literature suggests several possible mechanisms. Schollert et al. (2017) found that snow addition enhanced sesquiterpene, but not monoterpene, emission and altered leaf anatomy (via the density of glandular trichomes and proportion of spongy mesophyll). Kaser et al. (2013) attributed increases in emissions due to mechanical damage; senescent damage is thought to increase emissions due to degradation of cellular structures and oorganelles andimprove diffusion through the damaged cuticle and epidermis of the leaf (Mozaffar et al., 2018; Rottenberger et al., 2005).

Additionally, although the leaves were perceived to be dry during the study, water films can still exist and can influence both uptake and emission of volatile organic compounds (Fulgham

et al., 2020). Structural changes to the leaf's epicuticular wax occur as a result of snow (Grodzińska-Jurczak, 1998), which can in turn affect the emission of monoterpenes (Despland et al., 2016). Further investigation of leaf physiological changes and thus VOC emissions are necessary for tulip trees and other lesser studied emitting species.

The contribution of emitted monoterpenes to atmospheric hydroxyl radical reactivity further differs by day (Figure 3.3). Pre-snow, the overall monoterpene contribution was dominated by limonene. d-Limonene also dominated hydroxyl radical reactivity until the end of senescence (14 October), at which point β-ocimene almost exclusively dominated (>96%) OH reactivity. Both on 10 October and 14 October, where net emissions were negative (i.e., indicating net uptake of monoterpenes), we saw an increased hydroxyl radical reactivity compared to pre-snow conditions. This slight increase in the more reactive β-ocimene drives the increase in hydroxyl radical reactivity, despite the suppression of d-limonene emissions. Without isomeric speciation, the overall decrease in emitted monoterpenes would incorrectly suggest a decrease in hydroxyl radical reactivity, thus underestimating the atmospheric burden of snow.

We investigate the contribution of measured emissions to potential SOA formation using SOA yields from Lee et al. (2006), though we note that yields for many of these isomers are poorly constrained in the literature. In addition to limonene's dominance in emission rate and OH reactivity up to 4 days after snow, limonene dominates SOA formation over this period, contributing to over 90% of SOA formation until 14 October. Due to the low SOA yield (<1% per Morales et al. (2021)), β-ocimene's contribution to SOA is negligible until 14 October. By the end of measurements (14 October), SOA contributors become more diverse, with substantial contributions from α-pinene (>50%), β-ocimene (>20%), β-pinene (>10%), and terpinolene (>5%), when calculated considering SOA yields from Lee et al. (2006).

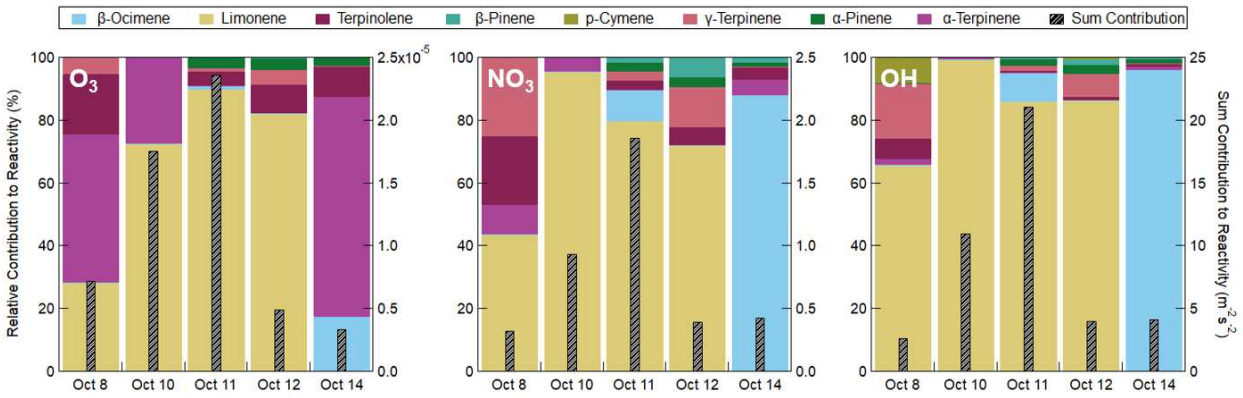

Figure 3.3. Stacked bar charts of the relative contribution of each monoterpene (left axis) and sum contribution to reactivity (right axis) for ozone (left plot), NO3 (center plot), and hydroxyl radical (right plot). Snow began on 10 October. Sum contribution to reactivity is relative to volume sampled through sorbent tubes (4L) and presented as a proxy to provide context for fractional reactivity; units are provided as reactivity per meter squared of leaf area per second. Reaction rate constants used for these calculations are detailed in the SI.

Consistent with previous plant surveys (Farmer & Riches, 2020), pre-snow CO_2 assimilation, stomatal conductance, and monoterpene isomers varied substantially across leaves of the same plant (Figure 3.4). This exceptional variability is consistent with previous survey measurements. For example, we see a 31% relative standard deviation in limonene emissions, comparable to the 35% seen by Dominguez-Taylor et al. (2007) (*Pinus patula,* October) and the 33% seen by Farmer and Riches (2020) (*Citrus limon x Citrus medica*, Summer). We note that these values differ greatly by species; for example, Kim et al. (2005) observed a 96% relative standard deviation in limonene emission in *Pinus koraiensis*. This variability is likely higher than that of the summer months, as previously reported (Kim et al., 2005; Malik et al., 2019; Staudt et al., 2002). Between 8 October and 14 October, which had comparable daily temperatures (Figure 3.1) and where RH was maintained at 50%, most monoterpene emission rates decreased. However, not all monoterpenes followed this trend. For example, despite being in the same family, α-pinene showed a significant decrease while β-pinene had no significant change. Despite the overall

decrease in monoterpene emissions, the leaf-to-leaf variability in isomer emissions generally increased, except for d-limonene. Two isomers behave differently from the other monoterpenes, with enhanced emissions after the snow event: β-ocimene and β-pinene. The leaf-to-leaf variability of β-ocimene decreased substantially, with the relative standard deviation dropping from 750% pre-snow to 75% post-snow. The impact of this variability extends beyond direct emissions to the subsequent atmospheric impact. For example, differences in β-ocimene emission dominates hydroxyl radical and NO_3 reactivity, but it is the smaller change in α-terpinene emission rates (Figure 3.2) that dominates ozone reactivity (Figure 3.3). Thus, the SOA forming potential with regards to OH differs drastically throughout the observational period, from the snow day (over 5x that of pre-snow) to the following monoterpene burst day (over 10x that of pre-snow), decaying down by the last day of measurements (a tenth of pre-snow).

Senescence thus either enhances or suppresses speciated monoterpene emissions – but it does so in a consistent manner for any given isomer. The differences in variability again do not trend with photosynthesis, where CO_2 assimilation and stomatal conductance both saw a significant decrease in leaf-to-leaf variability.

The temperature dependence of monoterpene emission rates on pre-snow and post-snow days were not consistent, despite the two sampling days (8 October and 14 October, respectively) having comparable ambient temperatures. In contrast to monoterpene emissions, the overall shape of the temperature response curve for CO_2 assimilation was consistent across these sample days. This observation suggests that the plant retains some metabolic functionality (i.e. are able to take up and metabolize CO_2), even as senescence develops.

While the shape of CO_2 assimilation response remained the same pre-snow and post-snow (Figure 3.5c), monoterpene isomers were affected in one of three ways: enhancement, diminution,

or no change. Three species saw an enhancement of the temperature response (β-ocimene, β-pinene, and α-pinene). Two species saw a diminution of the temperature response (γ-terpinene and terpinolene). Three species saw no clear change in the temperature response (α-terpinene, d-limonene, and p-cymene). Figure 3.5 shows a representative example of enhancement (5a) and diminution (5b) in the temperature responses. We once again identify differences in species of the same structural families (α-terpinene and γ-terpinene), and no relationship between physical properties and snow-induced impact on emission profiles of different monoterpene isomers.

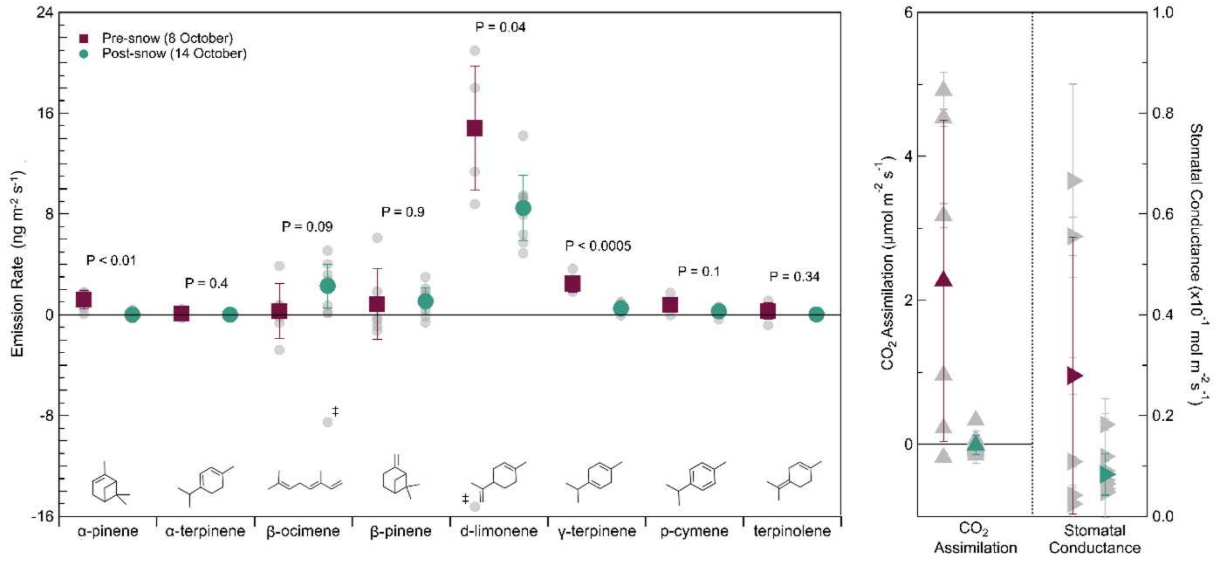

Figure 3.4. Emission rate of eight monoterpene isomers before a snow event (pre-snow, 8 October, red squares are average; grey are individual leaves) and after a snow event (post-snow, 14 October, teal circles) on several leaves (n=6 pre-snow, n=10 post-snow), as well as CO_2 assimilation (up triangles) and stomatal conductance (sideways triangles). Data was collected on days of comparable temperature (Figure 3.1). Whiskers represent standard deviation, and P-values are results of pre- vs post-snow T-tests. Outliers are labeled with a double dagger. RH was maintained at 50% on both days, so no correction factor has been applied.

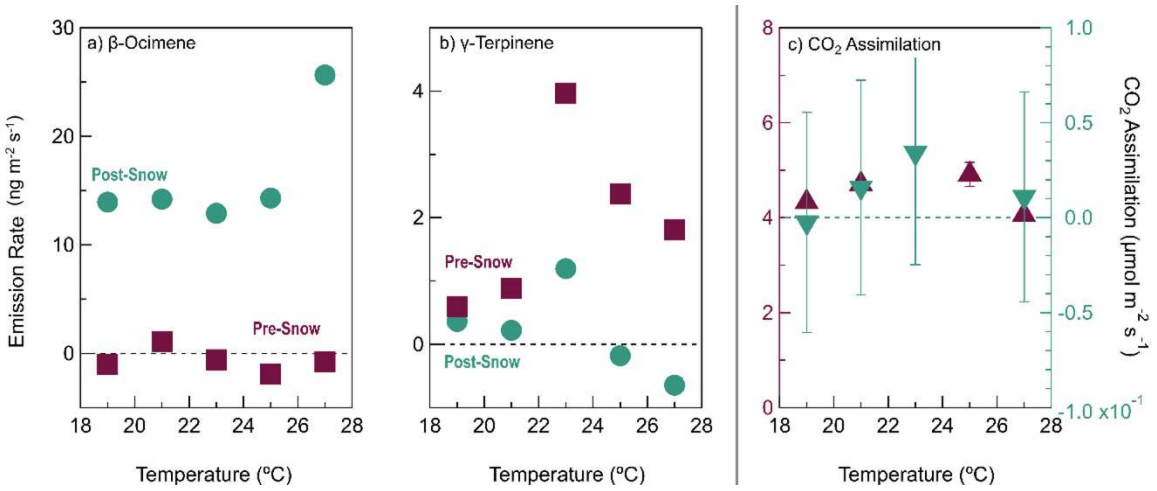

Figure 3.5. Emission rates of β-ocimene (a) and γ-terpinene (b) as leaf temperature changes. CO_2 assimilation (c) response curves are also shown. Emission rates pre-snow (October 8, red squares) and post-snow (October 14, teal circles) are representative of other compounds. CO_2 assimilation shows pre-snow (red triangles, left axis) and post-snow (teal inverted triangles, right axis). Results are for a single leaf. Whiskers denote standard deviation.

4. Conclusion

Biogenic emission models such as the Model of Emissions of Gases and Aerosols from Nature version 2.1 (MEGAN2.1) provide a much-needed simplification of the major processes that drive volatile organic compound emissions but can miss the complex role of environmental conditions in affecting plant emissions. However, in that simplification, the complex role of environmental conditions that affect plant emissions may be underrepresented. For example, MEGAN 2.1 considers emissions to be dominantly driven by light and temperature (Guenther et al., 2012), but underestimates monoterpene emissions during weather events including seasonal storms (Haase et al., 2011; Holzinger et al., 2006). Holzinger (2006) found that the model underpredicted the emissions resulting from the first seasonal snow by 300%, highlighting the opportunity for improvement in these models.

One such opportunity may be to introduce a burst leaf-age proxy (e.g., mature to senescent over the course of days rather than weeks/months) to align with the first seasonal snowfall (e.g.,

seasonal precipitation under freezing temperatures) for deciduous species. However, additional studies would need to corroborate emission profiles between snow and non-snow senesced leaves.

Our measurements here further demonstrate that the monoterpene cassettes measured during standard atmospheric conditions are often not representative of those emitted during and after weather events. Extreme weather events are increasing with climate change (National Academies of Sciences & Medicine, 2016), and weather-induced changes in plant volatile emissions may be relevant to climate feedbacks and air quality through contributions to OH reactivity and potential formation of secondary organic aerosol. Our measurements further highlight the potential for ambient relative humidity to impact monoterpene emissions and remains an environmental driver of interest in understanding biogenic emissions.

The prevalence of proton transfer reaction mass spectrometry measurements means that atmospheric measurements of monoterpenes are not commonly segregated by isomers. Biogenic emissions models often only distinguish a sub-set of these isomers. Our results show that lumping isomers in models or measurements would limit our capacity to capture changes in emissions and OH reactivity. For example, limonene, β-ocimene, α-pinene and β-pinene would be distinguished in MEGAN2.1, while p-cymene, α-terpinene, γ-terpinene and terpinolene – accounting for over 25% of pre-snow emissions – would be grouped together.

All leaves do not behave identically in terms of monoterpene emission or plant physiology, even on the same plant. Leaf-to-leaf variability remains an important factor to consider during experimental design of measurements and in sensitivity analyses of model emissions. In the case of d-limonene in standard, pre-snow conditions, our measurements show that a single leaf could be up to 133% different from the mean of 4 leaves (outlier omitted). This observed variance in

leaf-to-leaf variability confirms the need for more comprehensive measurements for constraining model parameterizations.

Models are further limited by the number of available studies to constrain plant emissions. Tulip trees are considered monoterpene non-emitters (Wang et al., 2016), though our study supports the findings of Matsunaga et al. (2017), who showed that specific cultivars of otherwise non-emitting species can emit substantial quantities of biogenic hydrocarbons. Thus cultivar-to-cultivar variability is an additional form of variance that must be considered in field measurements and selection of data for model development.

While storms are typically sporadic deviations from normal weather conditions, our data demonstrate that such events can substantially impact biogenic emissions in complex, isomer-specific ways. The extent to which monoterpene emission profiles change over time due to repeated weather events remains an open question for future measurements. These storm-specific, speciated VOC studies with adequate variability constraints are vital to provide the context necessary to improve biogenic emission models.

Support statement

We thank the National Science Foundation (grants 1614315 and 1932849) and the Eppley Foundation for Research for funding. We also thank ARC-MMA at Colorado State University for instrumental support. Additional thanks to Tyson Berg, Alex Riches, and Nathan Gasparovic for assistance in sample collection.

References

Atkinson, R. (1990). Gas-phase tropospheric chemistry of organic compounds: a review. *Atmospheric Environment. Part A. General Topics, 24*(1), 1-41.

Bonn, B., Magh, R.-K., Rombach, J., & Kreuzwieser, J. (2019). Biogenic isoprenoid emissions under drought stress: different responses for isoprene and terpenes. *Biogeosciences, 16*(23), 4627-4645.

Chen, J.-W., & Cao, K.-F. (2008). Changes in activities of antioxidative system and monoterpene and photochemical efficiency during seasonal leaf senescence in Hevea brasiliensis trees. *Acta Physiologiae Plantarum, 30*(1), 1-9.

Copolovici, L., Kännaste, A., Remmel, T., Vislap, V., & Niinemets, Ü. (2011). Volatile emissions from Alnus glutionosa induced by herbivory are quantitatively related to the extent of damage. *Journal of Chemical Ecology, 37*(1), 18-28.

Faiola, C. L., Buchholz, A., Kari, E., Yli-Pirilä, P., Holopainen, J., Kivimäenpää, M., et al. (2018). Terpene composition complexity controls secondary organic aerosol yields from scots pine volatile emissions. *Scientific reports, 8*(1), 1-13.

Faiola, C. L., VanderSchelden, G. S., Wen, M., Elloy, F. C., Cobos, D. R., Watts, R. J., et al. (2014). SOA formation potential of emissions from soil and leaf litter. *Environmental science & technology, 48*(2), 938-946.

Farmer, D. K., & Riches, M. (2020). Measuring Biosphere–Atmosphere Exchange of Short-Lived Climate Forcers and Their Precursors. *Accounts of Chemical Research, 53*(8), 1427-1435.

Guenther, A., Hewitt, C. N., Erickson, D., Fall, R., Geron, C., Graedel, T., et al. (1995). A Global-Model of Natural Volatile Organic-Compound Emissions. *Journal of Geophysical Research-Atmospheres, 100*(D5), 8873-8892.

Guenther, A., Jiang, X., Heald, C. L., Sakulyanontvittaya, T., Duhl, T., Emmons, L., & Wang, X. (2012). The Model of Emissions of Gases and Aerosols from Nature version 2.1 (MEGAN2. 1): an extended and updated framework for modeling biogenic emissions. *Geoscientific Model Development, 5*(6), 1471-1492.

Guenther, A., Zimmerman, P. R., Harley, P. C., Monson, R. K., & Fall, R. (1993). Isoprene and monoterpene emission rate variability: model evaluations and sensitivity analyses. *Journal of Geophysical Research: Atmospheres, 98*(D7), 12609-12617.

Haase, K. B., Jordan, C., Mentis, E., Cottrell, L., Mayne, H., Talbot, R., & Sive, B. (2011). Changes in monoterpene mixing ratios during summer storms in rural New Hampshire (USA). *Atmospheric Chemistry and Physics, 11*(22), 11465-11476.

Holzinger, R., Lee, A., McKay, M., & Goldstein, A. (2006). Seasonal variability of monoterpene emission factors for a ponderosa pine plantation in California. *Atmospheric Chemistry and Physics, 6*(5), 1267-1274.

Isidorov, V., Smolewska, M., Purzyńska-Pugacewicz, A., & Tyszkiewicz, Z. (2010). Chemical composition of volatile and extractive compounds of pine and spruce leaf litter in the initial stages of decomposition. *Biogeosciences, 7*(9), 2785-2794.

Janson, R. W. (1993). Monoterpene emissions from Scots pine and Norwegian spruce. *Journal of geophysical research: atmospheres, 98*(D2), 2839-2850.

Jardine, K. J., Jardine, A. B., Holm, J. A., Lombardozzi, D. L., Negron-Juarez, R. I., Martin, S. T., et al. (2017). Monoterpene 'thermometer'of tropical forest-atmosphere response to climate warming. *Plant, cell & environment, 40*(3), 441-452.

Kaser, L., Karl, T., Guenther, A., Graus, M., Schnitzhofer, R., Turnipseed, A., et al. (2013). Undisturbed and disturbed above canopy ponderosa pine emissions: PTR-TOF-MS

measurements and MEGAN 2.1 model results. *Atmospheric Chemistry and Physics, 13*(23), 11935-11947.
Kesselmeier, J., & Staudt, M. (1999). Biogenic volatile organic compounds (VOC): an overview on emission, physiology and ecology. *Journal of atmospheric chemistry, 33*(1), 23-88.
Kuhn, U., Rottenberger, S., Biesenthal, T., Wolf, A., Schebeske, G., Ciccioli, P., et al. (2004). Seasonal differences in isoprene and light-dependent monoterpene emission by Amazonian tree species. *Global Change Biology, 10*(5), 663-682.
Litvak, M. E., & Monson, R. K. (1998). Patterns of induced and constitutive monoterpene production in conifer needles in relation to insect herbivory. *Oecologia, 114*(4), 531-540.
Loreto, F., Fischbach, R. J., Schnitzler, J. P., Ciccioli, P., Brancaleoni, E., Calfapietra, C., & Seufert, G. (2001). Monoterpene emission and monoterpene synthase activities in the Mediterranean evergreen oak Quercus ilex L. grown at elevated CO2 concentrations. *Global Change Biology, 7*(6), 709-717.
Loreto, F., & Schnitzler, J.-P. (2010). Abiotic stresses and induced BVOCs. *Trends in plant science, 15*(3), 154-166.
Maffei, M. E. (2010). Sites of synthesis, biochemistry and functional role of plant volatiles. *South African Journal of Botany, 76*(4), 612-631.
Matsunaga, S. N., Shimada, K., Masuda, T., Hoshi, J., Sato, S., Nagashima, H., & Ueno, H. (2017). Emission of biogenic Volatile Organic compounds from trees along streets and in Urban Parks in tokyo, Japan. *Asian Journal of Atmospheric Environment, 11*(1), 29-32.
National Academies of Sciences, E., & Medicine. (2016). *Attribution of extreme weather events in the context of climate change*: National Academies Press.
Nishimura, H., Shimadera, H., Kondo, A., Bao, H., Shrestha, K. L., & Inoue, Y. (2015). Evaluation of light dependence of monoterpene emission and its effect on surface ozone concentration. *Atmospheric Environment, 104*, 143-153.
Owen, S., Harley, P., Guenther, A., & Hewitt, C. (2002). Light dependency of VOC emissions from selected Mediterranean plant species. *Atmospheric Environment, 36*(19), 3147-3159.
Owen, S., & Peñuelas, J. (2005). Opportunistic emissions of volatile isoprenoids. *Trends in plant science, 10*(9), 420-426.
Riches, M., Lee, D., & Farmer, D. K. (2020). Simultaneous leaf-level measurement of trace gas emissions and photosynthesis with a portable photosynthesis system. *Atmospheric Measurement Techniques, 13*(8), 4123-4139.
Schade, G. W., Goldstein, A. H., & Lamanna, M. S. (1999). Are monoterpene emissions influenced by humidity? *Geophysical Research Letters, 26*(14), 2187-2190.
Singh, H. B. (1995). *Composition, chemistry, and climate of the atmosphere*: Van Nostrand Reinhold New York.
Snow, M. D., Bard, R. R., Olszyk, D. M., Minster, L. M., Hager, A. N., & Tingey, D. T. (2003). Monoterpene levels in needles of Douglas fir exposed to elevated CO2 and temperature. *Physiologia Plantarum, 117*(3), 352-358.
Staudt, M., Rambal, S., Joffre, R., & Kesselmeier, J. (2002). Impact of drought on seasonal monoterpene emissions from Quercus ilex in southern France. *Journal of Geophysical Research: Atmospheres, 107*(D21), ACH 15-11-ACH 15-19.
Staudt, M., & Seufert, G. (1995). Light-dependent emission of monoterpenes by holm oak (Quercus ilex L.). *Naturwissenschaften, 82*(2), 89-92.

Tingey, D. T., Manning, M., Grothaus, L. C., & Burns, W. F. (1980). Influence of light and temperature on monoterpene emission rates from slash pine. *Plant Physiology, 65*(5), 797-801.

Trenberth, K. E., Miller, K., Mearns, L., & Rhodes, S. (2000). *Effects of changing climate on weather and human activities*. Retrieved from

Wang, B., Shugart, H. H., Shuman, J. K., & Lerdau, M. T. (2016). Forests and ozone: Productivity, carbon storage and feedbacks. *Scientific reports, 6*(1), 1-7.

Wu, C., Pullinen, I., Andres, S., Carriero, G., Fares, S., Goldbach, H., et al. (2015). Impacts of soil moisture on de novo monoterpene emissions from European beech, Holm oak, Scots pine, and Norway spruce. *Biogeosciences, 12*(1), 177-191.

CHAPTER 4

HUMIDITY AND TEMPERATURE AS DISCRETE AND SYNERGISTIC DRIVERS OF VOLATILE ORGANIC COMPOUND EMISSION AND PHOTOSYNTHESIS[4]

1. Introduction

Plants are the largest source of nonmethane volatile organic compounds to the atmosphere, with ~90% of global emission into the atmosphere coming from biogenic sources (Monson, 2002) and half of global volatile organic compound emissions coming from tropical woodlands (Guenther et al., 1995). The oxidation of these biogenic volatile organic compounds (BVOCs) in the atmosphere leads to secondary organic aerosol formation and ozone production (Fuentes et al., 2000; Scott et al., 2014), meaning that BVOC emissions impact human health (Kumar et al., 2019; Nel, 2005), climate (Peñuelas & Staudt, 2010; Stocker, 2014), forest ecosystem wellness (Franz et al., 2018; Matyssek & Sandermann, 2003), and crop productivity (Bhatia et al., 2012; Mahmood et al., 2020). Understanding BVOC emissions adequately for modeling is clearly important for accurate predictions of climate and air quality relevant parameters. However, the identity and quantity of BVOC emissions by plants is dependent on several factors including temperature and light (Harley et al., 2014; Sharkey & Loreto, 1993; Tarvainen et al., 2005; Tingey et al., 1980), though other notable forces include pathogens (Scala et al., 2013), drought (Ebel et al., 1995), and humidity (Lamb et al., 1993). The role of these parameters on BVOC emissions is poorly understood for many ecosystems.

[4] Riches M, Alwe H, Millet D, Farmer DK. *Manuscript in preparation*.

BVOCs represent a diverse class of compounds that are highly reactive in the atmosphere despite observed atmospheric mixing ratios on the order of parts-per-trillion (ppt) to parts-per-billion (ppb) (Kesselmeier & Staudt, 1999). While isoprene (C_5H_8) dominates BVOC emissions globally, other VOCs such as monoterpenes ($C_{10}H_{16}$) account for ~15% of global BVOC emissions and are dominant emissions over pine forests (Guenther et al., 2012). Monoterpenes are often measured as an integrated sum, but this class of compounds includes numerous isomers such as limonene, α-pinene, β-pinene, and β-ocimene. The reactivity of these isomers varies substantially – for example, ozone reaction rate constants cover three orders of magnitude (Griffin et al., 1999) and secondary organic aerosol yields are likewise variable, for example yields for β-ocimene are < 1% (Morales et al., 2021) whereas yields for β-pinene are ~50% (Mutzel et al., 2016). BVOCs that are emitted in low quantities can have an out-sized effect on the atmosphere, meaning that a comprehensive understanding of BVOC emissions, their speciation, and the factors that control their emissions is essential to accurately predict reactivities and secondary organic aerosol formation.

Current models provide a much-needed simplification for the estimation of BVOC emissions, but the sparsity and incongruity of observational constraints lead to disparities between modeled and observed emissions. The Model of Emissions of Gases and Aerosols in Nature (MEGAN) is widely used to extrapolate leaf and canopy level observations using leaf area, temperature, light, and plant functional type, among other parameters (Guenther et al., 2012). However, due to a lack of observational constraints, these models do not well integrate key environmental parameters like senescence (Gomez et al., 2021), weather events (Kaser et al., 2013), and severe drought (Opacka et al., 2022). With limited measurements, BVOC emissions from plant functional types such as cropland trees (Mishra et al., 2021), crops (Gomez et al., 2021)

and understory species (Šimpraga et al., 2019) are also often underrepresented. Widespread geographical data is also lacking, leading to underestimations in urban (Gao et al., 2022; Ma et al., 2021) and arctic (Opacka et al., 2021) regions. As far as chemical speciation, MEGAN considers ~150 compounds which are separated into 19 compound classes, including 10 speciated terpenes, a class for other monoterpenes, and a class for other sesquiterpenes. With the diversity of BVOCs emissions, there are compounds excluded from MEGAN including compounds like methyl vinyl ketone and methacrolein, which are confirmed to be directly emitted from plants (Jardine et al., 2012), in addition to the longstanding acknowledgement of their existence as atmospheric oxidation products of isoprene. Finally, the short-term nature of these measurements means that broader meteorological or other effects may reduce the accuracy of these emissions; inter-annual comparison of data collected at the same location may alleviate this challenge (Clifton et al., 2020; He et al., 2021).

Much work has been done on coniferous evergreens, providing a solid basis upon which additional parameters can be built; by developing a more thorough understanding of a single ecosystem and a single species we can improve upon existing models. Coniferous evergreen forests make up 20% of global tree cover (UNEP, 2020) and several studies have investigated BVOC emissions across both boreal and temperate forests (e.g., Borbon et al., 2004; Fulgham et al., 2019; Hakola et al., 2003; Harrison et al., 2001; Holzinger et al., 2006; Kaser et al., 2013; Müller et al., 2006; Ortega et al., 2014; Schade & Goldstein, 2001; Son et al., 2015). Ponderosa pine (*Pinus ponderosa)* has been a focus in literature. Previous studies have included gas-phase, aerosol and reactivity measurements at the canopy level (Fulgham et al., 2019; Link et al., 2021; Nakashima et al., 2014; Zhou et al., 2015), branch-enclosure measurements (Bouvier-Brown et al.,

2009; Fulgham et al., 2019; Kaser et al., 2013; S. Kim et al., 2010), and leaf-level measurements (Harley et al., 2014; Kaser et al., 2013).

Leaf-level emission studies investigate the direct effects of different parameters necessary for the observational constraints of models. However, the leaf-to-leaf and plant-to-plant emissions can vary substantially (Dominguez-Taylor et al., 2007; Farmer & Riches, 2020; Guenther et al., 1993; Kim et al., 2005), so a thorough investigation of variability is necessary for measurements such as these. While variability is indisputable, trends in emission forcers tend to remain representative. BVOC emissions of ponderosa pine are largely temperature and light dependent, though there remains discussion as to whether emissions are influenced by photosynthetic parameters (Harley et al., 2014; Kaser et al., 2013; Lamanna & Goldstein, 1999; Lerdau et al., 1994; Schade & Goldstein, 2001, 2002). Furthermore, there remains few studies or parameterization on the effects of humidity on BVOC emissions, despite its precedence as an influencer of such emissions (Schade et al., 1999). To improve our understanding of the drivers behind BVOC emissions, we must revisit these well-established sites and investigate variability and understudied parameters like humidity.

Here, we investigate the discrete and combined effects of temperature and humidity on leaf-level BVOC emissions and photosynthesis at a well-characterized semi-rural field site. We summarize findings of seven compounds, from their emission rates to their implications on atmospheric chemistry, and we suggest revisions the commonly used MEGAN model to account for changes in relative humidity. Finally, we address the needle-level variation and recommend considerations moving forward with conducting leaf-level measurements and interpreting such data.

2. Methods

2.1 Field site description

The Flux Closure Study (FluCS) took place at the Manitou Experimental Forest Observatory in Woodland Park, Colorado, USA. The field site is located at 39.1006°N, 105.0942°W, approximately 83 km southwest of Denver, Colorado, and 30 km northwest of Colorado Springs, Colorado, and 16 km north of the nearest town, Woodland Park, Colorado. The research facility is a semi-arid montane forest with primarily ponderosa pine (*Pinus ponderosa*) trees. This site is well described by Ortega et al. (2014).

2.1.1 Meteorological information

We made measurements between 25 August through 24 September 2020 and 7 August through 26 September 2021. The summer of 2020 was characterized by periods of intense, aged smoke largely due to wildfires in California and Colorado. The median daytime temperature was 21 °C and the median daytime humidity was 26% relative humidity. Snow fell on 9 September, and temperatures between 8 and 10 September were unusually cold, with a low of -4 and high of 12 °C. There was 29 mm of precipitation; 7 mm fell during the snowstorm and 20 mm fell by 30 August, leading to a substantial period of dryness. The summer of 2021 had less transported wildfire smoke and more frequent thunderstorms. The median daytime temperature was 24 °C and the median daytime humidity was 23% relative humidity. The 25 mm of precipitation that fell in 2021 was spread throughout the season.

The National Center for Atmospheric Research Atmospheric Chemistry Observations and Modeling (https://doi.org/10.5065/D61V5CDP) provides additional meteorological data (accessed on 2 May 2022) and the National Oceanic and Atmospheric Administration (NOAA) JSTAR Mapper (https://star.nesdis.noaa.gov/jpss/mapper) provides qualitative representations of smoke intensity (accessed on 2 May 2022).

2.2 Measurements

We coupled a portable photosynthesis system with a proton transfer reaction quadrupole-interface time-of-flight mass spectrometer (PTR-QiTOF) and sorbent tubes for analysis using thermal desorption gas chromatography mass spectrometry (TD-GC/MS). We made measurements with the PTR-QiTOF throughout the summer of 2020, accompanied by occasional measurements with the TD-GC/MS. The summer 2021 measurements were made exclusively by TD-GC/MS.

We describe the coupling of the portable photosynthesis system with online and offline chemical instrumentation in detail elsewhere (Riches et al., 2020). The portable photosynthesis system subsamples air both prior to and following the leaf enclosure. Two 30 m heated inlets (PFA Teflon, ¼" o.d.; Clayborn Labs, California, USA) kept at 50 °C connect the subsampling ports to a sampling manifold that switches between pre- or post-leaf emissions at any given time. For TD-GC/MS measurements, we pull air directly from the subsampling ports through the sorbent tubes. Total flow from the portable photosynthesis system is kept below 3 L min^{-1}, with mass spectrometers receiving dilution from ultra-high purity nitrogen or zero air as needed.

For each measurement, we enclosed 9 to 10 needles in the chamber of the portable photosynthesis system and allowed them to acclimate until CO_2 assimilation and stomatal conductance stabilized. Selected needles were at least 7 cm in length and visually appeared healthy. Leaf area of the sampled needles were calculated using the 6 cm of length that occupied the chamber and the radius (measured by digital calipers) to calculate area based on fascicles of two or three needles (Svenson & Davies Jr, 1992).

We describe measurements herein as the emission rate of each compound per leaf area (nmol m^{-2} min^{-1}). These numbers are derived from the difference in post-leaf and pre-leaf emissions, over a given time and per unit of leaf area.

2.2.1 *Experiments*

We conducted two types of experiments: i) response curves, wherein either temperature or humidity changed while other environmental parameters remained constant and ii) survey measurements, wherein environmental conditions remained the same as we measured different bundles of needles. Unless otherwise noted, relative humidity was maintained at 50%, temperature at 25 °C, light at 750 μmol m^{-2} s^{-1} photon flux density, and CO_2 at 400 parts-per-million (ppm).

2.3 *Instrumentation*

2.3.1 *Portable Photosynthesis System*

The portable photosynthesis system (LI-6800, LI-COR, Nebraska, USA) clamps onto the needles and controls the temperature, light, CO_2, and humidity within the leaf chamber. To control these parameters, ambient air travels through a column of soda lime to remove CO_2, a column of Drierite to remove water, and a column of stuttgarter masse to add water, after which additional CO_2 is added as necessary. A heat exchange unit near the chamber regulates temperature, and a light source (LI-6800-03, LI-COR, Nebraska, USA) maintains light intensity and color.

The portable photosynthesis system uses two infrared gas analyzers to determine the water and CO_2 exchange of the leaf and calculates several physiological parameters including CO_2 assimilation, stomatal conductance, and leaf vapor pressure deficit. This system further measures the chamber leak (i.e., flow pulled from the chamber), allowing us to quantify the flow rates of the gas-phase instruments.

2.3.2 *Proton Transfer Reaction Mass Spectrometer*

We measured VOCs using proton-transfer-reaction quadrupole-interface time-of-flight mass spectrometry (PTR-QiTOF), as described by Millet et al. (2018). With this technique, the sampled air flows continuously through a drift tube reaction chamber containing H_3O^+ ions produced by hollow cathode discharge. Analytes are ionized via proton transfer, extracted from the drift region via quadrupole ion guide, and subsequently detected by high-resolution TOF-MS.

For these experiments the PTR drift tube was maintained at 3.3 hPa with a drift voltage of 830 V (E/N = 131 Td). The TOF employed an extraction period of 32.5 ms, a mass range of 0-337 amu, and was calibrated via continuous addition of diiodobenzene. Calibration curves and instrument zeros were obtained before and after each day's measurements using zero air generated by passing ambient air through a Pt-bead catalyst (3.2 mm diameter; Shimadzu Corp.) heated to 400 °C. Multipoint calibrations for the species reported here were collected via dynamic dilution of certified, gravimetrically prepared, ppm-level compressed standards into zero air. Humidity dependencies were quantified post-campaign and propagated to the field data based on the measured $H_3O+(H_2O)$ and H_3O^+ signals. For acetone, this yielded a mean sensitivity of 1070 cps/ppb with a mass resolution of 3970.

2.3.3 Thermal Desorption Gas Chromatography Mass Spectrometry

The TD-GC/MS enables speciation and quantification of monoterpenes. We used inert-coated stainless steel sorbent tubes with Tenax-TA to preconcentrate BVOCs prior to offline GC/MS analysis. Handheld low-flow pumps pulled air from either the reference or sample ports through the sorbent tubes for 20 minutes; the portable photosynthesis quantified the exact flow through the tubes, which we used to calculate the total air volume sampled by the tubes.

A UNITY-xr thermal desorption unit (Markes International, UK) thermally desorbs compounds from the tubes, the latter of which are heated to 300 °C and compounds are then pre-concentrated on a coldtrap. The sample is then transferred to a gas chromatograph (TRACE 1310, Thermo Scientific, Massachusetts, USA) and a mass spectrometer (ISQ, Thermo Scientific). We use Chromeleon 7 (Thermo Scientific) to analyze chromatograms. We used the NIST MS spectral database to identify monoterpenes, and then further verified and quantified each compound identified in this work using standards. This analysis includes all monoterpenes that were both

quantifiable and unambiguously identifiable from samples (e.g., Δ-3-carene is identified, but not yet quantified). Riches et al. (2020) provide further details on the TD-GC/MS methods.

2.4 Compounds of interest

Table 4.1 summarizes properties of the compounds investigated herein. In general, the PTR-QiTOF measures organic acids, ketones, alcohols, and alkenes. Compounds observed using PTR-QiTOF are not speciated, and multiple compounds may exist at the same m/z. Methyl vinyl ketone (MVK) and methacrolein (MACR) are indistinguishable and thus referred to as [MVK+MACR]. Likewise, the sum of 2-methyl-3-buten-2-ol (MBO) and isoprene are referred here as [MBO+iso]. For ponderosa pine, MBO is the dominant emission with isoprene contributing to only 10% of the observed emission (Kaser et al., 2013). TD-GC/MS measures speciated monoterpenes, where the PTR-QiTOF measures a summed total of compounds with the $C_{10}H_{16}$ molecular formula. Monoterpenes are referred to as ΣMT when measured via PTR-QiTOF and by isomer-specific names when measured by TD-GC/MS.

Table 4.1. Properties of compounds described herein.

Compound	Formula	Structure	$\times 10^{-13}$ k_{OH} [a]	$\times 10^{-18}$ k_{O3} [a]	PTR ion
Acetic Acid	$C_2H_4O_2$	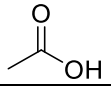	6.9[b]	---	61.0283
Glycoaldehyde	$C_2H_4O_2$	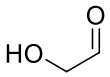	800[b]	---	61.0283
Formic Acid	CH_2O_2	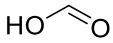	4.5[b]	---	47.0128
Acetone	C_3H_6O		1.8[b]	---	59.0496
Methyl vinyl ketone (MVK)	C_4H_6O	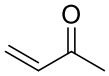	203[c]	5.4[d]	71.0494
Methacrolein (MACR)	C_4H_6O	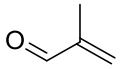	279[c]	1.3[d]	71.0494
2-Methyl-3-buten-2-ol (MBO)	$C_5H_{10}O$	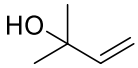	630[b]	8.6[e]	87.0802
Isoprene	C_5H_8	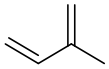	100[b]	13[f]	87.0802
Monoterpenes	$C_{10}H_{16}$				137.1338
Limonene[g]	$C_{10}H_{16}$	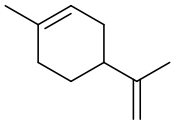	1710	200	
α-Pinene[g]	$C_{10}H_{16}$	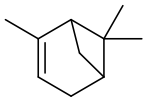	537	86.6	
β-Pinene[g]	$C_{10}H_{16}$	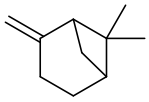	789	15	
β-Ocimene[g]	$C_{10}H_{16}$	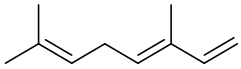	2520	540	
Sesquiterpenes	$C_{15}H_{24}$		variable	variable	205.1900

a. Units of cm^3 $molecules^{-1}$ s^{-1}
b. "Preferred values" from Atmospheric Chemical Kinetic Data Evaluation Data Sheets (https://iupac-aeris.ipsl.fr/index.html#)
c. From Gierczak et al. (1997)
d. From Neeb et al. (1998)
e. From Fantechi et al. (1998)
f. From Neeb and Moortgat (1999)
g. k_{OH} and k_{O3} values from Griffin et al. (1999)

2.5 MEGAN model

The emission (F) of each chemical compound class is calculated in MEGAN as

$$F = \gamma \sum \varepsilon\chi \quad (1)$$

which considers the emission factor at specified standard conditions (ε), the areal coverage grid cell of the vegetation type (χ), and an emission activity factor (γ) (Guenther et al., 2012). The emission activity factor is where changes in emissions induced by different environmental factors are considered. The emission activity factor is dominated by light, temperature, and CO_2 responses in calculations, though soil moisture and leaf age are also considered. Humidity is included as a piece of the meteorology component and goes into parameterizing the canopy environment, specifically the temperature of leaves at different depths of the canopy via a leaf energy balance model (Guenther et al., 2012; A. Guenther et al., 1999). MEGAN often groups together compounds without known emission activity parameters.

Temperature dependence of BVOC emission is approximated using an exponential relationship as described by Guenther et al. (1993) where the emission rate of a compound (E) at leaf temperature (T) are dependent on the emission rate at standard temperature (E_s and T_s) and an empirical coefficient (β) as

$$E = E_s \times \exp(\beta(T - T_s)) \quad (2)$$

Thus, while the temperature-independent coefficient E_s determines the vertical scaling of the relationship, the empirical coefficient (β) dictates the strength of the temperature dependence.

3. Results and discussion

The portable photosynthesis system controls environmental conditions at the leaf-level to quantify VOC emissions using the chemical instrumentation. We performed four temperature response curves at 50% relative humidity, four temperature response curves at 30% relative

humidity, and several survey measurements (i.e., measuring numerous bundles of needles at the same environmental conditions). Here we investigate the driving factors on these emissions and the variability of emission rates observed in the field.

3.1 Temperature and humidity as drivers of photosynthesis and BVOC emissions

We conducted temperature and humidity response curves to determine the influence of each variable on VOC emissions, both separately and combined. Humidity response curves give a direct measure of humidity's role on emissions, which we compare to results observed in temperature response curves conducted both at 30% and 50% relative humidity. The combination of these effects on each compound is described in Figure 4.1.

Numerous physiological and physiochemical factors contribute to the emission of BVOCs and there remains much discussion about the convoluted mechanisms behind emission. Diffusion through the cuticle is possible, especially for lipophilic compounds like monoterpenes, but the rates of diffusion via this avenue is often considered negligible (Niinemets & Reichstein, 2003; Widhalm et al., 2015). Thus, BVOC emissions are generally considered independent of stomatal control, rather driven by diffusivity through concentration and partial pressure gradients (Kesselmeier & Staudt, 1999; Niinemets et al., 2004; Sharkey, 1991). However, the extent of stomatal control is related to the Henry's law constant of the species (Niinemets et al., 2002), lending towards a stronger stomatal regulation for more water-soluble species like organic acids. Further complications arise in linking stomatal control and BVOC emissions in terms of production versus emission; for example, isoprene may trend with photosynthesis due to active biosynthesis (Loreto et al., 1996). Additional complications are introduced when considering the physiological mechanisms behind humidity dependence, including leaf water potential (Aasamaa and Sõber). Thus, while we discuss the correlation between photosynthesis and BVOC emissions, we caution against attributing causation.

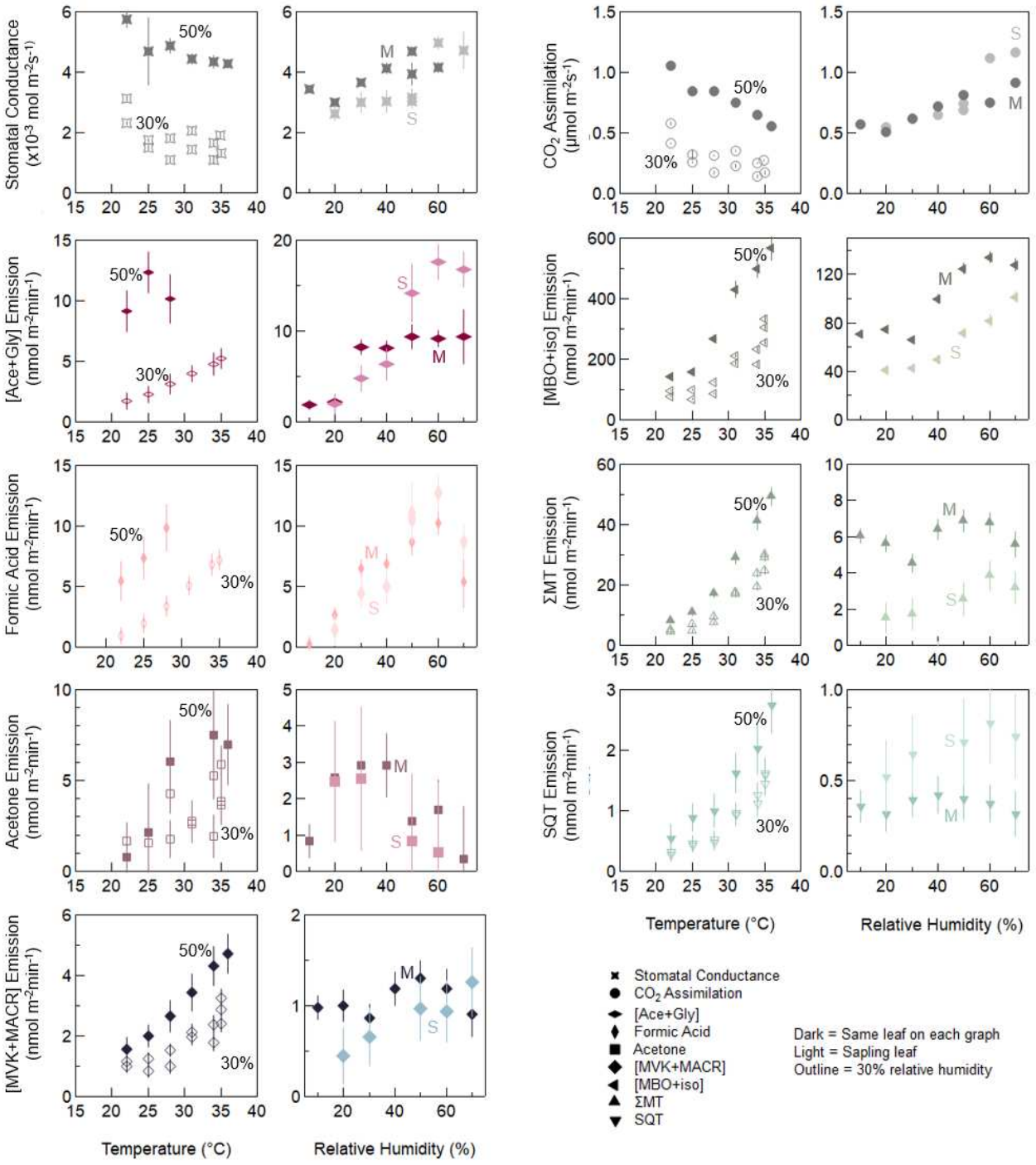

Figure 4.1. The effects of temperature and relative humidity on photosynthesis and seven VOC emissions. Temperature response curves for each compound (left) show emission rates of the same needle bundle on a mature plant at 50% relative humidity (dark, closed) and at 30% relative humidity (outlines). Humidity response curves for each compound (right) detail two separate leaves; the mature needles (M) are of the same as the temperature curves, and the light markers are those from a needle bundle of a sapling (S). Emissions above 30 °C are omitted for [Ace+Gly] and formic acid due to loss from condensation in the lines. Error bars are standard deviation.

The literature-established temperature response of photosynthesis and BVOC emissions are well captured here (Figure 4.1 and Table 4.2). Photosynthesis has a negative correlation with temperature in Ponderosa pine trees; a finding that has been previously reported in the literature (Gray et al., 2003; Harley et al., 1998) and there is a low correlation between stomatal conductance and BVOC emissions (SI Table 4.1). Increases in temperature increase BVOC emission for each compound, as is consistent with the literature (Gray et al., 2003; Guenther et al., 1991; Harley et al., 2014; Harley et al., 1998; Holzinger et al., 2006; Kaser et al., 2013; Kesselmeier et al., 1997; Lamb et al., 1985; Rissanen et al., 2021; Schade et al., 2000; Staudt & Bertin, 1998; M Staudt & Lhoutellier, 2011; Tigney, 1991). The experimentally derived exponential coefficient (β) of temperature response for each compound and MEGAN values are provided in Table 4.2.

The role of relative humidity on BVOC emissions is more ambiguous. Although the extent varies, most emissions increase with increasing humidity, with acetone a clear exception. While an immediate explanation may be stomate driven emissions, the lack of consensus between our observations (SI Table 4.1) and the reasons listed above suggest other mechanisms. Croteau (1977) suggested that hydration of the cuticle increased permeability and attributed their observed short-term enhancement of monoterpene emissions as such, though this theory has not been thoroughly investigated since. Schade et al. (1999) also observed enhancement of monoterpene emissions at higher humidity, attributing their results to adsorption of water onto leaf surfaces. Surface water has also been discussed as a potential reservoir for organic acids (He et al., 2006). It is unlikely that any one factor is driving this humidity-dependent emission, and investigations into the mechanism behind this release are necessary to best integrate such results into models.

Although we are unable to define the mechanism behind humidity-dependent BVOC emissions, we are able to characterize the effect. The temperature-dependence of emissions for

each compound changes when relative humidity is reduced from 50% to 30%. In all cases, the standard emission (E_s) is lesser at lower humidity, from slight changes as is the case for [MBO+iso] to substantial changes as is the case for sesquiterpenes (Table 4.2). Other compounds experience only a slight change in standard emission rates, but the exponential coefficient may change substantially, as is the case for acetone. Despite the discrete influence of humidity on BVOC emissions, the synergistic response of humidity and temperature are more complex. Below we discuss emission trends for different VOCs.

3.1.1 Acetone

The β of acetone temperature dependence is greatly reduced at a lower humidity, almost halved, and it is the only compound which demonstrates a strong inverse relationship during the humidity response curves. Humidity has been shown to have a negative correlation with acetone emission fluxes on a forest floor (Mäki et al., 2019) and a synergistic effect with temperature on Norway spruce (Cojocariu et al., 2004). Acetone is the least correlated with stomatal conductance (SI Table 4.1), providing strong evidence against the dependence on stomatal control, though transpiration should be investigated as a potential driver (Rissanen et al., 2018).

Table 4.2. Changes in the standard emission rate (ΔE_s) in per cent and temperature-dependent empirical coefficient (β) at 50% and 30% relative humidity (± standard deviation) and literature values. Empirical coefficients from the MEGAN model are in bold. Kaser and Schade and Goldstein results are canopy flux measurements from Ponderosa pine. Geron results are flux measurements from Loblolly pine (*Pinus taeda*). Kim and Bouvier-Brown are from branch enclosure measurements on Ponderosa pine. Bourtsoukidis results are from a branch enclosure on Norway spruce (*Picea abies*). Error values of Geron data are standard error.

Compound	ΔE_s	$\beta_{50\%}$	$\beta_{30\%}$	$\beta_{Literature}$	Citations
ΣMT	20	0.136 ±0.006	0.14 ±0.01	**0.10** 0.12 ± 0.01 0.15 0.13 ± 0.04	Guenther et al. (2012) Kaser et al. (2013) Kim et al. (2010) Bouvier-Brown et al. (2009)
Acetone	31	0.15 ±0.04	0.08 ±0.01	**0.1** 0.15 ± 0.01 0.11	Guenther et al. (2012) Kaser et al. (2013) Schade and Goldstein (2001)
[Ace+Gly]	---	---	0.085 ±0.004	**0.13** 0.15 ± 0.01	Guenther et al. (2012) Kaser et al. (2013)
[MVK+MACR]	51	0.081 ±0.003	0.077 ±0.008	0.10[a]	Guenther et al. (2012)
SQT	1800	0.110 ±0.007	0.113 ±0.008	**0.17** (0.09 ± 0.01) to (0.12 ± 0.02)[b] (0.02 ± 0.002) to (0.27 ± 0.04)[c] 0.16 0.07 ± 0.05	Guenther et al. (2012) Bourtsoukidis et al. (2012) Bourtsoukidis et al. (2012) Kim et al. (2010) Bouvier-Brown et al. (2009)
MBO	11	0.11 ±0.01	0.10 ±0.01	**0.13** (0.10±0.01) to (0.17±0.03)[b]	Guenther et al. (2012) Geron et al. (2016)
Formic Acid	---	---	0.15±0.02	**0.13**	Guenther et al. (2012)

[a]From the "Other VOC" category in the MEGAN model
[b]Seasonal variability
[c]Day-to-day variability

3.1.2 Methyl Vinyl Ketone and Methacrolein

We provide, to our knowledge, the first directly measured β values for [MVK+MACR] (methyl vinyl ketone and methacrolein) and evidence of the humidity dependence of these emissions. Temperature dependence of [MVK+MACR] has been mentioned in the literature; Montzka et al. (1995) found that [MVK+MACR] in a pine plantation trended slightly with temperature (r^2= 0.25 to 0.4) and Copeland et al. (2012) noted that [MVK+MACR] trended with variations in temperature over a plantation of grasses and willow. Both observations were ambient measurements, which do not differentiate between directly emitted versus oxidation product [MVK+MACR], and there remain no studies which directly investigate this temperature and

humidity response. As [MVK+MACR] are known to be emitted from leaves in addition to their atmospheric production via reactions with isoprene (Cappellin et al., 2019), elucidating the mechanism and driving factors behind direct emission is required to decouple observations of reacted versus emitted [MVK+MACR].

3.1.3 Sesquiterpenes

The standard emission rate of sesquiterpenes is severely diminished by decreased humidity, though the β of the temperature dependence changes to a much lesser degree. The β values we derive are about 30% lower than that which is used by MEGAN, but still fall within the range described elsewhere in the literature (Table 4.2). Matsunaga et al. (2009) hypothesized that SQT emissions may be enhanced during drier conditions, though authors noted that they did not have the data to support or disprove this hypothesis. While we did not control for soil moisture or precipitation, our results indicate that decreases in relative humidity (at least when incidental) only served to decrease SQT emissions. We also note the distinct shape of the humidity dependence of SQT emissions, which has been observed before in corn (Gouinguené & Turlings, 2002). The shape of this dependence suggests that there is a certain range of humidity where emissions are minimally affected, a necessary consideration for stepwise (e.g., daytime versus nighttime) changes that may not be as substantial for gradual changes (e.g., ongoing diel measurements).

3.1.4 Acetic Acid and Glycoaldehyde

[Ace+Gly] (acetic acid and glycoaldehyde) display a strong humidity response, though the subsequent impact on temperature dependence is uninvestigated here due to a lack of data. However, there is a clear decrease in the standard emission rate, as evident both in the humidity response curve and the drastic difference between what data is available for the temperature response curves at 30% and 50% relative humidity. Should humidity hold any synergistic effects

with temperature, this may explain the notably smaller β at 30% relative humidity than that of MEGAN and the literature (Table 4.2).

3.1.5 Formic Acid

Formic acid emissions follow a strong positive correlation with humidity. Parameterization of our humidity-dependence resolves the observed decrease in formic acid emissions at 25 °C within 30%. However, as with [Ace+Gly], the lack of data at 50% relative humidity prohibits comparison of temperature dependent β values at two humidity conditions. Our ability to deduce discrete and synergistic effects between the two variables is thus limited, though our observed β at 30% relative humidity agrees well with the value included in MEGAN, suggesting that the standard emission rate (E_s) may be the only factor which changes.

3.1.6 Monoterpenes

The β of monoterpene temperature dependence is enhanced at a lower humidity. Ambient humidity is suggested to play a role in long-term monoterpene emission variations (Tigney, 1991), whereas short-term variations are considered to be largely driven by temperature (Guenther et al., 1993). Our results highlight the control that short-term variations in humidity have over monoterpene emissions, while supporting the temperature dominated emission factor. While our β at both relative humidity are greater than that included in the MEGAN model, they remain representative of literature values.

3.1.7 MBO and Isoprene

Despite the clear relationship between humidity and emissions, we find that neither the β values nor the standard emission rates are substantially impacted by this dependence. Parameterization of our humidity-dependence resolves differences in the temperature response curves within 60% at 25 °C. The β values are on the low end of the literature precedence (Table 4.2) but remain represented at both 30% and 50% relative humidity. We conclude that, while humidity plays some role in emission, the effect of this relationship may be minimal for Ponderosa

pine; however, we find that this impact can indeed be defined through analysis of a humidity response curve. These results suggest the necessity to investigate other species, and we suggest isoprene-dominated species should be given a focus in future studies.

3.2 Variability in emissions

Although the variability in emission rates varies greatly depending on the compound, we observe some similarities in compounds of similar structural classes (Figure 4.2). Formic acid and [Ace+Gly] have similar emission rates and relative standard deviations. Ketones (acetone and [MVK+MACR]) also present with the same relative standard deviation and emit on the same order of magnitude. However, variability cannot be simplified for all classes, such as terpenes (MT, SQT, and [MBO+iso]), which have gross differences in their relative standard deviations between one another. Similarities in the extent of variability within alkenes are likely limited. Should the variability in emissions among certain functional groups remain similar, variability of a representative compound may be used to interpolate variability in other compounds, providing a basis for error propagation for studies where measurements are limited.

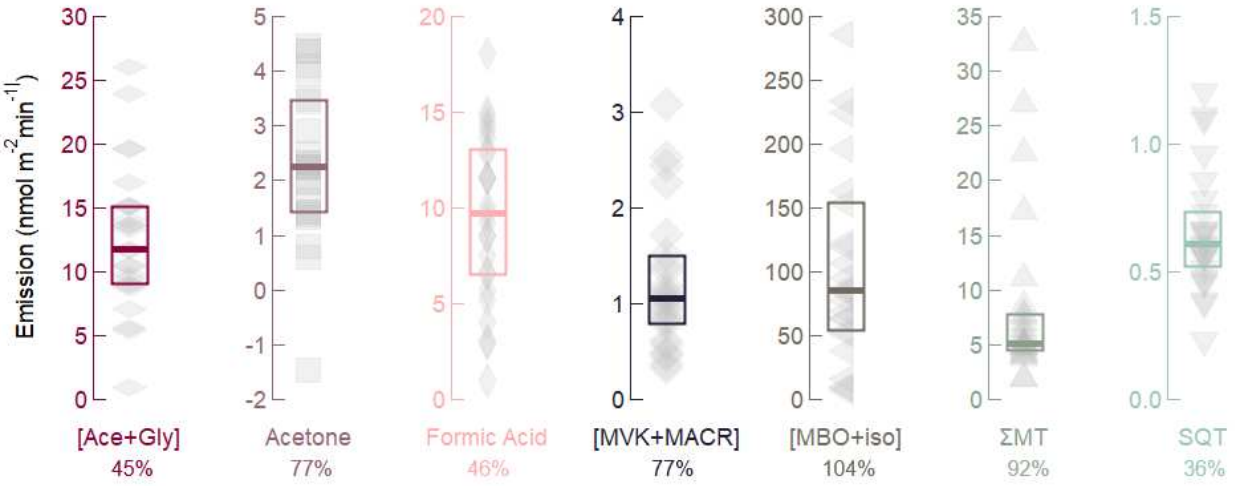

Figure 4.2. Box and whisker plots of emission rates for each compound. The central line is the median, with boxes describing the 25% and 75% quartiles. A single outlier described by a Grubbs' test ($\alpha = 0.05$) have been removed from each of [Ace+Gly], [MBO+iso], and [MVK+MACR]. Relative standard deviations (deviation / mean * 100%) are given below each compound.

As with ΣMT, variability in speciated monoterpenes is broad and cannot yet be resolved. Day-to-day variability (Figure 4.3a) highlights the differences of magnitude in both sum and speciated monoterpenes. Neither sum not speciated monoterpene emissions are explained by CO_2 assimilation (Figure 4.3b) or stomatal conductance.

Relative contributions are likewise wildly variable (Table 4.3), and we find a substantial contribution of an often-excluded monoterpene- β-ocimene. We find that β-pinene often dominates emissions, with significant contributions by d-limonene and α-pinene. However, β-ocimene makes a prominent contribution, and dominates (>50% relative contribution) emissions in a quarter of the measurements (Figure 4.3). This β-ocimene prominence differs from the general literature precedence, which describes Ponderosa pine emissions as largely dominated by α-pinene, β-pinene, and limonene (Harley et al., 2014; Latta et al., 2000; Lerdau et al., 1994). However, Loreto et al. (2000) found that β-ocimene was the primary constituent of emissions in healthy needles, whereas substantial emission of other monoterpenes was limited to wounded needles.

Table 4.3. Median and ranges of relative contributions to total monoterpene emission of each speciated compound. Values are complimentary to those in Figure 4.3b.

Compound	Median	Range
β-pinene	39%	0-67%
α-pinene	9%	0-26%
d-limonene	21%	1-62%
β-ocimene	16%	0-97%

Differences in speciated monoterpene emissions do not correlate well with one another, further complicating generalizations. We do find that β-pinene is well correlated with α-pinene (r^2 = 0.83), whereas d-limonene is less so (r^2 = 0.30) and β-ocimene not at all (r^2 = 0.03). Thus, we find that α-pinene and β-pinene, which share the same biosynthetic pathway are well-agreed and could be used to estimate relative contributions of one another. However, β-ocimene, which may be synthesized through different means (Cui et al., 2016; Loreto et al., 2000), prevents estimations

in terms of sum monoterpene contributions. Lerdau et al. (1994) observed that α-pinene and β-pinene correlated with total monoterpene emissions, but β-ocimene drives our monoterpene emissions ($r^2 = 0.71$). As such, while α-pinene or β-pinene could be used to estimate the emission of one another, neither can be used to estimate the contribution of other compounds or the sum emission.

We find that although β-ocimene is prominent in >20% of leaves, and although its variability is drastic, it is well represented in the MEGANv2.1 model where it is given a relative contribution to sum monoterpenes of 23% (Sindelarova et al., 2014). Thus, the issue in variability is of greater importance in other leaf-level experiments, where limited measurements may misrepresent speciated monoterpene emission rates. This variability complicates generalization of these compounds as necessary for model integration, but they are largely consequential. For example, β-ocimene plays a larger role than any other monoterpene herein to atmospheric reactivity. The high k_{O3} and k_{OH} compared to other compounds (Table 4.1) highlight the extent of which β-ocimene drives atmospheric reactivity. However, β-ocimene has a very low (<1%) contribution to SOA yield (Morales et al., 2021), and thus has more implications on atmospheric oxidation than on SOA formation. When considering three needles of roughly the same emission but different relative contributions, sum OH reactivity ranges from 1.2 to 2.2 $m^{-2}\ s^{-2}$ and sum O_3 reactivity ranges from 7.2 to 14.2 $x10^{-7}\ m^{-2}\ s^{-2}$ (units are an artifact of emission rate per leaf area). While comparable in sum emission rates, these values do not account for the fact that most of the β-ocimene dominated compounds have the highest emissions.

Smoke events (Figure 4.3, shaded grey) contribute to variability in sum monoterpene emissions, but do not drive variability in speciated emissions. During smoke events (grey shading), we see both substantial emissions (>5 nmol $m^{-2}\ min^{-1}$ sum) and deposition, suggesting that

deposition of smoke onto leaf surfaces may enhance deposition of monoterpenes, though this bidirectional exchange can occur regardless of the status of the needles (Guenther, 2015; Millet et al., 2018). As shown in Figure 4.3b, smoke events neither drive changes in photosynthesis nor speciated monoterpenes. Thus, while smoke events increase leaf-to-leaf variability, the paucity in data prohibits exhaustive investigation into the extent to which this occurs.

It is important to note here that these results are limited to the needle-level. Results here highlight the diversity of these emissions, but canopy-level measurements of non-speciated compounds largely discount this speciation. Despite this simplification, extrapolating the results of non-speciated emissions into reactivities or SOA yields are thus complicated. Likewise, due to the differences in chemical properties (e.g., vapor pressure), differences in contributions to temperature or humidity response curves are likely to vary, and it is likely that the humidity-dependence of emissions from temperate species differs from the results of semi-arid species. Our understanding of the mechanisms behind these needle-level emissions are still confounded and further studies must be conducted to accurately integrate these findings into models.

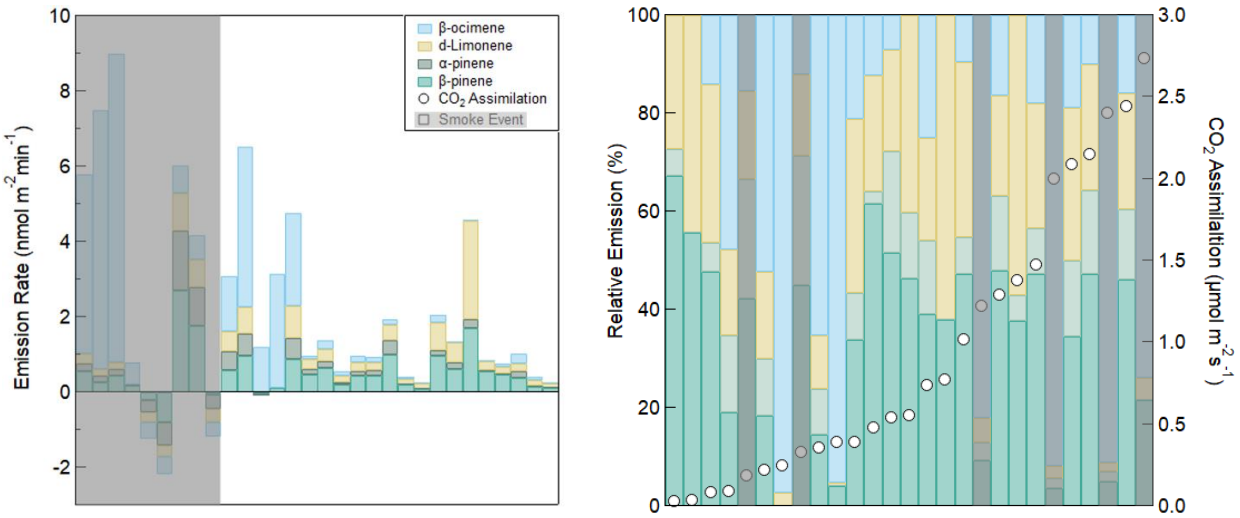

Figure 4.3. Emission of speciated monoterpenes of different leaves. The left graph describes differences in emission rates; negative values indicate deposition of compounds. The right graph describes differences in the relative emissions (%) of emitting-only leaves (left axis) and CO_2 assimilation (right axis), organizing by increasing values of the latter. In both graphs, results obtained on smoke days are highlighted in grey.

4. Conclusion

Humidity governs BVOC emissions synchronously with temperature. Although temperature always remains the dominant driver in BVOC emissions, humidity can change both the intensity of the temperature dependence and the standard emission rate. Compounds are each impacted differently and to a different degree; at a lower humidity, the standard emission rate of sesquiterpenes are drastically decreased whereas the empirical coefficient of temperature dependence (β) is drastically decreased in the case of acetone. There is no ubiquitous relationship with stomatal conductance which adequately explains this humidity dependence, and the mechanism behind this dependence cannot be explained solely by the results herein. However, integration of this humidity dependence may serve to explain the midday overestimation of BVOC emissions in empirical models like MEGAN (Niinemets & Reichstein, 2003), where relative humidity is at its lowest. We present compelling evidence that humidity must be investigated as a

driver of BVOC emissions, with a focus on compound-to-compound differences for accurate model integration.

We further identify β-ocimene as a significant contributor to monoterpene emissions, validating findings from Loreto et al. (2000), and highlight that its emission can nearly double OH and O_3 reactivities. We find no similarities in speciated monoterpene emissions with photosynthesis, nor in the sum monoterpene emissions with occurrent smoke exposure. Promisingly, however, we find that similarly functionalized compounds vary similarly with one another; this finding could simplify variability calculations in empirical models and provide a basis for variability in compounds that have yet to be investigated at this level. Thus, while we find that leaf-to-leaf variability is substantial and must be accounted for, generalization of functional groups can simplify estimations and inclusion of monoterpene speciation can improve our understanding of the atmospheric impacts of these emissions.

Ongoing analyses are underway to incorporate these findings into MEGAN, where the impact of these changes can be inferred on regional and global scales. Vapor pressure deficit is also being investigated as a driver behind BVOC emissions. Further experiments are required to investigate humidity dependence on other prevalent emissions and on speciated monoterpenes.

Support statement

We would like to acknowledge those who participated in FluCS. The field site and tower were maintained and made available by the National Center for Atmospheric Research and the United States Forest Service. Many thanks to Steve Alton for his on-site assistance and humor and to Paula Fornwalt for ensuring this project could progress despite a global pandemic. We thank NSF AGS 1932771 for funding.

References

Aasamaa, K., & Sõber, A. (2011). Stomatal sensitivities to changes in leaf water potential, air humidity, CO2 concentration and light intensity, and the effect of abscisic acid on the sensitivities in six temperate deciduous tree species. *Environmental and Experimental Botany*, *71*(1), 72-78.

Bhatia, A., Tomer, R., Kumar, V., Singh, S., & Pathak, H. (2012). Impact of tropospheric ozone on crop growth and productivity–a review.

Borbon, A., Coddeville, P., Locoge, N., & Galloo, J.-C. (2004). Characterising sources and sinks of rural VOC in eastern France. *Chemosphere, 57*(8), 931-942.

Bourtsoukidis, E., Bonn, B., Dittmann, A., Hakola, H., Hellén, H., & Jacobi, S. (2012). Ozone stress as a driving force of sesquiterpene emissions: a suggested parameterisation. *Biogeosciences, 9*(11), 4337-4352.

Bouvier-Brown, N. C., Holzinger, R., Palitzsch, K., & Goldstein, A. H. (2009). Large emissions of sesquiterpenes and methyl chavicol quantified from branch enclosure measurements. *Atmospheric Environment, 43*(2), 389-401.

Cappellin, L., Loreto, F., Biasioli, F., Pastore, P., & McKinney, K. (2019). A mechanism for biogenic production and emission of MEK from MVK decoupled from isoprene biosynthesis. *Atmospheric Chemistry and Physics, 19*(5), 3125-3135.

Clifton, O. E., Fiore, A. M., Massman, W. J., Baublitz, C. B., Coyle, M., Emberson, L., et al. (2020). Dry deposition of ozone over land: processes, measurement, and modeling. *Reviews of Geophysics, 58*(1), e2019RG000670.

Cojocariu, C., Kreuzwieser, J., & Rennenberg, H. (2004). Correlation of short-chained carbonyls emitted from Picea abies with physiological and environmental parameters. *New Phytologist, 162*(3), 717-727.

Copeland, N., Cape, J. N., & Heal, M. R. (2012). Volatile organic compound emissions from Miscanthus and short rotation coppice willow bioenergy crops. *Atmospheric Environment, 60*, 327-335.

Croteau, R. (1977). Effect of irrigation method on essential oil yield and rate of oil evaporation in mint grown under controlled conditions [Mentha piperita, Mentha spicata]. *HortScience*.

Cui, H., Wei, J., Su, J., Li, C., & Ge, F. (2016). Elevated O3 increases volatile organic compounds via jasmonic acid pathway that promote the preference of parasitoid Encarsia formosa for tomato plants. *Plant Science, 253*, 243-250.

Dominguez-Taylor, P., Ruiz-Suarez, L., Rosas-Perez, I., Hernandez-Solis, J., & Steinbrecher, R. (2007). Monoterpene and isoprene emissions from typical tree species in forests around Mexico City. *Atmospheric Environment, 41*(13), 2780-2790.

Ebel, R. C., Mattheis, J. P., & Buchanan, D. A. (1995). Drought stress of apple trees alters leaf emissions of volatile compounds. *Physiologia Plantarum, 93*(4), 709-712.

Fantechi, G., Jensen, N., Hjorth, J., & Peeters, J. (1998). Mechanistic studies of the atmospheric oxidation of methyl butenol by OH radicals, ozone and NO3 radicals. *Atmospheric Environment, 32*(20), 3547-3556.

Farmer, D. K., & Riches, M. (2020). Measuring biosphere–atmosphere exchange of short-lived climate forcers and their precursors. *Accounts of Chemical Research, 53*(8), 1427-1435.

Franz, M., Alonso, R., Arneth, A., Büker, P., Elvira, S., Gerosa, G., et al. (2018). Evaluation of simulated ozone effects in forest ecosystems against biomass damage estimates from fumigation experiments. *Biogeosciences, 15*(22), 6941-6957.

Fuentes, J. D., Lerdau, M., Atkinson, R., Baldocchi, D., Bottenheim, J., Ciccioli, P., et al. (2000). Biogenic hydrocarbons in the atmospheric boundary layer: a review. *Bulletin of the American Meteorological Society, 81*(7), 1537-1575.

Fulgham, S. R., Brophy, P., Link, M., Ortega, J., Pollack, I., & Farmer, D. K. (2019). Seasonal flux measurements over a Colorado pine forest demonstrate a persistent source of organic acids. *ACS Earth and Space Chemistry, 3*(9), 2017-2032.

Gao, Y., Ma, M., Yan, F., Su, H., Wang, S., Liao, H., et al. (2022). Impacts of biogenic emissions from urban landscapes on summer ozone and secondary organic aerosol formation in megacities. *Science of The Total Environment, 814*, 152654.

Geron, C. D., Daly, R. W., Arnts, R. R., Guenther, A. B., & Mowry, F. L. (2016). Canopy level emissions of 2-methyl-3-buten-2-ol, monoterpenes, and sesquiterpenes from an experimental Pinus taeda plantation. *Science of The Total Environment, 565*, 730-741.

Gierczak, T., Burkholder, J. B., Talukdar, R. K., Mellouki, A., Barone, S., & Ravishankara, A. (1997). Atmospheric fate of methyl vinyl ketone and methacrolein. *Journal of Photochemistry and Photobiology A: Chemistry, 110*(1), 1-10.

Gomez, L. G., Loubet, B., Lafouge, F., Ciuraru, R., Bsaibes, S., Kammer, J., et al. (2021). Effect of senescence on biogenic volatile organic compound fluxes in wheat plants. *Atmospheric Environment, 266*, 118665.

Gouinguené, S. P., & Turlings, T. C. (2002). The effects of abiotic factors on induced volatile emissions in corn plants. *Plant Physiology, 129*(3), 1296-1307.

Gray, D. W., Lerdau, M. T., & Goldstein, A. H. (2003). Influences of temperature history, water stress, and needle age on methylbutenol emissions. *Ecology, 84*(3), 765-776.

Griffin, R. J., Cocker III, D. R., Flagan, R. C., & Seinfeld, J. H. (1999). Organic aerosol formation from the oxidation of biogenic hydrocarbons. *Journal of Geophysical Research: Atmospheres, 104*(D3), 3555-3567.

Guenther, Jiang, X., Heald, C. L., Sakulyanontvittaya, T., Duhl, T., Emmons, L., & Wang, X. (2012). The Model of Emissions of Gases and Aerosols from Nature version 2.1 (MEGAN2. 1): an extended and updated framework for modeling biogenic emissions. *Geoscientific Model Development, 5*(6), 1471-1492.

Guenther, Zimmerman, P. R., Harley, P. C., Monson, R. K., & Fall, R. (1993). Isoprene and monoterpene emission rate variability: model evaluations and sensitivity analyses. *Journal of Geophysical Research: Atmospheres, 98*(D7), 12609-12617.

Guenther, A. (2015). Bidirectional exchange of volatile organic compounds. In *Review and integration of biosphere-atmosphere modelling of reactive trace gases and volatile aerosols* (pp. 107-113): Springer.

Guenther, A., Baugh, B., Brasseur, G., Greenberg, J., Harley, P., Klinger, L., et al. (1999). Isoprene emission estimates and uncertainties for the Central African EXPRESSO study domain. *Journal of Geophysical Research: Atmospheres, 104*(D23), 30625-30639.

Guenther, A., Hewitt, C. N., Erickson, D., Fall, R., Geron, C., Graedel, T., et al. (1995). A global model of natural volatile organic compound emissions. *Journal of Geophysical Research: Atmospheres, 100*(D5), 8873-8892.

Guenther, A., Jiang, X., Heald, C. L., Sakulyanontvittaya, T., Duhl, T., Emmons, L., & Wang, X. (2012). The Model of Emissions of Gases and Aerosols from Nature version 2.1 (MEGAN2. 1): an extended and updated framework for modeling biogenic emissions. *Geoscientific Model Development, 5*(6), 1471-1492.

Guenther, A. B., Monson, R. K., & Fall, R. (1991). Isoprene and monoterpene emission rate variability: observations with eucalyptus and emission rate algorithm development. *Journal of Geophysical Research: Atmospheres, 96*(D6), 10799-10808.

Guenther, A. B., Zimmerman, P. R., Harley, P. C., Monson, R. K., & Fall, R. (1993). Isoprene and monoterpene emission rate variability: model evaluations and sensitivity analyses. *Journal of Geophysical Research: Atmospheres, 98*(D7), 12609-12617.

Hakola, H., Tarvainen, V., Laurila, T., Hiltunen, V., Hellén, H., & Keronen, P. (2003). Seasonal variation of VOC concentrations above a boreal coniferous forest. *Atmospheric Environment, 37*(12), 1623-1634.

Harley, P., Eller, A., Guenther, A., & Monson, R. K. (2014). Observations and models of emissions of volatile terpenoid compounds from needles of ponderosa pine trees growing in situ: control by light, temperature and stomatal conductance. *Oecologia, 176*(1), 35-55.

Harley, P., Fridd-Stroud, V., Greenberg, J., Guenther, A., & Vasconcellos, P. (1998). Emission of 2-methyl-3-buten-2-ol by pines: A potentially large natural source of reactive carbon to the atmosphere. *Journal of Geophysical Research: Atmospheres, 103*(D19), 25479-25486.

Harrison, D., Hunter, M., Lewis, A., Seakins, P., Nunes, T., & Pio, C. (2001). Isoprene and monoterpene emission from the coniferous species Abies Borisii-regis—implications for regional air chemistry in Greece. *Atmospheric Environment, 35*(27), 4687-4698.

He, C., Clifton, O., Felker-Quinn, E., Fulgham, S. R., Juncosa Calahorrano, J. F., Lombardozzi, D., et al. (2021). Interactions between air pollution and terrestrial ecosystems: perspectives on challenges and future directions. *Bulletin of the American Meteorological Society, 102*(3), E525-E538.

He, Y., Zhou, X., Hou, J., Gao, H., & Bertman, S. B. (2006). Importance of dew in controlling the air-surface exchange of HONO in rural forested environments. *Geophysical Research Letters, 33*(2).

Holzinger, R., Lee, A., McKay, M., & Goldstein, A. (2006). Seasonal variability of monoterpene emission factors for a ponderosa pine plantation in California. *Atmospheric Chemistry and Physics, 6*(5), 1267-1274.

Jardine, K. J., Monson, R. K., Abrell, L., Saleska, S. R., Arneth, A., Jardine, A., et al. (2012). Within-plant isoprene oxidation confirmed by direct emissions of oxidation products methyl vinyl ketone and methacrolein. *Global Change Biology, 18*(3), 973-984.

Kaser, L., Karl, T., Guenther, A., Graus, M., Schnitzhofer, R., Turnipseed, A., et al. (2013). Undisturbed and disturbed above canopy ponderosa pine emissions: PTR-TOF-MS measurements and MEGAN 2.1 model results. *Atmospheric Chemistry and Physics, 13*(23), 11935-11947.

Kesselmeier, J., Bode, K., Hofmann, U., Müller, H., Schäfer, L., Wolf, A., et al. (1997). Emission of short chained organic acids, aldehydes and monoterpenes from Quercus ilex L. and Pinus pinea L. in relation to physiological activities, carbon budget and emission algorithms. *Atmospheric Environment, 31*, 119-133.

Kesselmeier, J., & Staudt, M. (1999). Biogenic volatile organic compounds (VOC): an overview on emission, physiology and ecology. *Journal of atmospheric chemistry, 33*(1), 23-88.

Kim, J.-C., Kim, K.-J., Kim, D.-S., & Han, J.-S. (2005). Seasonal variations of monoterpene emissions from coniferous trees of different ages in Korea. *Chemosphere, 59*(11), 1685-1696.

Kim, S., Karl, T., Guenther, A., Tyndall, G., Orlando, J., Harley, P., et al. (2010). Emissions and ambient distributions of Biogenic Volatile Organic Compounds (BVOC) in a ponderosa

pine ecosystem: interpretation of PTR-MS mass spectra. *Atmospheric Chemistry and Physics, 10*(4), 1759-1771.

Kumar, P., Druckman, A., Gallagher, J., Gatersleben, B., Allison, S., Eisenman, T. S., et al. (2019). The nexus between air pollution, green infrastructure and human health. *Environment international, 133*, 105181.

Lamanna, M. S., & Goldstein, A. H. (1999). In situ measurements of C2-C10 volatile organic compounds above a Sierra Nevada ponderosa pine plantation. *Journal of Geophysical Research: Atmospheres, 104*(D17), 21247-21262.

Lamb, B., Gay, D., Westberg, H., & Pierce, T. (1993). A biogenic hydrocarbon emission inventory for the USA using a simple forest canopy model. *Atmospheric Environment. Part A. General Topics, 27*(11), 1673-1690.

Lamb, B., Westberg, H., Allwine, G., & Quarles, T. (1985). Biogenic hydrocarbon emissions from deciduous and coniferous trees in the United States. *Journal of Geophysical Research: Atmospheres, 90*(D1), 2380-2390.

Latta, R. G., Linhart, Y. B., Lundquist, L., & Snyder, M. A. (2000). Patterns of monoterpene variation within individual trees in ponderosa pine. *Journal of chemical ecology, 26*(6), 1341-1357.

Lerdau, M., Dilts, S. B., Westberg, H., Lamb, B. K., & Allwine, E. J. (1994). Monoterpene emission from ponderosa pine. *Journal of Geophysical Research: Atmospheres, 99*(D8), 16609-16615.

Link, M. F., Brophy, P., Fulgham, S. R., Murschell, T., & Farmer, D. K. (2021). Isoprene versus Monoterpenes as Gas-Phase Organic Acid Precursors in the Atmosphere. *ACS Earth and Space Chemistry, 5*(6), 1600-1612.

Loreto, F., Ciccioli, P., Cecinato, A., Brancaleoni, E., Frattoni, M., & Tricoli, D. (1996). Influence of environmental factors and air composition on the emission of [alpha]-pinene from Quercus ilex leaves. *Plant Physiology, 110*(1), 267-275.

Loreto, F., Nascetti, P., Graverini, A., & Mannozzi, M. (2000). Emission and content of monoterpenes in intact and wounded needles of the Mediterranean pine, Pinus pinea. *Functional Ecology, 14*(5), 589-595.

Ma, M., Gao, Y., Ding, A., Su, H., Liao, H., Wang, S., et al. (2021). Development and Assessment of a High-Resolution Biogenic Emission Inventory from Urban Green Spaces in China. *Environmental science & technology, 56*(1), 175-184.

Mahmood, F., Khokhar, M. F., & Mahmood, Z. (2020). Examining the relationship of tropospheric ozone and climate change on crop productivity using the multivariate panel data techniques. *Journal of Environmental Management, 272*, 111024.

Mäki, M., Aalto, J., Hellén, H., Pihlatie, M., & Bäck, J. (2019). Interannual and seasonal dynamics of volatile organic compound fluxes from the boreal forest floor. *Frontiers in Plant Science, 10*, 191.

Matsunaga, S. N., Guenther, A. B., Greenberg, J. P., Potosnak, M., Papiez, M., Hiura, T., et al. (2009). Leaf level emission measurement of sesquiterpenes and oxygenated sesquiterpenes from desert shrubs and temperate forest trees using a liquid extraction technique. *Geochemical Journal, 43*(3), 179-189.

Matyssek, R., & Sandermann, H. (2003). Impact of ozone on trees: an ecophysiological perspective. *Progress in botany*, 349-404.

Millet, D. B., Alwe, H. D., Chen, X., Deventer, M. J., Griffis, T. J., Holzinger, R., et al. (2018). Bidirectional ecosystem–atmosphere fluxes of volatile organic compounds across the mass spectrum: How many matter? *ACS Earth and Space Chemistry, 2*(8), 764-777.

Mishra, A., Sinha, B., Kumar, R., Barth, M., Hakkim, H., Kumar, V., et al. (2021). Cropland trees need to be included for accurate model simulations of land-atmosphere heat fluxes, temperature, boundary layer height, and ozone. *Science of The Total Environment, 751*, 141728.

Monson, R. K. (2002). Volatile organic compound emissions from terrestrial ecosystems: a primary biological control over atmospheric chemistry. *Israel Journal of Chemistry, 42*(1), 29-42.

Montzka, S. A., Trainer, M., Angevine, W. M., & Fehsenfeld, F. C. (1995). Measurements of 3-methyl furan, methyl vinyl ketone, and methacrolein at a rural forested site in the southeastern United States. *Journal of Geophysical Research: Atmospheres, 100*(D6), 11393-11401.

Morales, A. C., Jayarathne, T., Slade, J. H., Laskin, A., & Shepson, P. B. (2021). The production and hydrolysis of organic nitrates from OH radical oxidation of β-ocimene. *Atmospheric Chemistry and Physics, 21*(1), 129-145.

Müller, K., Haferkorn, S., Grabmer, W., Wisthaler, A., Hansel, A., Kreuzwieser, J., et al. (2006). Biogenic carbonyl compounds within and above a coniferous forest in Germany. *Atmospheric Environment, 40*, 81-91.

Mutzel, A., Rodigast, M., Iinuma, Y., Böge, O., & Herrmann, H. (2016). Monoterpene SOA–Contribution of first-generation oxidation products to formation and chemical composition. *Atmospheric Environment, 130*, 136-144.

Nakashima, Y., Kato, S., Greenberg, J., Harley, P., Karl, T., Turnipseed, A., et al. (2014). Total OH reactivity measurements in ambient air in a southern Rocky mountain ponderosa pine forest during BEACHON-SRM08 summer campaign. *Atmospheric Environment, 85*, 1-8.

Neeb, P., Kolloff, A., Koch, S., & Moortgat, G. K. (1998). Rate constants for the reactions of methylvinyl ketone, methacrolein, methacrylic acid, and acrylic acid with ozone. *International journal of chemical kinetics, 30*(10), 769-776.

Neeb, P., & Moortgat, G. K. (1999). Formation of OH radicals in the gas-phase reaction of propene, isobutene, and isoprene with O3: Yields and mechanistic implications. *The Journal of Physical Chemistry A, 103*(45), 9003-9012.

Nel, A. (2005). Air pollution-related illness: effects of particles. *Science, 308*(5723), 804-806.

Niinemets, Ü., Loreto, F., & Reichstein, M. (2004). Physiological and physicochemical controls on foliar volatile organic compound emissions. *Trends in plant science, 9*(4), 180-186.

Niinemets, Ü., & Reichstein, M. (2003). Controls on the emission of plant volatiles through stomata: Differential sensitivity of emission rates to stomatal closure explained. *Journal of Geophysical Research: Atmospheres, 108*(D7).

Niinemets, U., Reichstein, M., Staudt, M., Seufert, G., & Tenhunen, J. D. (2002). Stomatal constraints may affect emission of oxygenated monoterpenoids from the foliage of Pinus pinea. *Plant Physiology, 130*(3), 1371-1385.

Opacka, B., Müller, J.-F., Stavrakou, T., Bauwens, M., Sindelarova, K., Markova, J., & Guenther, A. B. (2021). Global and regional impacts of land cover changes on isoprene emissions derived from spaceborne data and the MEGAN model. *Atmospheric Chemistry and Physics, 21*(11), 8413-8436.

Opacka, B., Müller, J.-F., Stavrakou, T., Miralles, D. G., Koppa, A., Pagán, B. R., et al. (2022). Impact of Drought on Isoprene Fluxes Assessed Using Field Data, Satellite-Based GLEAM Soil Moisture and HCHO Observations from OMI. *Remote Sensing, 14*(9), 2021.

Ortega, J., Turnipseed, A., Guenther, A. B., Karl, T. G., Day, D., Gochis, D., et al. (2014). Overview of the Manitou Experimental Forest Observatory: site description and selected science results from 2008 to 2013. *Atmospheric Chemistry and Physics, 14*(12), 6345-6367.

Peñuelas, J., & Staudt, M. (2010). BVOCs and global change. *Trends in plant science, 15*(3), 133-144.

Riches, M., Lee, D., & Farmer, D. K. (2020). Simultaneous leaf-level measurement of trace gas emissions and photosynthesis with a portable photosynthesis system. *Atmospheric Measurement Techniques, 13*(8), 4123-4139.

Rissanen, K., Aalto, J., Gessler, A., Hölttä, T., Rigling, A., Schaub, M., & Bäck, J. (2021). Drought effects on volatile organic compound emissions from Scots pine stems. *Plant, cell & environment*.

Rissanen, K., Hölttä, T., & Bäck, J. (2018). Transpiration directly regulates the emissions of water-soluble short-chained OVOCs. *Plant, cell & environment, 41*(10), 2288-2298.

Scala, A., Allmann, S., Mirabella, R., Haring, M. A., & Schuurink, R. C. (2013). Green leaf volatiles: a plant's multifunctional weapon against herbivores and pathogens. *International journal of molecular sciences, 14*(9), 17781-17811.

Schade, G. W., & Goldstein, A. H. (2001). Fluxes of oxygenated volatile organic compounds from a ponderosa pine plantation. *Journal of Geophysical Research: Atmospheres, 106*(D3), 3111-3123.

Schade, G. W., & Goldstein, A. H. (2002). Plant physiological influences on the fluxes of oxygenated volatile organic compounds from ponderosa pine trees. *Journal of Geophysical Research: Atmospheres, 107*(D10), ACH 2-1-ACH 2-8.

Schade, G. W., Goldstein, A. H., Gray, D. W., & Lerdau, M. T. (2000). Canopy and leaf level 2-methyl-3-buten-2-ol fluxes from a ponderosa pine plantation. *Atmospheric Environment, 34*(21), 3535-3544.

Schade, G. W., Goldstein, A. H., & Lamanna, M. S. (1999). Are monoterpene emissions influenced by humidity? *Geophysical Research Letters, 26*(14), 2187-2190.

Scott, C., Rap, A., Spracklen, D., Forster, P., Carslaw, K., Mann, G., et al. (2014). The direct and indirect radiative effects of biogenic secondary organic aerosol. *Atmospheric Chemistry and Physics, 14*(1), 447-470.

Sharkey, T. D. (1991). Stomatal control of trace gas emissions. *Trace gas emissions by plants*, 335-339.

Sharkey, T. D., & Loreto, F. (1993). Water stress, temperature, and light effects on the capacity for isoprene emission and photosynthesis of kudzu leaves. *Oecologia, 95*(3), 328-333.

Šimpraga, M., Ghimire, R. P., Van Der Straeten, D., Blande, J. D., Kasurinen, A., Sorvari, J., et al. (2019). Unravelling the functions of biogenic volatiles in boreal and temperate forest ecosystems. *European Journal of Forest Research, 138*(5), 763-787.

Sindelarova, K., Granier, C., Bouarar, I., Guenther, A., Tilmes, S., Stavrakou, T., et al. (2014). Global data set of biogenic VOC emissions calculated by the MEGAN model over the last 30 years. *Atmospheric Chemistry and Physics, 14*(17), 9317-9341.

Son, Y.-S., Kim, K.-J., Jung, I.-H., Lee, S.-J., & Kim, J.-C. (2015). Seasonal variations and emission fluxes of monoterpene emitted from coniferous trees in East Asia: focused on Pinus rigida and Pinus koraiensis. *Journal of atmospheric chemistry, 72*(1), 27-41.

Staudt, M., & Bertin, N. (1998). Light and temperature dependence of the emission of cyclic and acyclic monoterpenes from holm oak (Quercus ilex L.) leaves. *Plant, cell & environment, 21*(4), 385-395.

Staudt, M., & Lhoutellier, L. (2011). Monoterpene and sesquiterpene emissions from Quercus coccifera exhibit interacting responses to light and temperature. *Biogeosciences, 8*(9), 2757-2771.

Stocker, T. (2014). *Climate change 2013: the physical science basis: Working Group I contribution to the Fifth assessment report of the Intergovernmental Panel on Climate Change*: Cambridge university press.

Svenson, S. E., & Davies Jr, F. T. (1992). Comparison of methods for estimating surface area of water-stressed and fully hydrated pine needle segments for gas exchange analysis. *Tree physiology, 10*(4), 417-421.

Tarvainen, V., Hakola, H., Hellén, H., Bäck, J., Hari, P., & Kulmala, M. (2005). Temperature and light dependence of the VOC emissions of Scots pine. *Atmospheric Chemistry and Physics, 5*(4), 989-998.

Tigney, D. (1991). Factors controlling the emissions of monoterpenes and other volatile organic compounds. *Trace gas emission by plants.*, 93-119.

Tingey, D. T., Manning, M., Grothaus, L. C., & Burns, W. F. (1980). Influence of light and temperature on monoterpene emission rates from slash pine. *Plant Physiology, 65*(5), 797-801.

UNEP, F. (2020). The state of the world's forests 2020. *Forests, Biodiversity and People. FAO*.

Widhalm, J. R., Jaini, R., Morgan, J. A., & Dudareva, N. (2015). Rethinking how volatiles are released from plant cells. *Trends in plant science, 20*(9), 545-550.

Zhou, L., Gierens, R., Sogachev, A., Mogensen, D., Ortega, J., Smith, J., et al. (2015). Contribution from biogenic organic compounds to particle growth during the 2010 BEACHON-ROCS campaign in a Colorado temperate needleleaf forest. *Atmospheric Chemistry and Physics, 15*(15), 8643-8656.

CONCLUSION

In Chapter 1, we emphasize the complexity of BVOC emissions, their atmospheric implications, and some of the approaches to quantifying these compounds, while Chapter 2 details the characterization and use of a technique which couples trace gas instruments to a portable photosynthesis system, the approach I used as a basis for this dissertation. Leaf-level emission studies are useful as they control environmental parameters, thereby allowing investigation of the mechanisms behind BVOC emissions. However, trustful measurements require a combination of well-characterized instrumentation. Compared to simpler branch enclosure or leaf cuvette methods, the standard techniques for leaf-level measurements, portable photosynthesis systems provide more physiological information (e.g., measurements of CO_2 assimilation, stomatal conductance, leaf vapor pressure deficit) while maintaining environmental parameters equally if not more effectively than other chamber techniques. In Chapter 2, we assess the viability of a coupling the portable photosynthesis system to an online instrument (chemical ionization mass spectrometry) and an offline instrument (thermal desorption gas chromatography mass spectrometry). Further, we detail the interferences in the system and how failure to thoroughly characterize portable photosynthesis systems can lead to over- and underestimations of speciated BVOC emissions. We provide several options to minimize background interferences and present the modularity and customization of the system to investigate different compounds by coupling to different trace gas instruments. Throughout the dissertation, we highlight the potential of this method to couple with several instruments both separately and combined for a more robust profile of BVOC emissions.

In addition to providing a case study of the field-deployment of our coupled portable photosynthesis system, Chapter 3 reveals the necessity of investigating seasonal weather events outside of the typical summer-oriented field research. In a rare opportunity, we measured the effects of the first seasonal snow event on a broad-leaf tree in an urban arboretum. With our targeted approach, we were able to define the effects of snow-induced senescence on a deciduous tree. Our observations showed a burst of monoterpene emissions brought upon by the event and the subsequent change in atmospheric reactivity. Our results explore the disparate, non-linear response of different monoterpenes to senescence, and the day-to-day evolution of senescence as the tree enters dormancy. These seasonal snow events are not often observed, least of all exclusively investigated; our work underscores the need to prioritize these events in seasonal measurements. Future studies should extend the duration of typical seasonal measurements when possible and weather events which occur during the study should be explored, rather than dismissed.

We deployed this coupled system in a longer field campaign to make in situ measurements of BVOC emissions using three separate trace-gas instruments. With the environmental control provided by the portable photosynthesis system, we were able to identify humidity as a parameter that should be included in BVOC emission models (Chapter 4). We find that some compounds are humidity-dependent, be it in changing the temperature dependence of the emission (e.g., acetone) or in drastically effecting the basal emission rate (e.g., sesquiterpenes). Furthermore, our findings indicate that there are additional compounds to be differentiated, improved upon, or included in models, including acetic acid and glycoaldehyde, and methyl vinyl ketone and methacrolein. We provide recommendations for including relative humidity dependence and additional BVOCs in

atmospheric models but note that this is just the beginning of improvements to this field; every iteration of these models improves upon their accuracy and include recent advances.

Although difficult to extensively integrate into models, a unifying theme of this dissertation is the necessity to explore and parameterize variability in plant emissions. While leaf-to-leaf and plant-to-plant variability is complex, we show that variability can be simplified with consideration to robust measurements; leaf-to-leaf variability can generally capture plant-to-plant variability (Chapter 1 and Chapter 2). Additional day-to-day variability is introduced because of weather events (Chapter 3) and leaf-to-leaf measurements press upon the drastic differences in speciated monoterpenes (Chapter 4) and the implications on atmospheric chemistry are appreciable. Besides the types of variability described in this work, there remains numerous opportunities for improvement in the field through investigation of other plant species, such as those found in the understory, and environmental events such as wildfires.

1. Future insights and research directions

Due to the extensive and expansive measurements made during field campaigns spread over two summers, we have identified two additional directions to explore: the effects of wildfire smoke on BVOC emissions and the array of BVOCs emitted by the understory. The measurements we made on these topics warrant additional focus beyond the scope of this dissertation, but we emphasize here the significance of these studies. These discussions are based on preliminary results for manuscripts that are in preparation.

Research has known of the importance of understory species for quite some time and recent studies are working to better characterize their importance (Barreira et al., 2017; Kivimäenpää et al., 2018; Mäki et al., 2019; Schallhart et al., 2018). However, understory species vary greatly by location and emissions vary greatly by plant species. To address this underrepresented source, we measured BVOC emissions from more than 10 understory species and analysis is ongoing to

identify and, when possible, quantify the extent of these emissions. We identified over 30 terpenoid compounds emitted from two understory species- preliminarily identified as mountain yarrow (*Achillea lanulosa*) and fringed sagebrush (*Artemisia frigida*). The chemical diversity is extensive, as is the diversity between species, with yarrow emitting primarily monoterpenes and sesquiterpenes and sagebrush primarily emitting oxidized compounds. Understory BVOC emissions remain a necessary area of consideration.

In additional to early-snow events, additional environmental perturbations that are likely to increase because of climate change need to be addressed, including the impact of wildfire smoke on leaves. While previous work characterized emissions of chemical constituents of wildfire smoke (Maleknia et al., 2009; Wang et al., 2009; Yokelson et al., 2003), the impact of wildfire smoke on direct leaf-level emissions remains to be studied. To address this knowledge gap, we took several measurements using our portable photosynthesis system coupling technique in the summers of 2020 and 2021, which were characterized by extended periods of wildfire smoke. Our leaf-level measurements highlight the potential for wildfire smoke to i) increase or decrease stomatal conductance, and ii) change the known trends of leaf-level BVOC emissions. By increasing the temperature (and thus the vapor pressure deficit) of the leaf, we find that tight stomates may be forced open, causing an increase in photosynthesis (Figure 5.1A), a burst of BVOC emissions (e.g., of formic acid and methyl salicylate), and a sudden release of smoke constituents like nitrophenol. Meanwhile, other wildfire smoke exposed leaves may behave antithetical to known trends, such as monoterpenes decreasing with temperature (Figure 5.1B), rather than increasing exponentially. These preliminary findings show the substantial implications that natural wildfire smoke has on leaf-level emissions and investigates the direct leaf-level

impacts of such smoke to a more comprehensive degree than has been published in literature at this time.

Table 5.1. Compounds emitted from yarrow flowers (*Achillea lanulosa*) and fringed sagrebrush (*Artemisia frigida*) at Manitou Experimental Forest Observatory (measured in 2021). Compounds have been identified using the NIST structural library. Identifications are preliminary (*manuscript in preparation*).

Class	Compound	Formula	Yarrow	Sagebrush
Monoterpenes				
	Camphene	$C_{10}H_{16}$	X	X
	β-Ocimene	$C_{10}H_{16}$	X	
	2-Thujene	$C_{10}H_{16}$	X	X
	α-Pinene	$C_{10}H_{16}$	X	X
	β-Pinene	$C_{10}H_{16}$	X	
	Sabinene	$C_{10}H_{16}$	X	
	Myrcene	$C_{10}H_{16}$	X	
	α-Terpinene	$C_{10}H_{16}$	X	
	Cymene	$C_{10}H_{16}$	X	X
	γ-Terpinene	$C_{10}H_{16}$	X	
	Bornylene	$C_{10}H_{16}$	X	
	Limonene	$C_{10}H_{16}$	X	
	β-Phellandrene	$C_{10}H_{16}$		X
Sesquiterpenes				
	Farnesene	$C_{15}H_{24}$	X	
	Sesquisabinene	$C_{15}H_{24}$	X	
	β-Sesquiphellandrene	$C_{15}H_{24}$	X	
Oxidized Terpenoids				
	p-Tert-butylphenol	$C_{10}H_{14}O$	X	X
	Chrysanthenone	$C_{10}H_{14}O$	X	X
	Car-3-en-5-one	$C_{10}H_{14}O$		X
	Ocimenone	$C_{10}H_{14}O$		X
	Carvone	$C_{10}H_{14}O$		X
	Verbenone	$C_{10}H_{14}O$		X
	Piperitenone	$C_{10}H_{14}O$		X
	α-Terpinen-7-al	$C_{10}H_{14}O$		X
	Eucarvone	$C_{10}H_{14}O$		X
	Filifolone	$C_{10}H_{14}O$		X
	Myroxide	$C_{10}H_{16}O$	X	
	Camphor	$C_{10}H_{16}O$	X	
	4-Thujanol	$C_{10}H_{18}O$	X	
	Eucalyptol	$C_{10}H_{18}O$		X
	Davanone	$C_{15}H_{24}O_2$		X

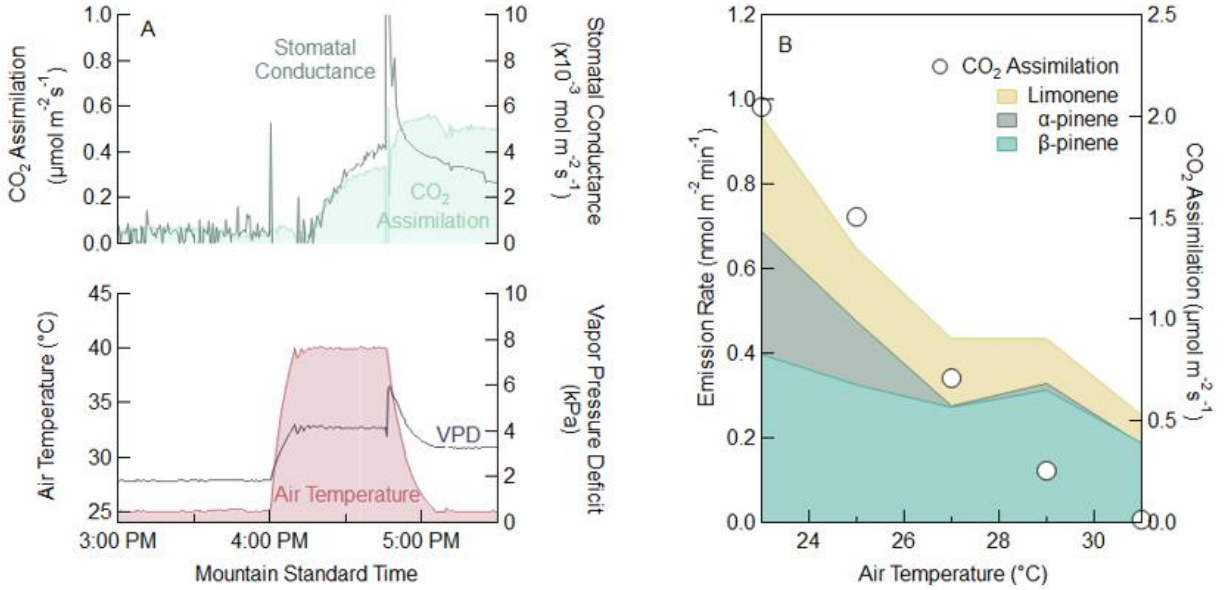

Figure 5.1. Preliminary data of the implications of wildfire smoke on photosynthesis and leaf-level monoterpene emissions. A) Timeseries of photosynthetic parameters shows that by increasing the temperature, stomatal conductance and CO_2 assimilation ramp up for the first time after a day of near-zero values (2020). Vapor pressure deficit (VPD) likewise responds to an increase in temperature. B) Temperature response curve of a different leaf (2021), showing a decreasing emission of monoterpenes as a response to temperature. *Manuscript in preparation.*

The results presented in this dissertation call for more field and laboratory measurements of speciated BVOCs emissions under specific weather conditions. This information is required to improve models that calculate BVOC emissions and thus models that predict future climate conditions. Specifically, more species must be investigated to improve a model's ability to address the accuracy and diversity of a model's plant functional types and measurements must be diverse in location to address changes in land cover. Lab studies may better investigate the mechanisms behind BVOC emissions, but these must be conducted with complementary field measurements to determine the implications of those findings. This dissertation contributes new ideas to a field that is constantly expanding with investigations that are improving both in quality and in breadth. With a field as broad and dynamic as this one, it truly takes a community effort to improve.

References

Feijo Barreira, L. M., Duporté, G., Parshintsev, J., Hartonen, K., Jussila, M., Aalto, J., et al. (2017). Emissions of biogenic volatile organic compounds from the boreal forest floor and understory: a study by solid-phase microextraction and portable gas chromatography-mass spectrometry. *Boreal Environment Research*.

Kivimäenpää, M., Markkanen, J.-M., Ghimire, R. P., Holopainen, T., Vuorinen, M., & Holopainen, J. K. (2018). Scots pine provenance affects the emission rate and chemical composition of volatile organic compounds of forest floor. *Canadian Journal of Forest Research, 48*(11), 1373-1381.

Mäki, M., Aalto, J., Hellén, H., Pihlatie, M., & Bäck, J. (2019). Interannual and seasonal dynamics of volatile organic compound fluxes from the boreal forest floor. *Frontiers in Plant Science, 10*, 191.

Maleknia, S. D., Bell, T. L., & Adams, M. A. (2009). Eucalypt smoke and wildfires: Temperature dependent emissions of biogenic volatile organic compounds. *International Journal of Mass Spectrometry, 279*(2-3), 126-133.

Schallhart, S., Rantala, P., Kajos, M. K., Aalto, J., Mammarella, I., Ruuskanen, T. M., & Kulmala, M. (2018). Temporal variation of VOC fluxes measured with PTR-TOF above a boreal forest. *Atmospheric Chemistry and Physics, 18*(2), 815-832.

Wang, Z., Bi, X., Sheng, G., & Fu, J. (2009). Characterization of organic compounds and molecular tracers from biomass burning smoke in South China I: Broad-leaf trees and shrubs. *Atmospheric Environment, 43*(19), 3096-3102.

Yokelson, R. J., Bertschi, I. T., Christian, T. J., Hobbs, P. V., Ward, D. E., & Hao, W. M. (2003). Trace gas measurements in nascent, aged, and cloud-processed smoke from African savanna fires by airborne Fourier transform infrared spectroscopy (AFTIR). *Journal of Geophysical Research: Atmospheres, 108*(D13).

APPENDIX A

CHAPTER 2 SUPPLEMENTAL INFORMATION[5]

S1 Additional Method Details on TOF-CIMS

For CIMS experiments, sample air is pulled from either the SAM or REF subsampling ports through 0.25 m of PFA tubing (6.35 mm o.d.) into an ion-molecule reaction chamber, where analytes of interest react with I^- reagent ions. We generate I^- ions by flowing ultrahigh purity nitrogen over a methyl iodide (CH_3I) permeation tube and through a ^{210}P ionizer. We detect analytes as $[I + analyte]^-$ adducts. TOF-CIMS mass resolution ($m/\Delta m$) = 4000 throughout experiments performed herein.

We calibrate our TOF-CIMS for formic acid (CH_2O_2) using a permeation tube standard (KIN-TEK Analytical, Inc.) housed in a homebuilt oven held at 50 °C. We flow UHP N_2 (Airgas) over the formic acid permeation tube to generate a steady calibrant flow (Brophy and Farmer, 2015). The TOF-CIMS detection limit for formic acid was 12 parts-per-trillion by volume (ppt_v) over a 60 second average, with a sensitivity of 2630 ± 40 normalized counts $second^{-1}$ ppt_v^{-1}.

S2 Additional Method Details on Thermal Desorption

We calibrated the TD GC/MS for monoterpenes using a mixed calibration standard. The calibration standard is a mixture of methanol (gradient grade OmniSolv®, CAS:67-56-1) and the same concentration of α-pinene (99%, CAS:80-56-8), β-pinene (99%, CAS:18172-67-3), α-terpinene (85%, CAS:99-86-5), p-cymene (99%, CAS:99-87-6), (R)-(+)-limonene (97%,

[5] Riches M, Lee D, Farmer DK. Simultaneous leaf-level measurement of trace gas emissions and photosynthesis with a portable photosynthesis system. Atmospheric Measurement Techniques. 2020 Aug 4;13(8):4123-39.

CAS:5989-27-5), γ-terpinene (97%, CAS:99-85-4), and terpinolene (technical, ≥85% (GC), CAS:586-62-9). All chemicals were purchased from Sigma Aldrich, Co. We created calibration standards at concentrations of 0.5, 1, 5, 25, 50, and 100 ng μL^{-1}, and we used a 1 μL syringe (Hamilton Co.) to inject aliquots of calibration standard in volumes of 0.5, 1.0 or 2.0 μL onto the front end of the sorbent tube. We observed a linear range between 0.25 and 100 ng mass loadings. Table 2.2 shows data from calibrations performed with mass loadings between 0.25 and 1 ng.

We collect gas phase samples using Tenax TA adsorbent material in inert-coated stainless steel tubes (Markes Intl., C1-CXXX-5003). We use a low-flow handheld sampling pump (ACTI-VOC, Markes Intl., C-LFP-01) at a constant flow rate of 0.20 L min^{-1} for 20 minutes, for a total sample volume of 4 L. Cartridges are sealed with brass storage caps and PTFE ferrules and are stored in an airtight container and refrigerated prior to sample analysis on the TD-GC/MS, typically within 10 days. The autosampler (Ultra-xr, Markes Intl.) and the thermal desorption unit (Unity-xr, Markes Intl.) desorb gases from the cartridge. Cartridges are pre-purged with helium for 3 min. The cartridge tubes are then heated to 300 °C for 6 min while carrier gas (high purity helium) flows through the tubes at a rate of 0.100 L min^{-1}. Desorbed analytes are focused onto a cold trap (Air Toxics Analyzer, Markes Intl.) at 20 °C before the trap is heated to 300 °C at a rate of 40 °C min^{-1}. The cold trap is maintained at 300°C for 7 min to allow the analytes to fully desorb.

Desorbed analytes are immediately sent through a gas chromatograph (TRACE 1310, Thermo Scientific with a ZB-5HT-MS column) mass spectrometer (TSQ 8000 Evo Triple Quadrupole GC-MS/MS, Thermo Scientific) with an electron impact source. A split ratio of 5.2:1 prevents overloading of the column during the desorption process. Helium carrier gas flows at 0.0012 L min^{-1}. The MS transfer line and the ion source temperatures are held at 300 °C. The GC oven temperature is maintained at 90 °C for 8 min and then raised to 280 °C (20 °C min^{-1}; hold at

280°C for 2.5 min). Full scan mass spectra covered *m/z* 35-300, while extracted ion chromatogram for monoterpenes were obtained using *m/z* 136, 135, 93, 91. BVOCs were identified using the NIST library and, when possible, retention time (RT) and mass spectra of available standards (Table 2.2). We also show the mass-based limit of detection (LOD) and emission rate LOD in Table 2.2. The emission rate LOD is calculated using the mass-based LOD, a 20 minute sampling time, and 6×10^{-4} m^2 leaf area. For background-subtracted emission measurements, the emission rate LOD depends on the background concentration of the analyte and should be calculated separately. For calibration, liquid standards are injected onto sorbent tubes by syringe. Standards and calibration methodology are described in detail in S1.

GC/MS peaks are integrated using Chromeleon™ Chromatography Data System 7.1 (Thermo Fisher Scientific). Integrated peaks of non-calibrated compounds are identified only if integrated area exceeded 50,000 counts×min and if a NIST library match score exceeded 500.

2.S3 Background Contamination Minimization Efforts

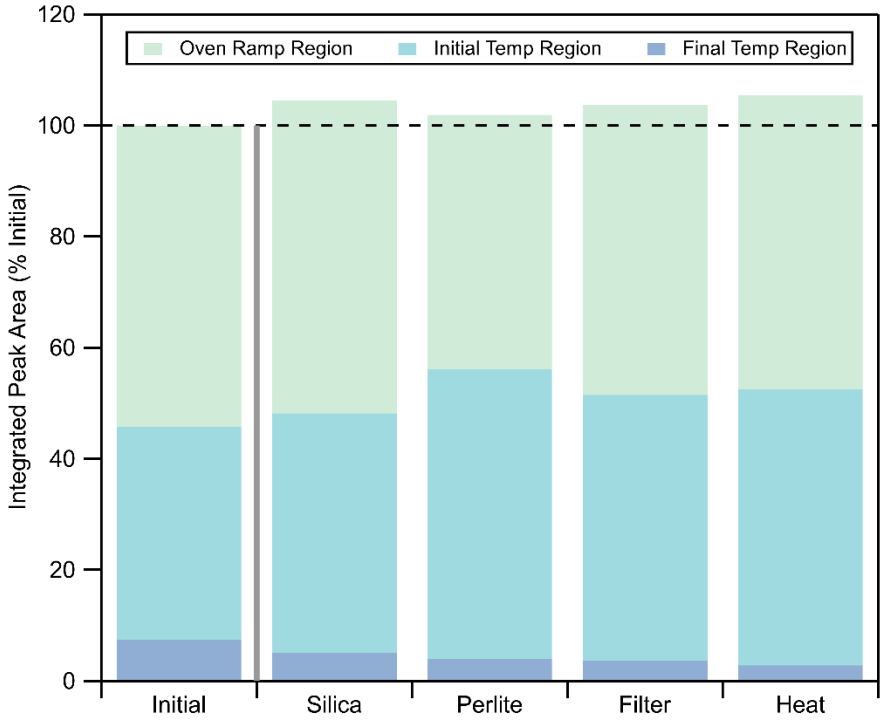

Figure 2.S3. Stacked bar chart of LI-6800 system blanks, resulting from different system alterations. We show the change in total ion counts of the resulting chromatograms in terms of % initial integrated peak area. The results are split into three regions, based on the GC oven program. The oven remains at 90 °C for 8 minutes (Initial Temp Region), then ramps at 20 °C min^{-1} for 9.5 minutes (Oven Ramp Region) and remains at 280 °C for 2.5 minutes (Final Temp Region). The solid line denotes 100% of initial integrated peak area, and the dashed line delineates initial conditions from the affected conditions.

2.S4 Plant Growth Conditions

Table 2.S4. Developmental stage, growth location, temperature variance and light conditions of species described.

Plant	Scientific Name	Developmental Stage	Grow Location	Diel Temperature Variance	Light Conditions
Basil	*Ocimum basilicum*	Mature, pre-flowering	Indoors, beside north-facing window	~ 19 – 23 °C	Primarily natural, some fluorescent, standard daylight hours
Mint	*Mentha spicata*	Mature, pre-flowering	Indoors, beside north-facing window	~ 19 – 23 °C	Primarily natural, some fluorescent, standard daylight hours
Ponderosa Lemon	*Citrus limon x Citrus medica*	Mature, fruiting	Indoors, greenhouse	~ 17 – 28 °C	Primarily natural, LED supplement, 16 hours of light
Ginkgo	*Ginkgo biloba*	Mature, 2.1 – 2.7 tall	Outdoors, arboretum	~ 16 – 33 °C	Natural light, standard daylight hours
Mulberry	*Morus alba*	Mature, 7.6 – 9.1 m tall	Outdoors, arboretum	~ 16 – 33 °C	Natural light, standard daylight hours
Walnut	*Juglans regia*	Mature, 3.0 – 4.6 m tall	Outdoors, arboretum	~ 16 – 33 °C	Natural light, Standard daylight hours

References

Brophy, P., and Farmer, D.: A switchable reagent ion high resolution time-of-flight chemical ionization mass spectrometer for real-time measurement of gas phase oxidized species: characterization from the 2013 southern oxidant and aerosol study, Atmos Meas Tech, 8, 2945-2959, 2015.

APPENDIX B

CHAPTER 3 SUPPLEMENTAL INFORMATION[6]

3.S1 Linear Fit Parameters of Monoterpene Emissions with Relative Humidity

Table 3.S1. Linear fit parameters of emission rate (ng m^{-2} min^{-1}) versus relative humidity (%) and description of direction of the associated correlation.

Compound	Slope [a]	Intercept [a]	r^2	Correlation
α-pinene	-0.08 ± 0.01	4.5 ± 0.6	0.94	Negative
α-terpinene	-0.001 ± 0.03	0.2 ± 1	0.0006	None
β-pinene	0.04 ± 0.2	-0.9 ± 7	0.02	None
β-ocimene	-0.22 ± 0.21	0.3 ± 9	0.006	None
d-limonene	-0.9 ± 0.1	55 ± 5	0.96	Negative
γ-terpinene	-0.12 ± 0.02	8.0 ± 0.8	0.94	Negative
p-cymene	0.04 ± 0.02	-0.7 ± 0.7	0.73	Positive
terpinolene	-0.04 ± 0.03	2 ± 1	0.49	Weakly Negative

[a] fit value ± error of fit

[6] Riches M, Snook J, Farmer DK. The first seasonal snowfall impacts plant photosynthesis and monoterpene emissions. *Reviewed and Resubmitted to Geophysical Research Letters*

3.S2 Changes in Emission Rates of Monoterpenes Before and After Snow Event

Table 3.S2. Emission rates (average ± standard deviation) and T-test p-values of monoterpenes before (Pre) and after (Post) the snow event.

Compound	Pre-Snow$_{50\%}$[a] ng m^{-2} s^{-1}	Pre-Snow$_{40\%}$[a,b] ng m^{-2} s^{-1}	Post-snow$_{40\%}$[c] ng m^{-2} s^{-1}	p-value[d]	Pre RSD[e]	Post RSD[e]
α-pinene	0.42 ± 0.25	1.19 ± 0.72	0.009 ± 0.25	0.009*	31	28000
α-terpinene	0.10 ± 0.23	0.10 ± 0.23	0.006 ± 0.04	0.4	230	619
β-ocimene	0.85 ± 2.79	0.85 ± 2.79	2.29 ± 1.73	0.09	748	75
β-pinene	0.29 ± 2.19	0.29 ± 2.19	1.09 ± 1.08	0.9	328	99
d-limonene	7.52 ± 2.5	14.81 ± 4.92	8.47 ± 2.6	0.04*	33	31
γ-terpinene	1.64 ± 0.43	2.47 ± 0.65	0.51 ± 0.35	<0.0005*	26	67
p-cymene	1.13 ± 0.85	0.77 ± 0.58	0.28 ± 0.30	0.1	75	106
terpinolene	0.16 ± 0.33	0.31 ± 0.65	0.03 ± 0.08	0.3	208	278

[a] n = 6 (n=5 for d-limonene)

[b] Emissions calculated using Pre-Snow$_{50\%}$ and RH-dependence parameters (Table S1)

[c] n = 10 (n=9 for β -ocimene)

[d] Statistical p-values from t-test comparison of Pre-Snow$_{40\%}$ and Post-Snow$_{40\%}$

[e] Relative Standard Deviation (RSD, %)

APPENDIX C

CHAPTER 4 SUPPLEMENTAL INFORMATION[7]

4.S1 Correlation Coefficients of VOCs with Stomatal Conductance

Table 4.S1. Compilation of the r^2 values of linear fits between respective compounds and stomatal conductance (CO_2 assimilation). Values are provided for survey measurements, temperature response curves at 50% ($TRC_{50\%}$) and 30% ($TRC_{30\%}$) relative humidity and humidity response curves (HRC). Each row summarizes a different experiment, and averages of each experiment of that type are provided in bold.

	[Ace+Gly]	Acetone	Formic Acid	[MBO + isoprene]	ΣMT	[MVK+ MACR]	SQT
Survey	0.00 (0.01)	0.00 (0.00)	0.02 (0.01)	0.18 (0.17)	0.10 (0.10)	0.20 (0.21)	0.21 (0.18)
$TRC_{50\%}$	0.09 (0.15)	0.00 (0.07)	0.04 (0.16)	0.80 (0.33)	0.43 (0.06)	0.72 (0.30)	0.50 (0.12)
	0.38 (0.53)	0.43 (0.62)	0.31 (0.43)	0.64 (0.86)	0.62 (0.88)	0.69 (0.92)	0.65 (0.92)
	0.77 (0.83)	0.00 (0.00)	0.60 (0.72)	0.03 (0.00)	0.26 (0.35)	0.01 (0.00)	0.34 (0.42)
	0.22 (0.27)	0.15 (0.22)	0.82 (0.91)	0.70 (0.76)	0.55 (0.64)	0.64 (0.66)	0.70 (0.77)
	0.37 (0.45)	**0.15 (0.23)**	**0.44 (0.56)**	**0.54 (0.49)**	**0.47 (0.48)**	**0.52 (0.47)**	**0.55 (0.56)**
average							
$TRC_{30\%}$	0.27 (0.85)	0.01 (0.45)	0.04 (0.98)	0.16 (0.36)	0.08 (0.45)	0.14 (0.41)	0.08 (0.46)
	0.48 (0.67)	0.04 (0.11)	0.49 (0.67)	0.17 (0.33)	0.26 (0.44)	0.14 (0.27)	0.30 (0.48)
	0.57 (0.60)	0.02 (0.02)	0.76 (0.78)	0.97 (0.98)	0.51 (0.51)	0.90 (0.88)	0.23 (0.21)
	0.55 (0.66)	0.32 (0.46)	0.64 (0.88)	0.03 (0.19)	0.64 (0.84)	0.67 (0.80)	0.61 (0.79)
	0.47 (0.70)	**0.10 (0.26)**	**0.48 (0.83)**	**0.33 (0.47)**	**0.37 (0.56)**	**0.46 (0.59)**	**0.31 (0.49)**
average							
HRC	0.96 (0.97)	0.94 (0.64)	0.46 (0.73)	0.98 (0.84)	0.24 (0.05)	0.86 (0.90)	0.58 (0.62)
	0.36 (0.50)	0.64 (0.63)	0.58 (0.73)	0.89 (0.87)	0.38 (0.28)	0.84 (0.78)	0.19 (0.25)
	0.64 (0.81)	0.13 (0.07)	0.36 (0.53)	0.77 (0.70)	0.09 (0.18)	0.04 (0.12)	0.00 (0.10)
	0.72 (0.65)	0.12 (0.10)	0.41 (0.39)	0.87 (0.78)	0.53 (0.53)	0.70 (0.60)	0.46 (0.45)
	0.67 (0.73)	**0.46 (0.36)**	**0.45 (0.60)**	**0.88 (0.80)**	**0.31 (0.26)**	**0.61 (0.60)**	**0.31 (0.36)**
average							

[7] Riches M, Alwe H, Millet D, Farmer DK. *Manuscript in preparation*.

4.S2 Variability of Speciated Monoterpene Emissions and Stomatal Conductance

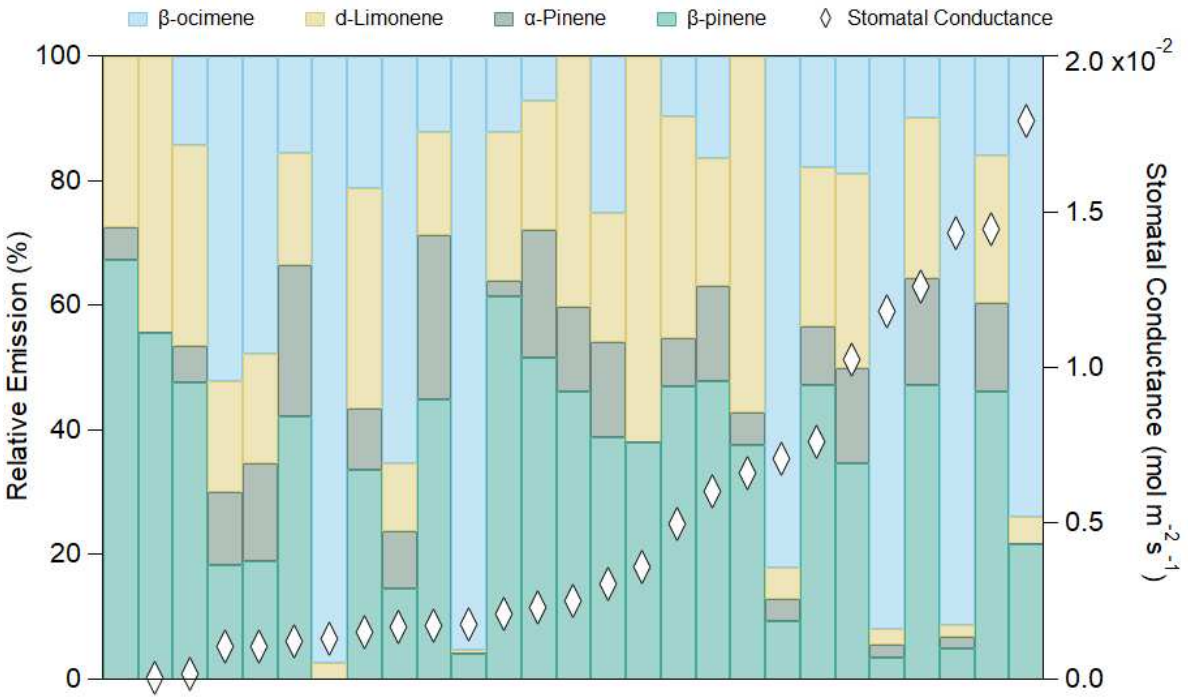

Figure 4.S2. Emission of speciated monoterpenes of different leaves. Differences in the relative emissions (%) of emitting-only leaves (left axis) and stomatal conductance (right axis), organized by increasing values of the latter.